ROADWAY SAFETY INSTITUTE

Human-centered solutions to advanced roadway safety

Positioning, Planning and Operation of Emergency Response Resources and Coordination between Jurisdictions

Yanfeng Ouyang
Siyang Xie
Kun An

Department of Civil and Environmental Engineering
University of Illinois at Urbana-Champaign

Final Report

CTS 18-03

University of Minnesota Driven to Discover℠ | The University of Akron | Illinois University of Illinois at Urbana-Champaign | Southern Illinois University Edwardsville | Western Michigan University

Technical Report Documentation Page

1. Report No.	2.	3. Recipients Accession No.	
CTS 18-03			
4. Title and Subtitle Positioning, Planning and Operation of Emergency Response Resources and Coordination between Jurisdictions		5. Report Date February 2018 6.	
7. Author(s) Siyang Xie, Kun An, Yanfeng Ouyang		8. Performing Organization Report No.	
9. Performing Organization Name and Address Department of Civil and Environmental Engineering University of Illinois at Urbana-Champaign 1209 Newmark Lab, 205 N. Mathews Ave., Urbana, IL 61801, USA		10. Project/Task/Work Unit No. CTS #2015058 11. Contract (C) or Grant (G) No. DTRT13-G-UTC35	
12. Sponsoring Organization Name and Address Roadway Safety Institute Center for Transportation Studies University of Minnesota 200 Transportation and Safety Building 511 Washington Ave. SE Minneapolis, MN 55455		13. Type of Report and Period Covered Final Report, 2014-2016 14. Sponsoring Agency Code	
15. Supplementary Notes http://www.roadwaysafety.umn.edu/publications/			
16. Abstract (Limit: 250 words) Railroad related rail incidents, particularly those involving hazardous material (hazmat), cause severe consequences and pose significant threats to safety, public health and the environment. Rail safety is a huge issue in Midwestern states such as Illinois, Wisconsin, and Minnesota. This project aims at strategically positioning and allocating emergency responders and resources in anticipation of potential accidents in a region that may be impacted by rail incidents. Mathematical models and solution techniques are developed to enable systematic analysis of the emergency response system associated with railroad incidents; e.g., to strategically position and allocate emergency responders and resources in anticipation of potential accidents along spatially distributed railroad networks. We consider the added complexity due to vulnerability of the emergency response system itself, such as the risk of disruptions to the transportation network for first-responders (e.g., blockage of railroad crossings). The outcomes from these tasks will provide fundamental understanding, operational guidelines, and practical tools to policy makers (e.g., federal and state agencies) to induce socio-economically favorable system that support safe and efficient railroad industry operations.			
17. Document Analysis/Descriptors Emergency response time, Strategic planning, Coordination, Contingency planning, Railroad safety		18. Availability Statement No restrictions. Document available from: National Technical Information Services, Alexandria, Virginia 22312	
19. Security Class (this report) Unclassified	20. Security Class (this page) Unclassified	21. No. of Pages 76	22. Price

Positioning, Planning and Operation of Emergency Response Resources and Coordination between Jurisdictions

FINAL REPORT

Prepared by:

Siyang Xie
Yanfeng Ouyang
Department of Civil and Environmental Engineering
University of Illinois at Urbana-Champaign

Kun An
Institute of Transport Studies
Monash University, Australia

February 2018

Published by:

Roadway Safety Institute
Center for Transportation Studies
University of Minnesota
200 Transportation and Safety Building
511 Washington Ave. SE
Minneapolis, MN 55455

ACKNOWLEDGMENTS

The funding for this project was provided by the United States Department of Transportation's Office of the Assistant Secretary for Research and Technology for the Roadway Safety Institute, the University Transportation Center for USDOT Region 5 under the Moving Ahead for Progress in the 21st Century Act (MAP-21) federal transportation bill passed in 2012.

Table of Contents

List of Tables

List of Figures

EXECUTIVE SUMMARY

Railroad is one of the leading modes for freight transportation, accounting for about half of the total ton-miles and about 30% of the hazardous material (hazmat) ton-miles transported in 2007 (Commodity Flow Survey, 2007). Recent years have witnessed significant increases in rail shipment of hazmat such as oil, gas, and ethanol (e.g., the highly volatile Bakken oil from North Dakota) in the Midwest Region. Rail safety becomes a huge issue in these areas because railroad-related rail incidents, particularly those involving hazmat, have caused severe consequences and posed significant threats to safety, public health and the environment. In response, U.S. federal and local regulators recently issued a number of orders to enhance prevention and preparedness in the context of rail safety (Gold and Stevens, 2014). In addition, railroad incidents involving a large number of hazmat cars often cause consequences that directly impact multiple jurisdictions. For example, MN DOT has explicitly expressed concerns over safety risks associated with large rail incidents (e.g., Bakken oil explosions) and has stressed the pressing need for city leaders, first responders and agencies from various jurisdictions to be better prepared for such major incidents (Hansen, 2014). The ideal systems should facilitate agreements among stakeholders to allow responders to go back and forth with specialized equipment on both sides of a boundary.

Considering the huge potential impacts of rail safety issues, the planning of emergency responses to railroad incidents is now a very important topic. Essentially, rail emergency resource planning involves facilty location and resource assignment decisions, which lie at the center of planning many infrastructure systems. For example, in practice, public agencies (e.g., governments) and private companies (e.g., retailers) both need to locate facilities to serve spatially distributed demands and customers. Governments locate various public facilities, e.g., hospitals, schools, fire stations, to provide public services; retail companies determine the locations of their facilities including warehouses, assembly plants, stores, etc, to sell goods and provide business. The design of all such facility systems generally involves considerations of fixed investment of facility construction and transportation cost of serving demands to maximize the operational efficiency and service profit of the system.

Recently, devastating infrastructure damages and catastrophic system failures (e.g., rail incidents) observed in natural and anthropogenic disasters show that facilities may become unavailable from time to time. In many real-world infrastructure systems, when a facility is disrupted, its customers have to seek service from other functioning facilities or even completely give up their services. Ignoring the possibility of facility disruptions often yields a suboptimal system design that is vulnerable to even infrequent facility disruptions. This emphasizes the necessity of taking real-world facility disruptions into consideration and thus complicates facility location planning.

This project aimed to develop a series of mathematical models and efficient solution techniques to enable systematic analysis of the emergency response system associated with railroad incidents. In particular, we plan to develop advanced reliability models to characterize and guide positioning and utilization of first-responder resources taking into account its own vulnerability and complex interactions among multiple agencies and jurisdictions. Based on the results of these models, we provide fundamental understanding, operational guidelines, and practical tools to policy makers (e.g., federal and state agencies) to induce socio-economically favorable systems that support safe and efficient railroad industry oper-

ations. The detailed methodologies are stated as follows.

First, in many real-world systems, facility disruptions exhibit spatial correlations (e.g., due to simultaneous exposition to shared hazards). Disruption correlations tend to have a strong impact on the performance of a reliable facility location design, but it is difficult to describe them with succinct mathematical models. In this project, therefore, we developed a systematic station structure framework to decompose correlated facility disruptions. First, we defined three commonly used probabilistic representations of correlated facility disruption profiles (i.e., with *scenario* probabilities, *marginal* probabilities and *conditional* probabilities), derived pairwise transformations between them and theoretically proved their equivalence. We also provided detailed formulas to transform these probabilistic representations into an equivalent adapted supporting station structure, which enabled us to decompose any correlated facility disruptions into a compact network structure that can be efficiently modeled with only independent failures. This, in turn, allowed us to avoid enumerating an exponential number of disruption scenarios in the system performance evaluation.

Building on the idea of supporting station structure, we next decomposed facility disruption correlations into an additional layer of supporting stations by properly connecting them to the candidate facility locations. The facility correlations could be caused by either "support failure" or "shared hazards," and the stations can either be representations of actual supporting infrastructures or virtual additions for capturing the effect of shared hazards, corresponding to the "support failure" and "shared hazards" correlation types, respectively. With the augmentation of stations, we developed a mixed-integer optimization model to determine the optimal facility location and customer assignment plans, which is capable of addressing correlations of both the two types, and for the first time, the station disruption probabilities are allowed to be site-dependent. Several customized solution approaches based on Lagrangian relaxation and branch and bound, with careful treatments of negative and mixed correlations, were also designed. Numerous hypothetical and empirical case studies involving correlations caused by shared hazards or support failures were conducted to demonstrate the performance and applicability of our methodology and to draw managerial insights.

This project also applied the reliable facility location modeling techniques to sensor deployment problems, where multiple facilities (i.e., sensors) work in combinations to provide service (e.g., positioning, surveillance coverage) to customers via trilateration process. This actually mimics the problem of coordination across multiple jurisdictions in the planning of emergency response resources. We incorporate impacts of sensor disruptions into a reliable sensor deployment framework. Since various sensor combinations may share common sensors, disruption of one combination could be directly related to that of another combination. This leads to internal correlation among the functionality of sensors and sensor combinations. We, therefore, addressed the problem of where to deploy sensors, which combinations of sensors to use, and in what sequence and probability to use these combinations in case of disruptions. A compact mixed-integer mathematical model was developed to formulate the problem, by combining and extending the ideas of assigning back-up sensors (Li & Ouyang, 2010, 2011, 2012) as well as correlation decomposition via supporting stations (Li et al., 2013; S. Xie et al., 2015, 2016). A customized solution algorithm based on Lagrangian relaxation and branch-and-bound was developed, together with several embedded approximation subroutines for sub-problems. A series of hypothetical examples were conducted to illustrate

the applicability and performance of the proposed methodology, while another empirical case study was investigated to draw managerial insights

Chapter 1

Introduction

1.1 Motivation

Railroad is one of the leading modes for freight transportation, accounting for about half of the total ton-miles and about 30% of the hazardous material (hazmat) ton-miles transported in 2007 (Commodity Flow Survey, 2007). Recent years have witnessed significant increase in rail shipment of hazmat such as oil, gas, and ethanol (e.g., the highly volatile Bakken oil from North Dakota) in the Midwest. Railroad-related rail incidents, particularly those involving hazmat, cause severe consequences and pose significant threats to safety, public health and the environment. Recent years have witnessed a series of rail crashes and derailments that have led to major oil spills, tanker fires or explosions that cause significant economic, environmental and social losses. Examples include catastrophic incidents that have occurred recently near Casselton, N.D., and in Quebec, Canada (Crummy, 2013; NBC News, 2013). In response, U.S. federal and local regulators recently issued a number of orders to enhance prevention and preparedness in the context of rail safety (Gold and Stevens, 2014).

Rail safety is a huge issue in Midwestern states such as Illinois, Wisconsin, and Minnesota because many of these hazmat trains go through Chicago, the Twin Cities and other towns and cross state boundaries. Railroad incidents involving a large number of hazmat cars often cause consequences that directly impact multiple jurisdictions. For example, MNDOT has explicitly expressed concerns over safety risks associated with large rail incidents (e.g., Bakken oil explosions) and has stressed the pressing need for city leaders, first responders and agencies from various jurisdictions to be better prepared for such major incidents (Hansen, 2014). The ideal systems should facilitate agreements among stakeholders to allow responders to go back and forth with specialized equipment on both sides of a boundary. However, in reality, state and local boundaries often can be a big barrier that prevents efficient prepositioning of rescue resources and efficient and coordinated response to incidents.

In light of these challenges, one research direction would be to strategically position and allocate emergency responders and resources in anticipation of potential accidents in a region that may be impacted by rail incidents. An embedded issue is to proactively develop coordinated and efficient response to emergence, e.g., by determining optimal operations for a random combination of large-scale incidents and dynamically route emergency vehicles in real-time. Both efforts would need to overcome the challenge associated with coordination

between the private rail industry and the public sector, as well as among multiple public agencies that can be involved with an incident.

1.2 Background

The planning of emergency responses and/or resources to railroad incidents is essentially a facilty location problem in the literature. Facility location decisions lie at the center of planning many infrastructure systems. In practice, public agencies (e.g., governments) and private companies (e.g., retailers) both need to locate their facilities to serve spatially distributed demands/customers. For example, governments locate various public facilities, such as hospitals, schools, and fire stations, to provide public services; retail companies determine the locations of their facilities including warehouses, assembly plants, stores, etc., to sell goods and provide business. The design of all such facility systems generally involves considerations of fixed investment of facility construction and transportation cost of serving demands, so as to maximize the operational efficiency and service profit of the system.

Recently, observations of uncertainties in many real-world infrastructure systems have further complicated facility location planning. There are two basic sources of uncertainties. First, demands could be stochastic and thus cannot be accurately identified beforehand, which introduces additional modeling difficulty compared to cases with deterministic demands. Plenty of research has been done to study demand uncertainties in the past few decades. The second source of uncertainties is facility disruptions, revealed by recent devastating infrastructure damages and catastrophic system failures observed in natural and anthropogenic disasters. Facilities may become unavailable from time to time due to either exogenous or endogenous factors. When a facility is disrupted, its customers have to seek service from other functioning alternatives or even completely give up their services. Therefore, ignoring the possibilities of facility disruptions often yields a suboptimal system design that is vulnerable to even infrequent facility disruptions. This emphasizes the necessity of taking real-world facility disruptions into consideration when planning a facility system (Snyder & Daskin, 2005).

Under probabilistic facility disruptions, one has to deal with a huge number of disruption scenarios, each of which is a unique combination of realized functioning states of the facilities. If each facility can be at one of two possible states (i.e., operating or disrupted) at any time, it is easy to see that the total number of disruption scenarios is two to the power of the facility count, and thus it grows exponentially with the system size. A reliable design needs to evaluate (and then optimize) the expected system performance across all these disruption scenarios, which is apparently a very tedious task. To get around this issue, many studies assume that facility disruptions occur independently (Snyder & Daskin, 2005; Chen et al., 2011). This assumption enables each individual facility's performance to be evaluated separately in a small polynomial time, which results in much less complexity of evaluating the expected system performance and further leads to fruitful developments of compact mathematical models and efficient solution algorithms for reliable facility location design (Cui et al., 2010; Daskin, 2011; Li & Ouyang, 2010).

However, in many real-world systems, facility disruptions exhibit spatial correlations (e.g., due to exposition to shared hazards). Disruption correlations tend to have a strong

impact on the performance of a reliable facility location design. Consider a simple network where two facilities A and B jointly serve one unit of demand from a customer. The costs for serving the demand from these two facilities are 10 and 20 units, respectively, and the penalty for not serving the demand is 100 units. When both facilities are perfectly reliable, the demand will obviously be served by A with a total cost of 10 units. When the facilities are subject to disruption, the demand will be served by A as long as A is functioning (i.e., event A), or by B if A is disrupted but B is functioning (i.e., event $\overline{A}B$), or the customer will bear the penalty if both A and B fail (i.e., event $\overline{AB}$). In the case where A and B fail independently with an equal probability of 0.5, the expected service cost is $10 \times (0.5) + 20 \times (0.5 \times 0.5) + 100 \times (0.5 \times 0.5) = 35$ units. If the facility disruptions are positively correlated, say $P(AB) = P(\overline{AB}) = 0.4, P(\overline{A}B) = P(A\overline{B}) = 0.1$, the expected service cost becomes $10 \times (0.1 + 0.4) + 20 \times 0.1 + 100 \times 0.4 = 47$ units. If the facility disruptions are negatively correlated, say $P(AB) = P(\overline{AB}) = 0.1, P(\overline{A}B) = P(A\overline{B}) = 0.4$, the expected service cost becomes $10 \times (0.1 + 0.4) + 20 \times 0.4 + 100 \times 0.1 = 23$ units. Although the marginal failure probability of each facility remains 0.5 in all the three cases, we can see that the presence of disruption correlations (both positive and negative) significantly affects the expected system service cost, and thus such factors should be carefully considered and incorporated.

In traditional facility location problems, each facility functions individually to serve customers. In some recent applications, however, several facilities work in combinations to provide integrated services and/or supplies. For example, in the supply chain context, downstream processes and/or services are typically in need of various types of products and/or materials from its upstream facilities and each upstream facility is capable of providing only part of these products, thus downstream customers seek services from multiple upstream facilities simultaneously. Similarly, in the sensor deployment context, sensors (which are facilities) are working in combinations to provide sensory coverage, and the effectiveness of the sensor system highly depends on the quality (working range and precision level) and quantity of sensors installed in the area. For sensor deployment problems, if we further consider the possibility of sensor disruptions, since various sensor combinations may share common sensors, disruption of one sensor combination could be directly related to that of another combination. This leads to internal correlation among the functionality of multiple sensors and sensor combinations. Therefore, where to deploy sensors, how to form sensor combinations, which sensor combinations to use, and in what sequence and probability to use them in case of sensor disruptions, are nontrivial questions and should be carefully investigated.

1.3 Contributions

The main objectives of this part of the proposed research are as follows:

(1) Develop a series of mathematical models and efficient solution techniques to enable systematic analysis of the emergency response system associated with railroad incidents. In particular, we plan to develop advanced reliability models to characterize and guide positioning and utilization of first-responder resources taking into account their own vulnerability and complex interactions among multiple agency and jurisdictions.

(2) Provide fundamental understanding, operational guidelines, and practical tools to policy makers (e.g., federal and state agencies) to induce socio-economically favorable systems that support safe and efficient railroad industry operations.

These objectives are widely recognized to be extremely complicated and challenging to tackle, due to the additional complexity associated with the new ingredients added to the traditional reliable facility location problems. In light of this, we propose several innovative methodologies as stated below.

First, this research develops a systematic supporting station structure framework, which was first introduced in Li et al. (2013), to decompose correlated facility disruptions. We then define three commonly-used probabilistic representations of generally correlated disruption profiles (i.e., with *scenario* probabilities, *marginal* probabilities and *conditional* probabilities) and derive pairwise transformations between them. These transformations unify the three different probabilistic representations that have appeared in past studies (Liu et al., 2009; Lu et al., 2015; Li & Ouyang, 2010) and theoretically prove their equivalence. We next provide detailed formulas to transform these probabilistic representations into an equivalent adapted supporting station structure. This enables us to essentially decompose any correlated facility disruptions into a compact network structure that can be efficiently modeled with only independent failures, which in turn allows us to avoid enumerating an exponential number of disruption scenarios in evaluating the system performance.

Building on the idea of supporting station structure, we decompose facility disruption correlations into an additional layer of supporting stations by properly connecting them to the candidate facility locations. The facility correlations could be caused by either "support failure" or "shared hazards," and the stations can either be representations of actual supporting infrastructures or virtual additions for capturing the effect of shared hazards, corresponding to the "support failure" and "shared hazards" correlation types, respectively. With the augmentation of stations, we develop a mixed-integer optimization model to determine the optimal facility location and customer assignment plans, which is capable of addressing correlations of both the two types, and for the first time, the station disruption probabilities are allowed to be site-dependent. We also designed several customized solution approaches based on Lagrangian relaxation and branch and bound, with careful treatments of negative and mixed correlations. Numerous hypothetical and empirical case studies involving correlations caused by shared hazards or support failures are also conducted to demonstrate the performance and applicability of our methodology and to draw managerial insights.

We also apply the reliable facility location modeling techniques to sensor deployment problems by incorporating the possible impacts of sensor disruptions. The reliable sensor deployment problem actually mimics the problem of coordination across multiple jurisdictions in the planning of emergence response resources. In the sensor system, an object is positioned or surveilled based on the distance measurements received from a combination of sensors via a traditional process. Various sensor combinations may share some common sensors, thus failure of a sensor could possibly affect multiple combinations, and the functioning state of one sensor combination could be directly related to that of another combination. Considering the interrelations among sensors and sensor combinations, where to deploy sensors, how to form sensor combinations, which sensor combinations to use, and in what sequence and probability to use them in case of disruptions, are nontrivial questions.

We address these questions by combining and extending the ideas of assigning back-up sensors (Li & Ouyang, 2010, 2011, 2012) as well as correlation decomposition via supporting stations (Li et al., 2013; S. Xie et al., 2015, 2016) into an overarching framework. A compact mixed-integer mathematical model is first developed to determine the optimal sensor location, sensor level assignment and combination selection plans. Then a customized solution algorithm based on Lagrangian relaxation and branch-and-bound is designed together with several embedded approximation subroutines for sub-problems. A series of hypothetical and empirical case studies are also conducted to illustrate the applicability and performance of the proposed methodology and to draw managerial insights.

1.4 Outline

This report is organized as follows. Chapter 2 summarizes the literatures in the reliable facility location context and in several extenstions. Chapter 3 proposes a systematic station structure framework to decompose facility disruption correlations into a succinct mathematical form. Chapter 4 formulates a mixed-integer optimization model for the reliable facility location problems with correlated facility disruptions. Chapter 5 develops a mixed-integer linear program and several solution approaches for the reliable sensor deployment problem.

Chapter 2

Literature Review

This chapter reviews work in reliable facility location literature, as well as its several extensions. There have been a lot of studies done on the reliable facility location problems, and most of them formulate the problems into discrete integer linear programs. The ideas of probabilistic disruptions, backup facility assignments, and expected system evaluation are widely adopted in these programs and models.

2.1 Reliable Facility Location Models

Facility location problems have been intensively studied in the past several decades, with the most original formulation dated back to 1909. Since then, there have been numerous studies and a large number of related models on facility location problems. (Drezner, 1995) reviews a series of classic mathematical models for deterministic location problems including covering problems, center problems, median problems, etc. Most of these traditional studies consider deterministic infrastructure service where each built facility is assumed functioning and available for service all the time (Drezner, 1995; Daskin, 2011). Recently, researchers began to recognize that facilities may lose functionalities due to various external/internal factors such as natural disasters, adverse weather, human factors, etc. And a series of new reliable facility location models have been proposed to furnish a facility system with proper redundancy to take real-world facility disruptions into consideration (Snyder & Daskin, 2005; Li & Ouyang, 2010; Cui et al., 2010).

In the reliable facility location literature, one stream of studies focused on design-related facility disruptions that can be prevented by fortification. Interdiction models were often used to identify critical components in an infrastructure system, and cost-effective fortification strategies were sought during facility location design (Church et al., 2004; Scaparra & Church, 2008a; Liberatore et al., 2011; Scaparra & Church, 2008b). Another stream of research focused on modeling the expected consequences of location-specific facility disruptions (Snyder & Daskin, 2005; Li & Ouyang, 2010). A comprehensive review can be found in Snyder (2006). Among a rich variety of efforts, Snyder & Daskin (2005) and Berman et al. (2009) formulated discrete models where facilities are subject to site-independent disruptions with identical failure probabilities. More recently, a series of reliable location models were proposed to allow site-dependent disruption probabilities. Berman et al. (2007) provided a

nonlinear mixed-integer programming formulation as well as an efficient heuristic solution approach. Li & Ouyang (2012) proposed a reliable sensor location model to optimize traffic system surveillance effectiveness where sensors are subject to site-dependent probabilistic failures. Cui et al. (2010) developed two distinct sets of models (discrete and continuous) and corresponding solution algorithms to allow the disruption probabilities to be site-dependent. Atamtürk et al. (2012) further presented reliable location-inventory models (which allowed facilities to be subject to failures due to inventory shortage) as well as an innovative conic programming solution approach. All these studies assume independent facility disruptions and furnish a facility system with proper redundancy so as to balance its efficiency in the normal scenario and its reliability when disruptions happen.

2.2 Extensions of RFL

2.2.1 Facility Correlations

Most reliable location models hold the assumption that facility disruptions are independent. However, in many real-world facility systems, the disruptions of facilities often exhibit complex correlations, and a straightforward modeling approach would need to enumerate or simulate an exponential number of scenarios; this makes it computationally difficult to even just evaluate the system performance under a given design. To the best of our knowledge, only a few efforts have been made to address correlated facility disruptions, either exactly or approximately (e.g., Liberatore et al. (2012); Li & Ouyang (2010); Lu et al. (2015)). Liberatore et al. (2012) considered the problem of optimally protecting a capacitated median system with a limited amount of protective resources subject to disruptions, a tri-level formulation of the problem and an exact solution algorithm based on a tree-search procedure were proposed. Li & Ouyang (2010) developed a continuum approximation model for the reliable uncapacitated fixed charge location problem where facilities are subject to spatially correlated disruptions that occur with site-dependent probabilities. Lu et al. (2015) allowed facility disruptions to be correlated with an uncertain joint distribution, and applied distributionally robust optimization to minimize the expected cost under the worst-case distribution. In addition, Huang et al. (2010) addressed a variant of the p-center model in case of large-scale emergencies, where correlated disruption was introduced by allowing many facilities to become functionless simultaneously. Gueye & Menezes (2015) considered a two-stage stochastic program model for a median problem under correlated facility disruptions, and asymptotic results were presented based on a scenario-based model formulation. Berman & Krass (2011) and Berman et al. (2013) introduced analytical approaches to help understand the effects of correlated failures in simpler spatial settings, e.g., along a line segment. Li et al. (2013) proposed a virtual station structure that transforms a facility network with correlated disruptions into an equivalent one with added virtual supporting stations, and the virtual stations were assumed to be subject to independent disruptions. An optimization model was developed to handle cases where facilities are positively correlated and the station disruption probabilities are all identical.

2.2.2 Sensor Deployment

Sensor deployement problems are natural applications where facilities work in combinations to provide services. Extensive researches have been conducted to study the sensor deployment problems. Gentili & Mirchandani (2012) provided a comprehensive literature review on existing sensor location models in traffic networks. Many of those studies aim at maximizing sensor coverage or minimizing the error/cost of estimation. Mirchandani et al. (2010) addressed the problem of locating surveillance infrastructure to cover a target surface; possible barriers that may block sensing signals were considered. Erdemir et al. (2008) developed models to study a location covering problem with consideration of both nodal and path-specific demand. Geetla et al. (2014) studied the deployment of omni-directional audio sensors that can detect vehicle crashes on a roadway. Eisenman et al. (2006) proposed a sensor location problem based on a simulation-based real-time network traffic estimation and prediction system. Fei & Mahmassani (2011) presented a multi-objective model that deploys a minimal number of passive point sensors in a roadway network considering link information gains and origin-destination demand coverage. Danczyk et al. (2016) developed a sensor location model to minimize the error of monitoring freeway traffic condition. Various customized solution methods for sensor location problems have also been developed. Among them, Wang et al. (2005) partitioned the sensing field into smaller sub-regions and deployed sensors in these sub-regions when the working range of a sensor forms an arbitrarily shaped region (i.e., polygon). Clouqueur et al. (2003) developed a sequential decision-making approach to maximize the exposure of network travel paths to a set of sensors. The overall goal was to minimize the system cost needed to achieve a desired exposure rate. Zou & Chakrabarty (2004) proposed a virtual force strategy for sensor deployment and a probabilistic target localization algorithm to enhance sensor coverage. He (2013) presented a graphical approach to find the smallest set of network links to locate sensors, so as to infer the traffic flow on all other links. Ouyang et al. (2009) and Peng et al. (2011) investigated ways to deploy wayside sensors in a railroad network to monitor railcar traffic. Studies on optimal sensor placement, especially those in the context of trilateration, are quite limited. While deploying directional sensors that collectively form regular convex polygons, X. Xie & Dai (2014) optimized the number of edges and length of these polygons so as to maximize coverage accuracy. As sensor deployment on a regular lattice is usually not optimal for trilateration, Roa et al. (2007) proposed a diversified local Tabu search method where omni-directional sensors can follow a non-regular configuration. De Stefano et al. (2015) investigated the placement of sensors on an engineering structure to detect the existence, location and extent of internal damage. These studies, however, assumed that the sensing targets are homogeneously distributed in a 2-dimensional plane; this is often unrealistic in the real world. Indeed, sensor locations are critical to the overall performance of the surveillance system. For example, Ahmed et al. (2014) demonstrated the significance of sensor location in influencing real-time traffic state prediction after traffic crashes.

Chapter 3

RFL with Facility Correlations: Decomposition of Correlations via Augmentation of Supporting Stations

3.1 Introduction

Most traditional studies on reliable facility location problems hold the assumption on independent facility disruptions. However, in many real-world infrastructure systems, the disruptions of facilities often exhibit complex correlations due to various types of interdependence and connections among them (e.g., shared external hazards, shared resources, or competition for resources). If each facility can be at one of two possible states (i.e., operating or disrupted) at any time, the total number of disruption scenarios is two to the power of the facility count, and thus a reliable design needs to evaluate (and then optimize) the expected system performance across all these disruption scenarios, which is apparently a very tedious task. There remains a lack of a systematic methodology framework that can model general disruption correlations (i.e., including both positive and general correlations) in a computationally-tractable way.

Therefore, in this chapter, we develop a systematic station structure methodology to decompose facility disruption correlations. Specifically, we first define three commonly-used probabilistic representations of generally correlated disruption profiles (i.e., with scenario probabilities, marginal probabilities and conditional probabilities) and derive transformations between them to unify these different representations that have appeared in past studies (Liu et al., 2009; Lu et al., 2015; Li & Ouyang, 2010) and to theoretically prove their equivalence. Then we introduce the supporting station structure and station representation of facility disruption profile, and provide detailed formulas to transform the probabilistic representations into an adapted station representation. This enables us to essentially decompose any correlated facility disruptions into a compact network structure that can be efficiently modeled with only independent failures, which in turn allows us to avoid enumerating an exponential number of disruption scenarios in evaluating system performance. This decomposition scheme largely reduces the complexity associated with system evaluation and optimization. Additional properties are discussed, and a set of illustrative numerical exper-

iments are conducted to demonstrate the proposed methodological framework and to cast interesting managerial insights.

3.2 Facility Disruption Representations

This section proposes various succinct representations of correlated facility disruptions. Section 3.2.1 describes three commonly used probabilistic representations of a general disruption profile, and the pairwise transformations between them. Section 3.2.2 introduces the new supporting station structure, its operational rules, properties, the station representation of disruption profile, and the transformations from probabilistic representations to the station representation.

3.2.1 Probabilistic representations

For a given set of facilities $\mathcal{J}$, the state of each facility $j \in \mathcal{J}$ can be denoted by a binary random variable V_j, which equals 1 if the facility is operating or 0 otherwise. The state of the entire facility set $\mathcal{J}$ is then specified by a random vector $\mathcal{V} := [V_j]_{j\in\mathcal{J}} \in \{0,1\}^{|\mathcal{J}|}$. We call a specific underlying disruption pattern of all facilities $\mathcal{J}$ (which determines how $\mathcal{V}$ realizes) a disruption profile, which can be described in three equivalent ways as follows.

We define each unique realization of $\mathcal{V}$ as a disruption scenario, which can be equivalently specified by the set of all disrupted facilities $J := \{j|V_j = 0, \forall j \in \mathcal{J}\}$ (i.e., no other facility fails). Let $S_J = Pr[V_j = 0, \forall j \in J \ \& \ V_j = 1, \forall j \in \mathcal{J}\backslash J]$ denote the probability for scenario J to occur. Any arbitrary disruption profile can be specified by set $\{S_J\}_{\forall J\subseteq\mathcal{J}}$, where $S_J \geq 0, \forall J \subseteq \mathcal{J}$ and $\sum_{J\subseteq\mathcal{J}} S_J = 1$. We call set $\{S_J\}_{\forall J\subseteq\mathcal{J}}$ a *scenario representation*, of the underlying disruption profile for convenience, which apparently includes a total of $2^{|\mathcal{J}|}$ elements.

A disruption profile can also be specified by marginal probabilities for subsets of set $\mathcal{J}$ to be disrupted, regardless of the states of all other facilities; i.e., $M_J = Pr[V_j = 0, \forall j \in J]$. Obviously, $M_{\{j\}} = q_j, \forall j \in \mathcal{J}$, where q_j is the disruption probability of facility j. Without loss of generality, we assume that $M_\emptyset = 1$. Then set $\{M_J\}_{J\subseteq\mathcal{J}}$, where $M_\emptyset = 1$ and $M_{J_1} \geq M_{J_2}, \forall J_1 \subseteq J_2 \subseteq \mathcal{J}$, specifies an arbitrary disruption profile, which we call a *marginal representation*. Note that it also includes $2^{|\mathcal{J}|}$ elements.

Similarly, a disruption profile can be also represented by conditional disruption probabilities; i.e., $C_{j|J} = Pr[V_j = 0|V_{j_1} = 0, \forall j_1 \in J], j \notin J$, which is the probability for facility $j \in \mathcal{J}$ to be disrupted given that all facilities in set $J \subseteq \mathcal{J}\backslash\{j\}$ have been disrupted. We call the collection of all conditional probabilities, i.e., $\{C_{j|J}\}_{\forall J\subseteq\mathcal{J}, j\notin J}$, a *conditional representation*. Note that it includes $|\mathcal{J}| \cdot 2^{|\mathcal{J}|-1}$ elements.

It is well-known that these three disruption profile representations can be transformed equivalently from one another. Obviously, by definition,

$$M_J = \sum_{J_1\supseteq J} S_{J_1}, \ \forall J \subseteq \mathcal{J}, \tag{3.1}$$

$$C_{j|J} = \frac{M_{j\cup J}}{M_J} = \frac{\sum_{J_1\supseteq j\cup J} S_{J_1}}{\sum_{J_2\supseteq J} S_{J_2}}, \ \forall j \notin J \subseteq \mathcal{J}. \tag{3.2}$$

Based on the Inclusion-Exclusion Principle Brualdi (2004), we conclude that,

$$S_J = \sum_{J_1 \supseteq J} (-1)^{|J_1|-|J|} M_{J_1}, \quad \forall J \subseteq \mathcal{J}. \tag{3.3}$$

Next, from the chain rule of conditional probability Russell & Norvig (2009), we have,

$$M_J = \prod_{i=1}^{|J|} C_{j_i|\{j_1,\cdots,j_{i-1}\}}, \quad \forall J := \{j_1, \cdots, j_{|J|}\} \subseteq \mathcal{J}. \tag{3.4}$$

3.2.2 Station structure representation

The idea of supporting station structure is first introduced in (Li et al., 2013). In a station structure, a set of virtual stations, $\mathcal{K}$, are added and connected to facilities in $\mathcal{J}$. Each supporting station $k \in \mathcal{K}$ fails independently at a site-dependent probability $P(\{k\})$, without loss of generality, we allow at most one station to be connected to the same subset of facilities (otherwise, these multiple stations can be consolidated to one with a failure probability equal to the product of the failure probabilities of all these stations). Then a supporting station can be specified by the set of facilities connected to it; i.e., let K_J denote the supporting station connected to all facilities in J but no other facilities, and $P(K_J)$ denote its failure probability. We further assume that a facility is operating if and only if at least one of its connected stations is functioning, and hence the operating state of a facility is determined collectively by all the functioning stations connected to it. For example, in Figure 3.1(b), facility j_1 is disrupted only when stations $k_{\{1\}}, k_{\{1,2\}}, k_{\{1,3\}}, k_{\{1,2,3\}}$ are all disrupted. Here k_J is the station connected to all and only facility locations in J; i.e., $l_{k_J j} = 1$ for all $j \in J$ and $l_{k_J j} = 0$ for all $j \notin J$. It can be proven that by properly adding and connecting the stations, the augmented facility-station structure can equivalently represent any facility disruption correlations. For convenience, we also define K_J^0 as the subset of supporting stations that are at least partially connected to facility set J, J_K as the subset of facilities supported only by the stations in K, and J_K^0 as the subset of facilities supported at least partially by the stations in set K. For example, in the structure in Figure 3.1(b), $J^0_{\{k_2,k_4,k_5\}} = \{j_1, j_2, j_3\}$, while $J_{\{k_2,k_4,k_5\}} = \{j_2\}$, and $K^0_{\{j_1,j_2\}} = \{k_1, k_2, k_3, k_4, k_5\}$, while $K_{\{j_1,j_2\}} = \{k_2\}$.

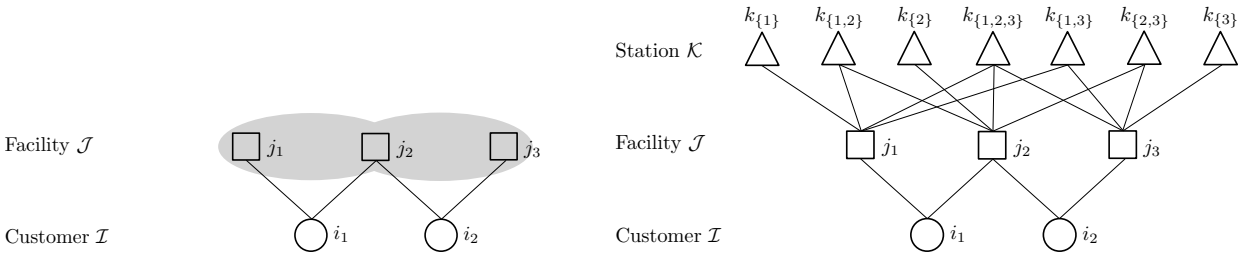

(a) Correlated facility disruption (b) Augmented station structure

Figure 3.1: Conceptual illustration of the station structure.

It is easy to see that correlation of original facilities could be captured by the station-facility connections. For example, if at any time facility $j \in J_k^0$ is disrupted, then station k

must have been disrupted, and hence all other facilities in J_k^0 would have a higher likelihood of being disrupted. With this set-up, we will prove in the following section that a correlated disruption profile of facility set $\mathcal{J}$ can be equivalently represented by a set of supporting station $\mathcal{K}$ with purely independent failures.

For the set of all possible supporting stations $\mathcal{K} = \{K_J\}_{\forall J \subseteq \mathcal{J}}$, the corresponding probability formulation is $\{P(K_J)\}_{\forall J \subseteq \mathcal{J}}$, which we now call a *station representation*. In the worst case, the maximum number of supporting stations can be up to $|\{P(K_J)\}_{\forall J \subseteq \mathcal{J}}| = |\mathcal{K}| = 2^{|J|}$. However, as we will show in Section 3.4.1, in most real-world cases, the number of necessary supporting stations in practice is likely to be quite small.

As a final remark, it shall be noted that although we call the supporting stations "virtual", there are many real-world infrastructure systems that emulate this supporting structure. For example, if a service facility requires material (e.g., power) obtained from supporting factories (e.g., power plants), then the stations can actually be real factories.

3.3 Decomposition of Correlated Disruptions

3.3.1 Independence and Correlation

We say that a disruption profile is independent if any subset of facilities $J \subseteq \mathcal{J}$ are independent; i.e., $M_J = M_{J_1} \cdot M_{J \setminus J_1}, \forall J_1 \subset J$. In this case, the three probabilistic representations can be simply expressed in terms of individual facility disruption probabilities $\{q_j\}_{\forall j \in \mathcal{J}}$, i.e.,

$$S_J = \prod_{j \in J} q_j \prod_{j \in \bar{J}} (1 - q_j), \quad M_J = \prod_{j \in J} q_j, \quad C_{j|J} = \frac{\prod_{j \in j \cup J} q_j}{\prod_{j \in J} q_j}, \quad \forall J \subseteq \mathcal{J}, j \notin J, \tag{3.5}$$

where $\bar{J} := \mathcal{J} \setminus J$.

More generally, a disruption profile may be correlated. Next, we define positive correlation for a disruption profile, $\{M_J\}_{\forall J \subseteq \mathcal{J}}$. We first define a set of cue fractions $\frac{M_J}{M_{J \setminus \{j\}}} \leq 1, \forall j \in J \subseteq \mathcal{J}$, and then consider a series of iterative operations. In the first iteration, we construct a new fraction with each of the cue fraction $\frac{M_J}{M_{J \setminus \{j\}}}$ as the denominator and $\frac{M_{J \setminus \{j'\}}}{M_{J \setminus \{j, j'\}}}$ as the numerator. The numerator is simply obtained by removing an arbitrary common subscript element $j' \in J, j' \neq j$ from every item in the original cue fraction. In each of the following iterations, we just take the resulting fractions from the previous iteration as cue fractions and repeat the same operation until the numerator of every resulting fraction contains an item of $M_\emptyset$. If every resulting fraction throughout the iterations is no greater than one we call the disruption profile positively correlated. Obviously, the disruptions are independent only if all of the resulting fractions at all iterations are equal to one. This definition is formally stated below.

Definition 1. *A set of facilities $J \subseteq \mathcal{J}$ are positively correlated if*

$$Q(J, J_1, j) := \frac{\prod\limits_{J_1 \setminus \{j\} \subseteq L \subseteq J \setminus \{j\}} M_L^{(-1)^{|L| - |J_1|}}}{\prod\limits_{J_1 \subseteq L \subseteq J} M_L^{(-1)^{|L| - |J_1| + 1}}} \leq 1, \quad \forall j \in J_1 \subseteq J \subseteq \mathcal{J}, \tag{3.6}$$

and $\exists j \in J_1 \subseteq J \subseteq \mathcal{J}$ *such that* $Q(J, J_1, j) < 1$*. If facilities are correlated but not positively correlated, we say they are generally correlated. If all facilities in* $\mathcal{J}$ *are positively (or generally) correlated, we say the disruption profile is positively (or generally) correlated.*

As a specific example, when $\mathcal{J}$ only has two facilities, say $\mathcal{J} := \{j_1, j_2\}$, then the above conditions are equivalent to $\frac{M_{\{j_1\}}/M_{\emptyset}}{M_{\mathcal{J}}/M_{\{j_2\}}} \leq 1$. This is obviously consistent with the classic definition of positively correlated disruptions $\frac{C_{j_1|\emptyset}}{C_{j_1|j_2}} = \frac{M_{\{j_1\}}M_{\{j_2\}}}{M_{\mathcal{J}}} < 1$, since $M_{\mathcal{J}}/M_{\{j_2\}} \leq 1$ by definition.

When facility disruptions are correlated, specifying any of the three probabilistic representations would typically require enumerating an exponential number of the representation elements. To circumvent this complexity, the following section describes how an arbitrary probabilistic disruption representation can be transformed into an equivalent station representation with only independent station failures.

3.3.2 Decomposition

Station structure with only independent station failures are much easier for analysis and design (Snyder, 2006; Chen et al., 2011). This section presents recipes for decomposing a facility system with an arbitrary positively correlated disruption profile (probabilistic representation) into an equivalent network with additional supporting stations (station representation).

Proposition 1. *For a given station representation* $\{P(K_J)\}_{\forall J \subseteq \mathcal{J}}$*, the equivalent probabilistic disruption profile representations are formulated as:*

$$S_J = \sum_{J_1 \supseteq J} (-1)^{|J_1|-|J|} \left[\prod_{J_2 : J_2 \cap J_1 \neq \emptyset} P(K_{J_2}) \right], \ \forall J \subseteq \mathcal{J}, \tag{3.7}$$

$$M_J = \prod_{J_1 : J_1 \cap J \neq \emptyset} P(K_{J_1}), \ \forall J \subseteq \mathcal{J}, \tag{3.8}$$

$$C_{j|J} = \prod_{J_1 \ni j, J_1 \subseteq \bar{J}} P(K_{J_1}), \ \forall J \subseteq \mathcal{J}, j \notin J. \tag{3.9}$$

Conversely, given a probabilistic disruption representations, we can construct an equivalent station representation by solving equations (3.7), (3.8) or (3.9). We prove in the following proposition that the station representation satisfying (3.7), (3.8) or (3.9) exists and is unique.

Proposition 2. *For any correlated disruption profile representation, there exists one and only one station representation* $\{P(K_J)\}_{\forall J \subseteq \mathcal{J}}$ *that satisfies* (3.7)*,* (3.8) *or* (3.9)*.*

Next, the following propositions show how to construct a supporting station structure (station representation) from a probabilistic disruption profile representation $\{C_{j|J}\}_{\forall J \subseteq \mathcal{J}, j \notin J}$, $\{M_J\}_{\forall J \subseteq \mathcal{J}}$, or $\{S_J\}_{\forall J \subseteq \mathcal{J}}$.

Proposition 3. *An arbitrary conditional representation* $\{C_{j|J}\}_{\forall J\subseteq\mathcal{J},j\notin J}$ *of a positively correlated disruption profile can be represented by a station representation* $\{P(K_J)\}_{\forall J\subseteq\mathcal{J}}$*, where:*

$$P(K_J)=\prod_{i=0}^{|J|-1}\left[\prod_{\substack{L\subseteq J\setminus\{j\}\\|L|=i}}C_{j|(\bar{J}\cup L)}\right]^{(-1)^i}=\prod_{L\subseteq J\setminus\{j\}}\left[C_{j|(\bar{J}\cup L)}\right]^{(-1)^{|L|}},\ j\in J,\ \forall J\subseteq\mathcal{J}. \tag{3.10}$$

Proposition 4. *An arbitrary marginal representation* $\{M_J\}_{\forall J\subseteq\mathcal{J}}$ *or scenario representation* $\{S_J\}_{\forall J\subseteq\mathcal{J}}$ *of a positively correlated disruption profile can be transformed into a station representation* $\{P(K_J)\}_{\forall J\subseteq\mathcal{J}}$*, where:*

$$P(K_J)=\prod_{i=0}^{|J|}\left[\prod_{\substack{L\supseteq\bar{J}\\|L|=|\bar{J}|+i}}M_L\right]^{(-1)^{i-1}}=\prod_{\mathcal{J}\supseteq L\supseteq\bar{J}}[M_L]^{(-1)^{|L|-|\bar{J}|+1}} \tag{3.11}$$

$$=\prod_{\mathcal{J}\supseteq L\supseteq\bar{J}}\left[\sum_{J_1\supseteq L}S_{J_1}\right]^{(-1)^{|L|-|\bar{J}|+1}},\ \forall J\subseteq\mathcal{J}. \tag{3.12}$$

This decomposition procedure could be illustrated using the simple three-facility system in Figure 3.1. Suppose the scenario-based disruption probabilities are given as input data, as shown in Table 3.1. Following (3.1) and (3.11), the marginal failure probability for facility 1, $M_{\{1\}}$, and failure propensity for a station solely connected to this facility, $P(k_{\{1\}})$, are computed respectively as follows,

$$M_{\{1\}}=S_{\{1\}}+S_{\{1,2\}}+S_{\{1,3\}}+S_{\{1,2,3\}}=0.60,$$
$$P(k_{\{1\}})=\frac{M_{\{1,2,3\}}}{M_{\{2,3\}}}=\frac{0.30}{0.35}=0.86.$$

In so doing, the entire marginal representation and associated station structure can be computed, and the results are summarized in Table 3.1.

Table 3.1: Different representations of the correlated disruption for the transformation example (S. Xie et al., 2015).

Scenario representation	$S_{\{1\}}$ 0.05	$S_{\{2\}}$ 0.05	$S_{\{3\}}$ 0.05	$S_{\{1,2\}}$ 0.15	$S_{\{1,3\}}$ 0.10	$S_{\{2,3\}}$ 0.05	$S_{\{1,2,3\}}$ 0.30
Marginal representation	$M_{\{1\}}$ 0.60	$M_{\{2\}}$ 0.55	$M_{\{3\}}$ 0.50	$M_{\{1,2\}}$ 0.45	$M_{\{1,3\}}$ 0.40	$M_{\{2,3\}}$ 0.35	$M_{\{1,2,3\}}$ 0.30
Station structure	$P(k_{\{1\}})$ 0.86	$P(k_{\{2\}})$ 0.75	$P(k_{\{3\}})$ 0.67	$P(k_{\{1,2\}})$ 0.93	$P(k_{\{1,3\}})$ 0.95	$P(k_{\{2,3\}})$ 1.00	$P(k_{\{1,2,3\}})$ 0.79

3.4 Discussions and Illustrations

This section illustrates some important properties and miscellaneous issues assoicated with the proposed supporting station structure.

3.4.1 Compactness of the supporting station structure

One may wonder how many stations will be needed to represent a complex correlation profile. The following theorem states that when the facility system is globally correlated, the number of needed stations is comparable to the number of scenario/marginal/conditional probabilities that are needed to describe the correlation.

Theorem 1. *In a facility system with facility set $\mathcal{J}$ and effective disruption scenario set $\mathcal{S}$, the maximum number of necessary supporting stations $|\mathcal{K}|$ is* $\min\left\{2^{|\mathcal{J}|}, \left|\left\{\bigcap_{J\in\widetilde{J}} J\right\}_{\forall \widetilde{J}\subseteq\mathcal{S}}\right|\right\}$. *Specially, $|\mathcal{K}| \leq |\mathcal{S}|+1$ if $\left\{\bigcap_{J\in\widetilde{J}} J\right\}_{\forall \widetilde{J}\subseteq\mathcal{S}} = \mathcal{S}\bigcup\emptyset$.*

When the facilities are more "locally" correlated, the number of stations $|\mathcal{K}|$ (generally larger than the number of facilities $|\mathcal{J}|$) shall be smaller than the number of scenarios $|\mathcal{S}|$. In particular, if the facility system $\mathcal{J}$ could be partitioned into N mutually exclusive subsets $\{J_n\}_{n=1,2,\cdots,N}$, such that the facilities within each subset J_i are correlated with one other, while facilities in different subsets are independent, then the maximum number of needed stations is $|\mathcal{K}| \leq \sum_{n=1}^{N} 2^{|J_n|}$, which is typically much smaller compared to the maximum number of scenarios that are used/needed to describe the correlation, $\mathcal{S} = 2^{|\mathcal{J}|}$. We state this in the following proposition without proof.

Proposition 5. *If $\mathcal{J} = \cup_{n=1,2,\cdots,N} J_n$ for some $N > 1$, such that for all $i = 1, 2, \cdots, N$, the disruptions of all facilities in J_i are independent of those in $\mathcal{J}\backslash J_i$, then the maximum number of needed stations $|\mathcal{K}|$ and the number of scenarios $|\mathcal{S}|$ satisfy $|\mathcal{K}| \leq \sum_{n=1}^{N} 2^{|J_n|}$ and $|\mathcal{S}| = 2^{\sum_{n=1}^{N}|J_n|}$, respectively, which further yields*

$$\frac{|\mathcal{K}|}{|\mathcal{S}|} \leq \frac{\sum_{n=1}^{N} 2^{|J_n|}}{2^{\sum_{n=1}^{N}|J_n|}} \leq \begin{cases} 1, & \text{if } N = 1 \text{ (globally correlated)} \\ \frac{\sum_{n=1}^{N} 2^{|J_n|}}{2^{|\mathcal{J}|}}, & \text{if } 2 \leq N \leq |\mathcal{J}|/2 \text{ (locally correlated)} \end{cases}$$

As an example, we consider a facility system $\mathcal{J} = \cup_{n=1,2,\cdots,N} J_n$ where $J_i = \{3i-2, 3i-1, 3i\}$, and the disruptions of J_i and $\mathcal{J}\backslash J_i$ are independent. Each J_i has a system structure as shown in Figure 3.1(a), and is subject to the scenario disruption profile in Table 3.1. For this particular system $\mathcal{J}$, the total number of scenarios is $|\mathcal{S}| = (2^3)^N = 8^N$, while the number of stations is only $|\mathcal{K}| = 6N$, which is much smaller than $|\mathcal{S}|$. As such, the formulations we will present in next chapter indicate that when $N = 4$, a scenario-based formulation would require at least $3N + 3N(3N+1)\cdot 8^N = 638988$ binary variables to describe the scenarios, while our proposed formulation will only need $3N + 3N(3N+1)(6N+1)R = 3900R + 12 \leq 93612$ binary variables, where R is a value less than or equal to $|\mathcal{K}|$.

3.4.2 Identical station failure probability

Our framework allows supporting stations to have site-dependent failure probabilities so as to reduce the supporting station structure size. This is very appealing. However, for location design models, it is sometimes convenient to have identical probabilities across stations (Snyder & Daskin, 2005). A station structure with identical probabilities can be constructed based on the following lemma.

Lemma 1. *Li et al. (2013) Given a station structure with site-dependent failure probabilities, all elements can be equivalently represented by powers of an identical constant $p > 0$, i.e.,*

$$P(K_J) = p^{I(K_J)},\ I(K_J) \in \mathbb{R}. \tag{3.13}$$

Where $I(K_J)$ is the corresponding exponent of $P(K_J)$. If we further limit the powers to be integers, these probabilities can be approximated arbitrarily accurately within error $\epsilon > 0$, i.e.,

$$P(K_J) \in \left[p^{N(K_J)} - \epsilon, p^{N(K_J)} + \epsilon\right],\ N(K_J) \in \mathbb{Z}. \tag{3.14}$$

Where $N(K_J)$ is the corresponding integer exponent of $P(K_J)$ under error ϵ.

The basic idea behind Lemma 1 is to split each original station into one or multiple new ones with identical failure probabilities. Hence, this transformation will undesirably increase the number of the necessary stations and introduce certain approximation errors.

The following example illustrates the effects of enforcing identical station failure probabilities. We consider a facility system $\mathcal{J} = \{1, 2, 3\}$, and arbitrarily generate facility disruption scenario representation as $S_{\{1\}} = 0.16, S_{\{2\}} = S_{\{3\}} = 0.12, S_{\{1,2\}} = S_{\{1,3\}} = 0.08, S_{\{2,3\}} = 0.07, S_{\{1,2,3\}} = 0.05$. After computing the station failure probabilities, we expand each station by introducing some identical stations with equal failure probabilities which are grouped together as a substitute of the orignal station. We further ensure that the difference between the approximated failure probability(multiplication of the probabilities of all grouped stations) and the accurate failure probability of each station is no larger than a pre-set approximation error. The station structure with site-dependent station failure probabilities and no approximation (corresponds to the last row), and the ones with identical failure probabilities under different approximation error tolerances are presented in Table 3.2. The values 0.1, 0.01, and 0.001 in this table are different required approximation error tolerances (i.e., ϵ in (3.14)), and the associated rows list the results of the corresponding cases.

It can be seen that as the approximation becomes more accurate, the number of necessary stations increases dramatically. Therefore, cautions shall be taken when one decides which supporting station structure to use.

3.4.3 Computational treatment

Consider a facility system $\mathcal{J}$ where all facilities are possible to be disrupted (otherwise we can simply ignore those which are always functioning). In a positively correlated disruption profile regarding this system, $\forall j \notin J \subseteq \mathcal{J}$, we shall have

Table 3.2: Comparison of station structures with site-dependent and identical failure probabilities.

	ϵ	$K_{\{1\}}$	$K_{\{2\}}$	$K_{\{3\}}$	$K_{\{1,2\}}$	$K_{\{1,3\}}$	$K_{\{2,3\}}$	$K_{\{1,2,3\}}$
Number of stations	0.1	25	25	25	3	3	5	4
	0.01	30	33	33	1	1	3	2
	0.001	653	712	712	19	19	68	51
Approx failure prob.	0.1	0.4167	0.4167	0.4167	0.9003	0.9003	0.8394	0.8693
	0.01	0.4167	0.3817	0.3817	0.9712	0.9712	0.9162	0.9433
	0.001	0.4167	0.3849	0.3849	0.9748	0.9748	0.9129	0.9339
Accurate failure prob.		0.4167	0.3846	0.3846	0.9750	0.9750	0.9135	0.9341

$$C_{j|J} = \frac{M_{\{j\}\cup J}}{M_J} \geq M_{\{j\}},\ \forall j \notin J \subseteq \mathcal{J}. \tag{3.15}$$

In such a case, $S_{\mathcal{J}} > 0$ must hold; otherwise if $S_{\mathcal{J}} = 0$, there must exist $j \notin J$ such that $M_{\{j\}} > 0, M_J > 0, M_{\{j\}\cup J} = 0$, which violates (3.15). Hence, according to the transformations from scenario reprentation to marginal and conditional representations, any element in both the marginal representation $\{M_J\}_{\forall J\subseteq\mathcal{J}}$ and the conditional representation $\{C_{j|J}\}_{\forall j\in\mathcal{J},J\subseteq\mathcal{J}\setminus\{j\}}$ must have a positive value, and it is always feasible to use (3.10)-(3.11) to construct a supporting station representation.

However, when facility disruptions are not positively correlated, or if observed data is incomplete, the probability for all facilities to simultaneously disrupt may be 0 ($S_{\mathcal{J}} = 0$), and our decomposition equations (3.10)-(3.11) for station construction would divide a positive value by 0. To avoid such a mathematical artifact, we introduce a sufficient small value $\epsilon > 0$ to replace $S_{\mathcal{J}}$ if $S_{\mathcal{J}} = 0$. In this way, the original $\frac{C}{0}$ and $\frac{0}{C}$ expressions in equations (3.10)-(3.11) become $\frac{C}{\epsilon}$ and $\frac{\epsilon}{C}$, respectively, and consequently our decomposition approach can continue to be applied. From the proof of Proposition 4, this simple treatment will preserve the equivalence of the disruption profile representations and the station structure, except that only the original probability $S_{\mathcal{J}}$ will bear a small approximation error ϵ. By setting ϵ sufficiently small, we can limit the approximation error within an acceptable tolerance.

3.5 Numerical Examples

This section illustrates application of the proposed methodological framework to three examples of disaster patterns as shown in Figure 3.2(a)-3.2(c). We also conduct sensitivity analysis to study how the station structure is dependent on various parameter settings.

3.5.1 Example 1: Earthquake

Figure 3.2(a) illustrates sixteen evenly distributed facility locations in an 8×8 square area. We assume that the epicenter of a potential earthquake hazard is at location 1, and the

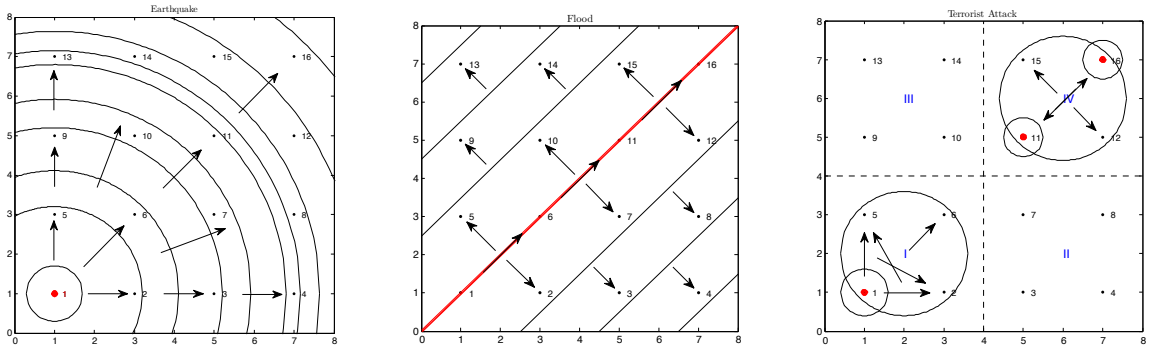

(a) Earthquake. (b) Flooding. (c) Terrorist attack.

Figure 3.2: Illustrative diagrams of different disaster patterns.

earthquake would disrupt all and only facilities within a random radius (due to a random earthquake magnitude). That is, facilities with the same distance from the epicenter are always disrupted simultaneously, and facilities closer to the source are always disrupted first. Such a correlated disruption pattern can be described by a scenario representation as listed in Table 3.3.

Table 3.3: Scenario representation of disruption profile under the earthquake hazard.

J	S_J
$\{1\}$	0.10
$\{1, 2, 5\}$	0.09
$\{1, 2, 5, 6\}$	0.08
$\{1, 2, 3, 5, 6, 9\}$	0.07
$\{1, 2, 3, 5, 6, 7, 9, 10\}$	0.06
$\{1, 2, 3, 5, 6, 7, 9, 10, 11\}$	0.05
$\{1, 2, 3, 4, 5, 6, 7, 9, 10, 11, 13\}$	0.04
$\{1, 2, 3, 4, 5, 6, 7, 8, 9, 10, 11, 13, 14\}$	0.03
$\{1, 2, 3, 4, 5, 6, 7, 8, 9, 10, 11, 12, 13, 14, 15\}$	0.02
$\{1, 2, 3, 4, 5, 6, 7, 8, 9, 10, 11, 12, 13, 14, 15, 16\}$	0.01

Marginal and conditional representations are first computed from (3.1) and (3.2), respectively, and part of the results are illustrated in Tables 3.4 and 3.5. It is observed that only positive correlation exists among the facility disruptions (and we can verify from Definition 1 that the disruption profile is positively correlated).

The supporting station structure from equation (3.11) includes 10 supporting stations, each with a site-dependent failure probability. Note that the number of stations is equal to the total number of input scenarios, indicating the compactness of the station structure. The detailed connections between the constructed stations and the facilities and the failure probabilities of each station are presented in Table 3.6. All stations have a failure probability between 0 and 1, which verifies that the disruption profile is positively correlated.

Table 3.4: Marginal disruption probabilities for some facilities under the earthquake hazard.

J	M_J	J	M_J	J	M_J	J	M_J
$\{1\}$	0.55	$\{5\}$	0.45	$\{9\}$	0.28	$\{13\}$	0.10
$\{2\}$	0.45	$\{6\}$	0.36	$\{10\}$	0.21	$\{14\}$	0.06
$\{3\}$	0.28	$\{7\}$	0.21	$\{11\}$	0.15	$\{15\}$	0.03
$\{4\}$	0.10	$\{8\}$	0.06	$\{12\}$	0.03	$\{16\}$	0.01
$\{1,2\}$	0.45	$\{1,6\}$	0.36	$\{2,6\}$	0.36	$\{1,2,3\}$	0.28
$\{1,2,6\}$	0.36	$\{2,3,6\}$	0.28	$\{2,5,6\}$	0.36	$\{1,2,5,6\}$	0.36

Table 3.5: Conditional disruption probabilities for some facilities under the earthquake hazard.

j	J	$C_{j\|J}$	j	J	$C_{j\|J}$
1	{2}	1.0000	1	{2,6}	1.0000
2	{1}	0.8182	2	{1,3}	1.0000
2	{5}	1.0000	2	{1,5}	1.0000
2	{6}	1.0000	2	{1,5,6}	1.0000
3	{2}	0.6222	3	{1,2}	0.6222
3	{6}	0.7778	3	{2,6}	0.7778
6	{1}	0.6545	6	{1,2,3}	1.0000
6	{2}	0.8000	6	{1,2,5}	0.8000

Table 3.6: Supporting stations and corresponding failure propensities under the earthquake hazard.

k	J_k	$P(\{k\})$	k	J_k	$P(\{k\})$
1	{16}	0.3333	6	{4,7,8,10,11,12,13,14,15,16}	0.7500
2	{12,15,16}	0.5000	7	{3,4,7,8,9,10,11,12,13,14,15,16}	0.7778
3	{8,12,14,15,16}	0.6000	8	{3,4,6,7,8,9,10,11,12,13,14,15,16}	0.8000
4	{4,8,12,13,14,15,16}	0.6667	9	{2,3,4,5,6,7,8,9,10,11,12,13,14,15,16}	0.8182
5	{4,8,11,12,13,14,15,16}	0.7143	10	{1,2,3,4,5,6,7,8,9,10,11,12,13,14,15,16}	0.5500

3.5.2 Example 2: Flooding

Now we consider a different type of hazard, flooding, for the same square area. Figure 3.2(b) illustrates a river passing diagonally through locations 1, 6, 11, 16, as illustrated by the red line. Flooding may start at any one of these four locations, and once it occurs, the impacted area may expand in all directions depending on the severity. The facility disruptions along the river direction could be either positively correlated (e.g., due to expansion of the flooding area), or generally correlated (e.g., due to release of flood water elsewhere), but the disruptions along the traverse direction are surely positively correlated (i.e., in a way similar to that of the earthquake example). For this example, a total of 16 input scenarios are listed in Table 3.7.

Similar to Example 1, we first transform the scenario representation into marginal and conditional representations (the tables showing these transformation results are omitted to

Table 3.7: Scenario representation of disruption profile under the flooding hazard.

J	S_J	J	S_J
$\{1\}$	0.10	$\{6, 11, 16\}$	0.06
$\{6\}$	0.10	$\{1, 6, 11, 16\}$	0.04
$\{11\}$	0.10	$\{1, 2, 5, 6\}$	0.05
$\{16\}$	0.10	$\{6, 7, 10, 11\}$	0.05
$\{1, 6\}$	0.08	$\{11, 12, 15, 16\}$	0.05
$\{6, 11\}$	0.08	$\{1, 2, 3, 5, 6, 7, 9, 10, 11\}$	0.03
$\{11, 16\}$	0.08	$\{6, 7, 8, 10, 11, 12, 14, 15, 16\}$	0.03
$\{1, 6, 11\}$	0.06	$\{1, 2, 3, 4, 5, 6, 7, 8, 9, 10, 11, 12, 13, 14, 15, 16\}$	0.01

save space). Then the supporting station structure is constructed from (3.11). Again, the station structure is compact with only 16 effective supporting stations (i.e., identical to the number of input scenarios). However, equations (3.11) now may yield greater-than-one $P(K_J)$ values, and thus now a $P(K_J)$ has to be interpreted as a propensity. The station-facility connections and the station propensities are presented in Table 3.8. The first subset of stations (#1 - 8) have disruption propensities less than 1 (i.e., providing positive support), while the other stations (#9 - 16) have disruption propensities larger than 1 (i.e., providing negative support). It can be also seen from the disruption profile representations that this disruption profile is generally correlated. For instance, the results of conditional and marginal representations show that $C_{6|\{11,16\}} = 0.5185 < M_{\{6\}} = 0.59$, which implies that disruption of facility 6 is generally correlated with disruptions of facilities 11 and 16. Meanwhile, $C_{1|\{6\}} = 0.4576 > M_{\{1\}} = 0.37$ shows that disruption of facility 1 is positively correlated with disruption of facility 6.

3.5.3 Example 3: Terrorist attack

This example uses a conditional profile representation to describe the risk of terrorist attacks in the same 8×8 square area. The terrorists have limited capacity and they can only threat regions I and IV as shown in Figure 3.2(c). We assume that their threats to these two regions are independent. In region I, only after facility 1 is attacked (i.e., disrupted) could facilities 2 and 5 be possibly attacked. Only after facilities 1, 2 and 5 are all attacked could facility 6 be possibly attacked. In region IV, facilities 11 and 16 must both have been disrupted before possible attacks may occur to facilities 12 and 15. The detailed conditional representation is listed in Table 3.9.

We first compute marginal and scenario representations by (3.4) and (3.3), then use (3.10) to calculate the failure propensities of 11 effective supporting stations. The results of stations are summarized in Table 3.10. We see that all propensities are less than 1 except for station #11. Therefore, the disruption profile contains both positive (e.g., in region I) and general (e.g., in region IV) correlations. Since the possible attacks in the two regions are independent, we only have stations connecting facilities within each subregion.

Table 3.8: Supporting stations and corresponding failure propensities under the flooding hazard.

k	J_k	$P(\{k\})$
1	{1,2,3,4,5,9,13}	0.2500
2	{4,8,12,13,14,15,16}	0.2500
3	{1,2,3,4,5,6,7,8,9,10,13,14}	0.4444
4	{2,3,4,5,7,8,9,10,12,13,14,15}	0.2000
5	{3,4,7,8,9,10,11,12,13,14,15,16}	0.4444
6	{1,2,3,4,5,7,8,9,10,12,13,14,15,16}	0.8167
7	{1,2,3,4,5,6,7,8,9,10,11,12,13,14,15}	0.7297
8	{2,3,4,5,6,7,8,9,10,11,12,13,14,15,16}	0.7297
9	{1,2,3,4,5,8,9,12,13,14,15,16}	1.3333
10	{1,2,3,4,5,7,8,9,10,12,13,14,15}	1.4286
11	{2,3,4,5,7,8,9,10,12,13,14,15,16}	1.4286
12	{1,2,3,4,5,6,7,8,9,10,12,13,14,15}	1.1667
13	{2,3,4,5,7,8,9,10,11,12,13,14,15,16}	1.1667
14	{1,2,3,4,5,6,7,8,9,10,12,13,14,15,16}	1.1768
15	{1,2,3,4,5,7,8,9,10,11,12,13,14,15,16}	1.1768
16	{1,2,3,4,5,6,7,8,9,10,11,12,13,14,15,16}	1.8158

Table 3.9: Conditional representation of disruption profile under terrorist attacks.

j	J	$C_{j\|J}$	J	$C_{j\|J}$	J	$C_{j\|J}$	J	$C_{j\|J}$
1	∅	9/10						
2	∅	0	{1}	2/5	{5}	1/2	{1,5}	1/2
5	∅	0	{1}	2/5	{2}	1/2	{1,2}	1/2
6	∅	0	{1}	1/15	{2}	1/6	{5}	1/6
	{1,2}	1/6	{1,5}	1/6	{2,5}	1/3	{1,2,5}	1/4
11	∅	3/5	{16}	3/5				
12	∅	0	{11}	1/4	{15}	1/3	{16}	1/4
	{11,15}	1/3	{15,16}	1/3	{11,16}	3/8	{11,15,16}	1/3
15	∅	0	{11}	1/4	{12}	1/3	{16}	1/4
	{11,12}	1/3	{12,16}	1/3	{11,16}	3/8	{11,12,16}	1/3
16	∅	3/5	{11}	3/5				

Table 3.10: Supporting stations and corresponding failure propensities under terrorist attacks.

k	J_k	$P(\{k\})$	k	J_k	$P(\{k\})$
1	{6}	0.3333	6	{12}	0.3333
2	{5,6}	0.5000	7	{15}	0.3333
3	{2,6}	0.5000	8	{11,12,15}	0.6667
4	{2,5,6}	0.8000	9	{12,15,16}	0.6667
5	{1,2,5,6}	0.9000	10	{11,12,15,16}	0.9000
11	{12,15}	1.1250			

Chapter 4

RFL with Facility Correlations: Facility Location Planning under Correlated Facility Disruptions

4.1 Introduction

The previous chapter develops a recipe for transforming any (positive, negative, or mixed) facility disruption correlations into an augmented network (with additional supporting stations). It was proven that with such a station structure, a system of interdependent facilities with generally correlated disruptions can be equivalently represented by one with independent stations that fail with site-dependent probabilities. How to optimally design the reliable locations of service facilities under site-dependent failures and negative/mixed correlations, however, remains an open nontrivial question. Therefore, a more complete systematic methodology framework is needed to design reliable facility locations under site-dependent correlated facility disruptions.

In this chapter, we extend the framework in the previous chapter to capture any pattern of facility disruption correlations (positive, negative, or mixed) by adding an additional layer of independent supporting stations with site-dependent failure probabilities. These stations, with proper connections to the facilities, can either represent actual support infrastructures, or virtually capture the effect of shared hazards. With these newly added stations, we are able to develop a compact mixed-integer mathematical model to optimize the facility location and customer assignment decisions in order to strike a balance between system reliability and cost efficiency. To hedge against the complexity associated with the optimization model, customized algorithms based on Lagrangian relaxation and approximation subroutines are developed. Multiple numerical case studies with various types of correlated facility disruptions are carried out to demonstrate the performance and applicability of our model and algorithms. Managerial insights are also drawn from the numerical results.

4.2 Model Formulation

In many real world infrastructure systems, facilities are correlated due to various types of connections and interactions among built facilities. Such correlations could be caused by either: (i) support failure; or (ii) shared hazards. In this section, we develop optimization models to address correlations from both the two types.

4.2.1 Support Failure

Facility disruptions do not always occur directly at the facilities themselves. The service functionality of a facility may also be effectively "disrupted" – even when facilities themselves are not damaged – if its external support infrastructures (e.g., power supply, transportation access) are lost. Often the external support infrastructures are shared, and hence will possibly affect, the functionality of multiple facilities, and hence the "failure" of these facilities will display complex correlation patterns. For example, in a ground transportation network consisting of intersecting highway and railway corridors, the highway paths between customers (e.g., residential neighborhoods) and facilities (e.g., fire stations) may cross by railways tracks. If railroad incidents happen and cause railroad blockage by stopped trains, the paths between customers and multiple facilities may be cut off as well. These customers are no longer able to receive service (e.g., emergency response) from their preferable facilities in time (e.g., imagine the firetrucks are blocked at railroad crossings), which could lead to catastrophic losses. Recent years have witnessed a series of rail crashes and derailments that have led to major oil spills, tanker fire or explosions Crummy (2013); NBC News (2013). The train carriages are forced to stop on the rail track, possibly blocking crossings for entrance to and exit from the affected region. Similar incidents could happen in many other contexts; e.g., in coastal areas or cities where rivers or lakes exist and partition the area into sub-regions. Bridges, as the only access points to enter/leave the sub-regions, link the partitioned subregions into an interconnected network. One distinct example would be the city of Venice, Italy. If a key bridge is blocked or disrupted due to external factors (e.g., structure or material damages, traffic accidents, congestions, etc.), multiple facilities in the region may become unreachable at the same time. In this chapter, we generally call these types of disruption correlations to be caused by "support failure".

We denote $\mathcal{I}$ as the set of customers, and each customer $i \in \mathcal{I}$ has a demand μ_i. Normally, each customer i seeks service by visiting its most preferred facility j that is supported by station k (defined as a station-facility pair (k, j) in the rest of the paper). In consideration of possible station-facility pair failures, each customer is also assigned to a set of another $R-1$ backup station-facility pairs as part of the service plan. We assume that the station-facility status is available to all customers after the realization of disruption(s), and hence each customer directly visits the assigned functioning station-facility pair that has the smallest backup level. For example, if the first and second backup choices are both disrupted, a customer will go directly to its third backup station-facility pair. The transportation cost for station-facility pair (k, j) to satisfy one unit of demand from customer i is denoted by d_{ikj}. In case correlations are caused by shared hazards, the stations do not physically exist, and d_{ikj}, for all k, is set to equal $\min\{d_{ij}, \forall j \in J_k^*\}$, where J_k^* is the set of built facilities that are connected to station k. For all $i \in \mathcal{I}, j_1, j_2 \in \mathcal{J}, k_1, k_2 \in \mathcal{K}$, let $c_{ik_1j_1k_2j_2} = 1$ if

$d_{ik_1j_1} \leq d_{ik_2j_2}$; or 0 otherwise. Moreover, a penalty cost π_i per unit demand will be imposed if customer i does not receive any service. This situation occurs if no facility is reachable, or if the cost of serving customer i by the nearest available station-facility pair already exceeds π_i.

While a customer may be assigned to multiple station-facility pairs (each at a distinct backup level), the following proposition states that a station will appear at no more than one of the backup levels of this customer.

Proposition 1. *A customer is assigned to a station at no more than one backup level.*

As such, each backup level corresponds to exactly one station, and a customer will visit its level-r station if all its level-1, $\cdots$, level-$(r-1)$ stations have been disrupted (the operating station is exactly the rth backup option). We assume that each customer can be assigned to at most a number R of stations. We further add a dummy *emergency* station with index $k = 0$ and a dummy *emergency* facility with index $j = 0$ to allow the "penalty assignment", i.e., when a customer loses service. Note that $l_{00} = 1$ and $q_0 = 0$, and we set the corresponding transportation cost to be the penalty cost, i.e., $d_{ikj}|_{k=0,j=0} = \pi_i, \forall i \in \mathcal{I}$. Typically, a customer shall be assigned to station-facility pair $(0, 0)$ at level $R+1$ as long as regular stations are available for backup levels $1, 2, \cdots, R$. However, if at some backup level $s \in \{1, 2, \cdots, R\}$, customer i cannot receive service from any station-facility pair (k, j) at a cost less than π_i (per unit demand), it will choose to pay the penalty cost π_i, i.e., visit the emergency station-facility pair at level s.

There are several sets of decision variables. First, variables $\mathbf{X} := \{X_j\}_{j\in\mathcal{J}}$ determine the facility locations as follows,

$$X_j = \begin{cases} 1 & \text{if a facility is build at } j; \\ 0 & \text{otherwise.} \end{cases}$$

Next, we use $\mathbf{Y} := \{Y_{ikjr}\}_{i\in\mathcal{I},k\in\mathcal{K}\cup\{0\},j\in\mathcal{J}\cup\{0\},r\in\{1,2,\cdots,R+1\}}$ to specify the assignment of customers to station-facility pairs at multiple backup levels

$$Y_{ikjr} = \begin{cases} 1 & \text{if customer } i \text{ is assigned to station-facility pair } (k, j) \text{ at level } r; \\ 0 & \text{otherwise.} \end{cases}$$

Finally, we define $\mathbf{Z} := \{Z_{ikjr}\}_{i\in\mathcal{I},k\in\mathcal{K}\cup\{0\},j\in\mathcal{J}\cup\{0\},r\in\{1,2,\cdots,R+1\}}$ where $Z_{ikjr} \in \mathbb{R}$ denotes the probability of customer i being assigned to station-facility pair (k, j) at level r. This could happen only when station k is not disrupted, station k and facility j are connected, and all the stations assigned to customer i at levels $1, 2, \cdots, r-1$ are unavailable. Therefore, the value of Z_{ikjr} depends on the assignments of customer i to station-facility pairs at levels $1, 2, \cdots, r-1$ (i.e., $\{Y_{ikjs}\}_{\forall(k,j),s=1,2,\cdots,r-1}$) and their corresponding probabilities (i.e., $\{Z_{ikjs}\}_{\forall(k,j),s=1,2,\cdots,r-1}$).

With all these decision variables and modeling considerations, the reliable facility-location problem with correlation of "support failure" type (RFL-SF) is formulated as the following

mixed-integer programming model:

$$\text{(RFL-SF)} \quad \min \quad \sum_{j\in\mathcal{J}} f_j X_j + \sum_{i\in\mathcal{I}} \sum_{k\in\mathcal{K}\cup\{0\}} \sum_{j\in\mathcal{J}\cup\{0\}} \sum_{r=1}^{R+1} \mu_i d_{ikj} Z_{ikjr} Y_{ikjr} \tag{4.1a}$$

$$\text{s.t.} \quad \sum_{r=1}^{R} Y_{ikjr} \le X_j, \quad \forall i \in \mathcal{I}, j \in \mathcal{J}, k \in \mathcal{K}, \tag{4.1b}$$

$$Y_{ikjr} \le l_{kj}, \quad \forall i \in \mathcal{I}, j \in \mathcal{J}\cup\{0\}, k \in \mathcal{K}\cup\{0\}, r = 1, 2, \cdots, R+1, \tag{4.1c}$$

$$\sum_{j\in\mathcal{J}} \sum_{r=1}^{R} Y_{ikjr} \le 1, \quad \forall i \in \mathcal{I}, k \in \mathcal{K}, \tag{4.1d}$$

$$\sum_{r=1}^{R+1} Y_{i00r} = 1, \quad \forall i \in \mathcal{I}, \tag{4.1e}$$

$$\sum_{k\in\mathcal{K}} \sum_{j\in\mathcal{J}} Y_{ikjr} + \sum_{s=1}^{r} Y_{i00s} = 1, \quad \forall i \in \mathcal{I}, r = 1, 2, \cdots, R+1, \tag{4.1f}$$

$$Z_{ikj1} = l_{kj}\,(1 - q_k)\,, \quad \forall i \in \mathcal{I}, j \in \mathcal{J}\cup\{0\}, k \in \mathcal{K}\cup\{0\}, \tag{4.1g}$$

$$Z_{ikjr} = l_{kj}\,(1 - q_k) \cdot \sum_{k'\in\mathcal{K}} \sum_{j'\in J} \frac{q_{k'}}{1 - q_{k'}} Z_{ik'j'(r-1)} Y_{ik'j'(r-1)}, \quad \forall i \in \mathcal{I}, j \in \mathcal{J}\cup\{0\}, k \in \mathcal{K}\cup\{0\}, r = 2, 3, \cdots, R+1, \tag{4.1h}$$

$$X_j, Y_{ikjr} \in \{0, 1\}, \quad \forall i \in \mathcal{I}, j \in \mathcal{J}\cup\{0\}, k \in \mathcal{K}\cup\{0\}, r = 1, 2, \cdots, R+1. \tag{4.1i}$$

The objective function (4.1a) presents the expected system cost including the fixed facility cost, the expected total transportation cost, and the expected penalty cost (associated with the dummy station-facility pair). Constraints (4.1b) and (4.1c) enforce that customers can only be assigned to open facilities in connected station-facility pairs. Constraints (4.1d) make sure that each customer's assignment will not involve any station at more than one backup level, as that stated in Proposition 1. Constraints (4.1e) postulate that each customer is assigned to the dummy emergency station-facility pair at a certain backup level, while constraints (4.1f) require that at each level r, a customer $i \in I$ is either assigned to a station-facility pair, or assigned to the dummy station-facility pair at an earlier level $s \le r$. Constraints (4.1g)–(4.1h) recursively define the assignment probabilities Z_{ikjr}: at level $r = 1$, the probability Z_{ikjr} is simply the probability for station k to function; at level $r > 1$, the value of Z_{ikjr} equals $(1 - q_k)q_{k'}/(1 - q_{k'})Z_{ik'j'r-1}$ if that customer i is assigned to $(k^{'}, j^{'})$ at level $r - 1$. Since propensity q_k can take a value large than 1, Z_{ikjr} can take any real value in $[\overline{M}_k, \widehat{M}_k]$, where

$$\overline{M}_k = \min_{\forall L\subseteq\mathcal{K}\setminus\{k\}} \left[(1 - q_k)\prod_{l\in L} q_l\right], \quad \widehat{M}_k = \max_{\forall L\subseteq\mathcal{K}\setminus\{k\}} \left[(1 - q_k)\prod_{l\in L} q_l\right], \quad \forall k \in \mathcal{K}.$$

Constraints (4.1i) are integrality constraints.

4.2.2 Shared Hazards

Facility disruptions could also be correlated when facilities are exposed to shared hazards or mutual interactions. Such correlations could be positive or negative, or mixed. For example, adjacent facilities in a local geographical region are prone to simultaneous damage by a natural disaster (e.g., earthquake, hurricane, flooding). If one facility is known to have been disrupted by an earthquake, its neighboring facilities will bear a higher likelihood of being disrupted as well – this shows a positive correlation. The correlation can also be negative: suppose multiple facilities along a river are all threatened by flooding. If one facility is known to have been disrupted by flooding, then its downstream peers become less likely to be disrupted due to the release of water pressure. Similar negative correlations may also exist when facilities compete for scarce resources. For simplicity, in the rest of this chapter, we generally call these types of disruption correlations to be caused by "shared hazards".

The reliable facility-location problem with correlations of "shared hazards" type (RFL-SH) is formulated as the following mixed-integer programming model:

$$\text{(RFL-SH)} \quad \min \quad \sum_{j\in\mathcal{J}} f_j X_j + \sum_{i\in\mathcal{I}} \sum_{k\in\mathcal{K}\cup\{0\}} \sum_{j\in\mathcal{J}\cup\{0\}} \sum_{r=1}^{R+1} \mu_i d_{ikj} Z_{ikjr} Y_{ikjr} \tag{4.2a}$$

$$\text{s.t.} \quad \sum_{r=1}^{R} Y_{ikjr} \le X_j, \quad \forall i \in \mathcal{I}, j \in \mathcal{J}, k \in \mathcal{K}, \tag{4.2b}$$

$$Y_{ikjr} \le l_{kj}, \quad \forall i \in \mathcal{I}, j \in \mathcal{J}\cup\{0\}, k \in \mathcal{K}\cup\{0\}, r = 1, 2, \cdots, R+1, \tag{4.2c}$$

$$\sum_{j\in\mathcal{J}} \sum_{r=1}^{R} Y_{ikjr} \le 1, \quad \forall i \in \mathcal{I}, k \in \mathcal{K}, \tag{4.2d}$$

$$\sum_{r=1}^{R+1} Y_{i00r} = 1, \quad \forall i \in \mathcal{I}, \tag{4.2e}$$

$$\sum_{k\in\mathcal{K}} \sum_{j\in\mathcal{J}} Y_{ikjr} + \sum_{s=1}^{r} Y_{i00s} = 1, \quad \forall i \in \mathcal{I}, r = 1, 2, \cdots, R+1, \tag{4.2f}$$

$$Y_{ikj_1r} \le Y_{ikj_2r} + c_{ikj_1kj_2} + 2 - X_{j_1} - X_{j_2}, \quad \forall i \in \mathcal{I}, j_1, j_2 \in \mathcal{J}, k \in \mathcal{K}, 1 \le r \le R, \tag{4.2g}$$

$$Y_{ik_1j_1r} + Y_{ik_2j_2,r+1} \le 1 + c_{ik_1j_1k_2j_2}, \quad \forall i \in \mathcal{I}, j_1, j_2 \in \mathcal{J}, k_1, k_2 \in \mathcal{K}, 1 \le r \le R-1, \tag{4.2h}$$

$$Z_{ikj1} = l_{kj}\,(1 - q_k), \quad \forall i \in \mathcal{I}, j \in \mathcal{J}\cup\{0\}, k \in \mathcal{K}\cup\{0\}, \tag{4.2i}$$

$$Z_{ikjr} = l_{kj}\,(1 - q_k) \cdot \sum_{k'\in\mathcal{K}} \sum_{j'\in J} \frac{q_{k'}}{1 - q_{k'}} Z_{ik'j'(r-1)} Y_{ik'j'(r-1)}, \quad \forall i \in \mathcal{I}, j \in \mathcal{J}\cup\{0\}, k \in \mathcal{K}\cup\{0\}, r = 2, 3, \cdots, R+1, \tag{4.2j}$$

$$X_j, Y_{ikjr} \in \{0, 1\}, \quad \forall i \in \mathcal{I}, j \in \mathcal{J}\cup\{0\}, k \in \mathcal{K}\cup\{0\}, r = 1, 2, \cdots, R+1. \tag{4.2k}$$

Two more constraints are added to address the difficulty associated with handling correlations of "shared hazards" type. Constraints (4.2g) make sure that a customer i is never assigned to the station-facility pair (k_2, j_2) when facilities j_1 and j_2 are both connected to station k and j_2 is farther than j_1. Constraints (4.2h) enforce that a customer is always assigned to the closest functioning station-facility pair for service; i.e., for any $1 \leq r < R-1$ and two arbitrary station-facility pairs $(k_1, j_1), (k_2, j_2)$ with $d_{ik_1j_1} \leq d_{ik_2j_2}$, a customer i cannot be assigned to (j_2, k_2) at levels r and (j_1, k_1) at level $r+1$.

We then show that the above formulation (RFL-SH) correctly captures disruption correlations caused by shared hazards. Proposition 2 proves the equivalence between our formulation (RFL-SH) (with station-based disruption representation) and the problem described by scenario-based disruptions.

Proposition 2. *When correlations are caused by shared hazards, for sufficiently large R, formulation (RFL-SH) with virtual supporting stations yields the exact optimal objective value and optimal solutions $\mathbf{X}, \mathbf{Y}$ as the scenario-based formulation.*

Next, we show in Proposition 3 that formulation (RFL-SH) also correctly handles disruption correlations caused by support failure, i.e., (4.2g) and (4.2h) in (RFL-SH) are redundant when the supporting stations are real/physical. Building upon Proposition 2, we only need to prove that the optimal solution to (RFL-SF) always satisfies these two constraints (4.2g) and (4.2h).

Proposition 3. *When correlations are caused by support failure, formulation (RFL-SH) based on physical supporting stations yields the true optimal objective value and optimal solutions $\mathbf{X}, \mathbf{Y}$, i.e., the optimal solution to (RFL-SF) and (RFL-SH) are identical.*

Proposition 3 and 2 together imply that formulation (RFL-SH) can be used to address correlations from both the "support failure" and "shared hazards" types. (RFL-SH) is nonlinear because the objectives and probability constraints (4.2j) contain nonlinear terms such as $Z_{ikjr}Y_{ikjr}$. However, since each $Z_{ikjr}Y_{ikjr}$ is a product of a bounded continuous variable and a binary variable, we can linearize it by applying a variant of the technique introduced by Sherali & Alameddine (1992), i.e., we replace each $Z_{ikjr}Y_{ikjr}$ by a new continuous variable W_{ikjr} and enforce their equivalence by adding the following four sets of constraints.

$$W_{ikjr} \leq Z_{ikjr} + \overline{M}_k(Y_{ikjr} - 1), \tag{4.3a}$$

$$W_{ikjr} \geq Z_{ikjr} + \widehat{M}_k(Y_{ikjr} - 1), \tag{4.3b}$$

$$W_{ikjr} \leq \widehat{M}_k Y_{ikjr}, \tag{4.3c}$$

$$W_{ikjr} \geq \overline{M}_k Y_{ikjr}. \tag{4.3d}$$

The model formulation (RFL-SH) is now transformed into the following linearized version

(LRFL):

$$\text{(LRFL)} \quad \min \quad \sum_{j\in\mathcal{J}} f_j X_j + \sum_{i\in\mathcal{I}} \sum_{k\in\mathcal{K}\cup\{0\}} \sum_{j\in\mathcal{J}\cup\{0\}} \sum_{r=1}^{R+1} \mu_i d_{ijk} W_{ikjr} \tag{4.4a}$$

$$\text{s.t.} \quad \text{(4.2b)} - \text{(4.2i)}, \tag{4.4b}$$

$$Z_{ikjr} = (1-q_k) \sum_{k'\in\mathcal{K}} \sum_{j'\in\mathcal{J}} \frac{q_{k'}}{1-q_{k'}} W_{ik'j'(r-1)}, \quad \forall i \in \mathcal{I}, j \in \mathcal{J}\cup\{0\}, k \in \mathcal{K}\cup\{0\}, r = 2,3,\cdots,R+1, \tag{4.4c}$$

$$\text{(4.3a)} - \text{(4.3d)}, \quad \forall i \in \mathcal{I}, j \in \mathcal{J}\cup\{0\}, k \in \mathcal{K}\cup\{0\}, r = 1,2,\cdots,R+1, \tag{4.4d}$$

$$X_j, Y_{ikjr} \in \{0,1\}, \quad \forall i \in \mathcal{I}, j \in \mathcal{J}\cup\{0\}, k \in \mathcal{K}\cup\{0\}, r = 1,2,\cdots,R+1. \tag{4.4e}$$

The mixed-integer linear program (LRFL) could in theory be solved by commercial solvers such as CPLEX and Gurobi. However, the existence of station-facility pairs as well as site-dependent probabilities exacerbates the model complexity; as we will show with numerical examples in Section 4.4, existing solvers generally incur extremely long computation time for practical instances. In light of this, we develop customized solution approaches in the next section.

4.3 Solution Approach

4.3.1 Lagrangian Relaxation

We choose to relax constraints (4.2b) in (LRFL) with Lagrangian multipliers $\{\lambda_{ikj}\}_{\forall i\in I,\forall k\in K,\forall j\in J}$ and move them as penalty terms to the objective function. The objective function becomes

$$\min \sum_{j\in\mathcal{J}} \left(f_j - \sum_{i\in\mathcal{I}} \sum_{k\in\mathcal{K}} \lambda_{ikj} \right) X_j + \sum_{i\in\mathcal{I}} \sum_{k\in\mathcal{K}\cup\{0\}} \sum_{j\in\mathcal{J}\cup\{0\}} \sum_{r=1}^{R+1} \mu_i d_{ikj} W_{ikjr} + \sum_{i\in\mathcal{I}} \sum_{k\in\mathcal{K}} \sum_{j\in\mathcal{J}} \lambda_{ikj} \sum_{r=1}^{R} Y_{ikjr}.$$

One could potentially further relax constraints (4.2g) and move them as penalty terms to the objective. However, as stated in the proof of Proposition 3, (i) when the correlations are caused by support failure, constraints (4.2g) can be omitted from (RFL), and (ii) when the correlations are caused by shared hazards, removing constraints (4.2g) never increases the objective value. Therefore, we suggest simply removing constraints (4.2g) from the relaxed problem; this treatment turns out to be very helpful. We will demonstrate this in Section 4.4.

The above relaxation of two sets of constraints (4.2b) and (4.2g) essentially decouples the location and assignment variables $\mathbf{X}$ and $\mathbf{Y}$. The remaining model can be decomposed into multiple disjoint parts. The part involving $\mathbf{X}$,

$$\min_{X_j\in\{0,1\},\forall j} \sum_{j\in\mathcal{J}} \left(f_j - \sum_{i\in\mathcal{I}} \sum_{k\in\mathcal{K}} \lambda_{ikj} \right) X_j,$$

can be solved by simple inspection; i.e., given any $\{\lambda_{ikj}\}$, we can easily find the optimal $\mathbf{X}$ as follows:

$$X_j = \begin{cases} 1 & \text{if } f_j - \sum_{i\in\mathcal{I}} \sum_{k\in\mathcal{K}} \lambda_{ikj} < 0, \\ 0 & \text{otherwise.} \end{cases}$$

We further notice that the remaining problem can be further separated into individual subproblems, one for each customer. The subproblem (RSFL_i) with respect to customer i is

$$\begin{aligned}
(\text{RSFL}_i) \quad \min \quad & \sum_{k\in\mathcal{K}\cup\{0\}} \sum_{j\in\mathcal{J}\cup\{0\}} \sum_{r=1}^{R+1} \mu_i d_{ikj} W_{kjr} + \sum_{k\in\mathcal{K}} \sum_{j\in\mathcal{J}} \lambda_{kj} \sum_{r=1}^{R} Y_{kjr} && \text{(4.5a)} \\
\text{s.t.} \quad & Y_{kjr} \le l_{kj}, \quad \forall j \in \mathcal{J}\cup\{0\}, k \in \mathcal{K}\cup\{0\}, r = 1, 2, \cdots, R+1, && \text{(4.5b)} \\
& \sum_{j\in\mathcal{J}} \sum_{r=1}^{R} Y_{kjr} \le 1, \quad \forall k \in \mathcal{K}, && \text{(4.5c)} \\
& \sum_{r=1}^{R+1} Y_{00r} = 1, && \text{(4.5d)} \\
& \sum_{k\in\mathcal{K}} \sum_{j\in\mathcal{J}} Y_{kjr} + \sum_{s=1}^{r} Y_{00s} = 1, \quad \forall r = 1, 2, \cdots, R+1, && \text{(4.5e)} \\
& Y_{k_1 j_1 r} + Y_{k_2 j_2, r+1} \le 1 + c_{ik_1 j_1 k_2 j_2}, \quad \forall j_1, j_2 \in \mathcal{J}, k_1, k_2 \in \mathcal{K}, 1 \le r \le R-1, && \text{(4.5f)} \\
& Z_{kj1} = 1 - q_k, \quad \forall j \in \mathcal{J}, k \in \mathcal{K}, && \text{(4.5g)} \\
& Z_{kjr} = (1 - q_k) \sum_{k'\in\mathcal{K}} \sum_{j'\in\mathcal{J}} \frac{q_{k'}}{1 - q_{k'}} W_{j'k'(r-1)}, \\
& \qquad \forall j \in \mathcal{J}, k \in \mathcal{K}, r = 2, 3, \cdots, R+1, && \text{(4.5h)} \\
& \text{(4.3a)} - \text{(4.3d)}, && \text{(4.5i)} \\
& Y_{kjr} \in \{0, 1\}, \quad \forall j \in \mathcal{J}, k \in \mathcal{K}, r = 1, 2, \cdots, R+1. && \text{(4.5j)}
\end{aligned}$$

Note that (RSFL_i), although still a mixed-integer linear program, is much smaller in size than the original (LRFL), and hence it can often be effectively handled by commercial solvers like CPLEX. However, solving this subproblem repeatedly (for each customer, and across Lagrangian relaxation iterations) could pose as a computational burden. Thus, Section 4.3.2 further proposes an optional customized algorithm.

It is well-known that the optimal objective values from the above relaxed subproblems provide a lower bound to the original problem. However, the decision variables may not satisfy the relaxed constraints. Nevertheless, we use simple heuristics to perturb the subproblem solutions in order to obtain a feasible solution to the original problem (and an upper bound). In so doing, we fix the optimal facility location decisions from the relaxed problem. For each customer i, we sort all built and connected station-facility pairs (i.e., (k, j) is considered if $X_j = 1, l_{kj} = 1$) in ascending order of d_{ikj}. If there exist $d_{ik_1j_1}$ and $d_{ik_2j_2}$ such that $d_{ik_1j_1} = d_{ik_2j_2}$, we break the tie based on index k, i.e., $d_{ik_1j_1}$ comes before

$d_{ik_2j_2}$ if $k_1 < k_2$. Then at every level r, we assign customer i to pair (k, j) with the smallest d_{ikj} as long as i has never been assigned to k in levels $1, 2, \cdots, r-1$ before. The following proposition, although proven only when $q_k \in [0, 1], \forall k$, indicates that the feasible solution from this simple approach is likely to have a good quality.

Proposition 4. *If $R \geq |\mathcal{K}|$ and $q_k \in [0, 1], \forall k$, then in any optimal solution $(\mathbf{X}, \mathbf{Y}, \mathbf{Z})$, a customer will be assigned to backup station-facility pairs based on the distances; i.e., if $Y_{ik_1j_1r} = 1$ and $Y_{ik_2j_2,r+1} = 1$ for some i, r, then $d_{ik_1j_1} \leq d_{ik_2j_2}$.*

Hence, when $|\mathcal{K}| \leq R$ and $q_k \in [0, 1], \forall k$, given the facility locations, this heuristic yields an optimal customer assignment and a tight upper bound. In case $|\mathcal{K}| > R$ or $\exists k$ such that $q_k > 1$, it can only guarantee a feasible but not necessarily optimal solution. Nevertheless, since the probabilities for large back-up levels to occur (i.e., the product of multiple station disruption propensities) are often smaller by orders of magnitudes, the solution given by this sorting/greedy heuristic shall be quite close to the optimal solution.

In the remainder of the Lagrangian solution framework, we use standard subgradient techniques Fisher (1981) to update the multipliers λ; i.e.,

$$\lambda_{ikj}^{n+1} = \lambda_{ikj}^{n} + t_j^n \left(\sum_r Y_{ikjr}^n - X_j^n \right), \tag{4.6}$$

$$t_j^n = \frac{\xi^n \left(Z^* - Z_D(\lambda^n) \right)}{\| \sum_r Y_{ikjr}^n - X_j^n \|^2}, \tag{4.7}$$

where λ_{ikj}^n represents a generic multiplier in the nth iteration, t^n is the step size, ξ^n is a scalar, and Z^* and $Z_D(\lambda^n)$ are the best upper bound and the current lower bound, respectively.

The above bounds, especially the lower bound, may be far from optimum (e.g., due to duality gaps from the relaxed constraints). If the Lagrangian relaxation algorithm fails to find a solution with small enough gap in a certain number of iterations, we embed it into a branch-and-bound (B&B) framework to further reduce the gap. We construct a binary tree by branching on $\mathbf{X}$. Specifically, among all unbranched variables, we select and branch on the one whose construction yields the least system cost. After building the branching tree, we run the Lagrangian relaxation algorithm at each node to determine the corresponding feasible solution and lower bound, and update them after finishing both child branches. While traversing the binary tree, depth-first search is found to perform slightly better than breadth-first or least-cost-first searches for small or moderate-sized instances (which are likely to be solved to optimality). However, if the instances are large, it is difficult to traverse the entire tree and completely close the gap. In such cases, least-cost-first search is preferable since it tends to yield a reasonably good lower bound before completely traversing the entire tree.

4.3.2 Approximate Solution to Subproblems

As mentioned before, although the relaxed problem is separable by customer i, each subproblem is still combinatorial and the worst-case complexity is exponential. Furthermore, considering the large number of nodes we need to explore during the branch-and-bound

process, even if we solve each subproblem (e.g., using commercial solvers) relatively quickly (e.g., 1-10s), it may take an excessively long time to complete the entire algorithm and find a good near-optimal solution. Therefore, in this section we develop an approximate algorithm which helps quickly find lower bounds to the relaxed subproblems.

Equations (4.5h) show that Z_{kjr} depends on $Z_{kj(r-1)}$ and $Y_{kj(r-1)}$, which builds connections across the decision variables and brings difficulty in solving subproblem (RSFL$_i$). Instead of having Z_{kjr} directly in the formulation, we approximate them with fixed numbers. Let $k_1, k_2, \cdots, k_{|\mathcal{K}|+1}$ be an ordering of the stations such that $q_{k_1} \leq q_{k_2} \leq \cdots \leq q_{k_{|\mathcal{K}|+1}}$. We define two additional sets of numbers $\{\alpha_{kr}\}_{\forall r \in \{1,2,\cdots,R+1\}}, \{\beta_r\}_{\forall r \in \{1,2,\cdots,R+1\}}$, such that

$$\alpha_{kr} = (1-q_k)\left(\prod_{l=1}^{r-1} q_{k_l}\right)^{1_{[q_k \leq 1]}} \left(\prod_{l=1}^{r-1} q_{k_{|\mathcal{K}|+1-l}}\right)^{1_{[q_k > 1]}}, \quad \beta_r = \prod_{l=1}^{r-1} q_{k_l}. \tag{4.8}$$

where $1_{[\cdot]} = 1$ when condition $[\cdot]$ holds, or 0 otherwise. When $q_k < 1$, α_{kr} is essentially based on the product of the $r-1$ smallest station failure probabilities; when $q_k > 1$, it is based on the product of the $r-1$ largest station failure probabilities.

We next replace Z_{kjr} and Z_{00r} respectively by their estimates, α_{kr} and β_r, and relax constraints (4.5f). The relaxed subproblem (RRSFL$_i$) of (RSFL$_i$) becomes

$$\text{(RRSFL}_i\text{)} \quad \min \quad \sum_{k\in\mathcal{K}}\sum_{j\in\mathcal{J}}\sum_{r=1}^{R+1} \left(\mu_i d_{ikj}\alpha_{kr} + \lambda_{kjr}\right) Y_{kjr} + \sum_{r=1}^{R+1} \mu_i d_{i00}\beta_r Y_{00r} \tag{4.9a}$$

$$\text{s.t.} \quad Y_{kjr} \leq l_{kj}, \quad \forall j \in \mathcal{J}\cup\{0\}, k \in \mathcal{K}\cup\{0\}, r = 1,2,\cdots,R+1, \tag{4.9b}$$

$$\sum_{j\in\mathcal{J}}\sum_{r=1}^{R} Y_{kjr} \leq 1, \quad \forall k \in \mathcal{K}, \tag{4.9c}$$

$$\sum_{r=1}^{R+1} Y_{00r} = 1, \tag{4.9d}$$

$$\sum_{k\in\mathcal{K}}\sum_{j\in\mathcal{J}} Y_{kjr} + \sum_{s=1}^{r} Y_{00s} = 1, \quad \forall r = 1,2,\cdots,R+1, \tag{4.9e}$$

$$Y_{kjr} \in \{0,1\}, \quad \forall j \in \mathcal{J}, k \in \mathcal{K}, r = 1,2,\cdots,R+1. \tag{4.9f}$$

We observe that (RRSFL$_i$) is a combinatorial generalized assignment problem, which can be solved by an adapted Hungarian algorithm as in Cui et al. (2010). (RRSFL$_i$) aims at assigning one station-facility pair to each level (up to $R+1$) based on the updated coefficients associated with each Y_{kjr}, so as to minimize the total expected system cost. However, the actual maximum assignment level $R_{\max}$ (i.e., the largest r such that $Y_{kjr} = 1$ for some (k,j) pair) may be smaller than R due to lower cost associated with the emergency station-facility pair than all other remaining pairs at some level $r < R$. The main challenge is to identify the level that the emergency station-facility pair should be assigned to. As such, we enumerate $R_{\max}$ from 0 to R and for each $R_{\max}$, we fix $Y_{00,R_{\max}+1} = 1$ and $Y_{kjr} = 0, r > R_{\max}+1$. In this way, the (RRSFL$_i$) is simplified into a standard assignment problem that can be solved by conventional Hungarian algorithm. We solve (RRSFL$_i$) and calculate the associated total

cost for each enumeration of $R_{\max}$. By comparison, the value of $R_{\max}$ corresponding to the lowest total cost is the actual maximum assignment level $R_{\max}$. After fixing $R_{\max}$, It is worth noting that in the enumeration process, the assignment solutions to model with $R_{\max} = r$ can be used as a warm start to the model with $R_{\max} = r + 1$, which helps expedite the computation. Specifically, if the penalty cost d_{i00} (or say π_i) is sufficiently large, we only need to solve (RRSFL$_i$) for one iteration, i.e., $R_{\max} = R$.

Proposition 5. *The solution to (RRSFL$_i$) provides a lower bound to the relaxed subproblem (RSFL$_i$).*

Proof. Let $\mathbf{Y}^*, \mathbf{Z}^*$ and $\mathbf{W}^*$ be the optimal solution to (RSFL$_i$). (RRSFL$_i$) can be built from (RSFL$_i$) by replacing Z^*_{kjr} and Z^*_{00r} with α_{kr} and β_r, respectively, and removing constraints (4.5f)–(4.5i). Since we are relaxing contraints, the solution $\mathbf{Y}^*, \mathbf{Z}^*$ and $\mathbf{W}^*$ should still be feasible to (RRSFL$_i$), and based on the construction of α_{kr} and β_r, we know that $\alpha_{kr}Y_{kjr}$ and $\beta_r Y_{00r}$ are lower bounds of W_{kjr} and W_{00r}, respectively. Moreover, removing constraints (4.5f) never increases the objective value of this minimization problem. Therefore the optimal objective value of (RRSFL$_i$) is a lower bound to the optimal objective value of (RSFL$_i$). This completes the proof. □

4.4 Case Studies

We apply the proposed model and solution algorithms to five examples so as to demonstrate their applicability and performance under different correlation patterns and parameter settings. The first example includes a series of hypothetical square grid networks with varying sizes. The second case focuses on planning railroad emergency response facility locations in the Chicago metropolitan area, where facility disruption correlations are caused by support failure that may occur at network access points (e.g., railroad crossing blockage). The main purpose of this example is to illustrate the impacts of various system settings (e.g., heterogeneity) on the optimal design. The latter three cases (from S. Xie et al. (2015)) deal with correlations caused by shared hazards; i.e., earthquake with positive correlation, flooding with general correlation, and terrorist attacks with local correlation, so as to illustrate the application of virtual station structures, and to demonstrate the impacts of spatial correlation.[a]

The proposed solution algorithms are programmed in C++ and run on a 64-bit Intel i7-3770 computer with 3.40 GHz CPU and 8G RAM. The mixed-integer linear programs LRFL and RSFL$_i$, if solved directly, are tackled by commercial solver CPLEX 12.4 using up to 4 threads. The reformulated problem RRSFL$_i$ is solved by the Hungarian algorithm.

4.4.1 Hypothetical Grid Networks

For $n \in \{4, 5, 6, 7, 8\}$, an $n \times n$ square grid network is generated to represent a hypothetical study region (e.g., a city like Venice) with n^2 cells (e.g., islands) and $2n(n-1)$ blockage segments (e.g., canal branches), as shown in Figure 4.1. The n^2 cell indices $1, 2, \cdots, n^2$ are

[a] All input data for these case studies will be available at webpage `http://web.engr.illinois.edu/~yfouyang`.

labeled from left to right (with increments of 1), and from top to bottom (with increments of n). The edge length of each cell is set to 1. The centroid of each cell is considered to be both an individual customer and a candidate facility location. For cell i, the demand is $9.5 + 0.5(\text{mod}(i, 5) + 1)$ and the fixed facility cost is $85 + 5(\text{mod}(i, 5) + 1)$.[b] The middle point of each edge represents the access point (e.g., bridge) through which customers may travel to service facilities. The site-dependent failure probability of the edge between cells i and j is assumed to be $0.01(\text{mod}(i + j, 5) + 1)$. The maximum assignment level is $R = 3$ for all cases.

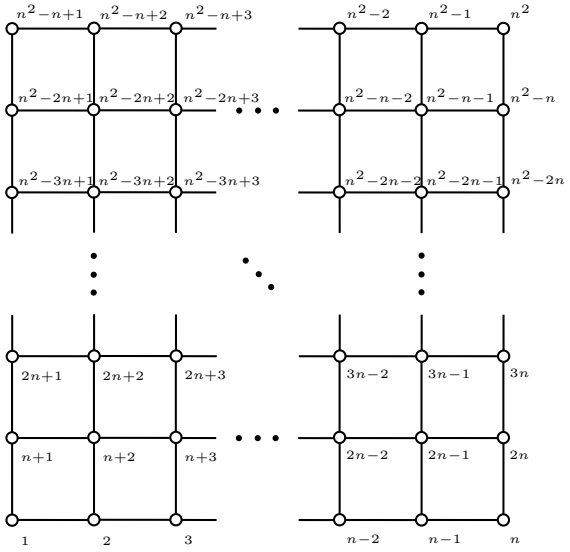

Figure 4.1: $n \times n$ hypothetical grid network.

To solve the reliable facility location problems in these networks, we use three solution approaches: (i) CPLEX directly applied to the linearized original problem (LRFL); (ii) Lagrangian relaxation based branch-and-bound algorithm with each subproblem (RSFL_i) solved by CPLEX (LR+B&B+CPLEX); and (iii) Lagrangian relaxation based branch-and-bound algorithm with each subproblem (RRSFL_i) solved by the approximate algorithm (LR+B&B+Approx.). The solution time limit is set to be 3600 seconds. Table 4.1 summarizes and compares the results obtained by the three approaches for a range of test instances.

Overall, it can be observed that the solution time and solution quality deteriorate with the network size, owing probably to the significant increase in the number of integer variables $\mathbf{Y}$. CPLEX cannot close the optimality gaps for the first three cases despite the relatively small network sizes. For the four larger networks, CPLEX ran out of memory and failed to provide even a feasible solution. The LR+B&B+CPLEX approach can provide a feasible solution within one hour for the first five cases, however, the optimality gaps are relatively large except for the smallest 4×4 network. This is because when network size is large, it takes CPLEX a long time to solve even one instance of subproblem (RSFL_i), and thus

[b]The demand and facility cost can be generated arbitrarily, e.g., one could choose $\text{mod}(i, n)$, but that may lead to a very special spatial pattern (e.g., low values on the left and high values on the right). So we choose $\text{mod}(i, 5)$ as an example, such that these values are "arbitrarily" distributed across the network.

Table 4.1: Algorithm performance comparison for the 5 hypothetical cases.

	Network size	No. of facilities	Opt. facility locations	Final UB	Final LB	Final gap (%)	CPU time (s)
CPLEX	4×4	2	5, 11	435.24	433.38	0.428	3600
	5×5	3	8, 17, 20	685.31	678.07	1.056	3600
	6×6	4	8, 11, 26, 29	945.44	930.46	1.584	3600
	7×7	–	–	–	–	fail	3600
	8×8	–	–	–	–	fail	3600
LR+B&B +CPLEX	4×4	2	5, 11	435.24	435.24	0.0	3378
	5×5	3	8, 17, 20	685.30	488.73	28.684	3600
	6×6	4	7, 10, 23, 33	995.45	643.71	35.334	3600
	7×7	5	10, 17, 20, 34, 37	1365.80	712.65	47.822	3600
	8×8	8	10, 15, 20, 25 37, 49, 56, 63	1809.37	1071.65	40.772	3600
LR+B&B +Approx.	4×4	2	5, 11	435.24	435.24	0.0	1.3
	5×5	3	8, 17, 20	685.30	685.30	0.0	21.2
	6×6	4	8, 11, 26, 29	945.34	945.34	0.0	118.1
	7×7	5	11, 16, 20, 37, 40	1283.29	1278.06	0.408	3600
	8×8	5	10, 15, 36, 50, 55	1671.51	1566.91	6.258	3600

the overall algorithm can only branch on a very limited number of nodes within the time limit. For the 10×10 and 15×15 networks, the LR+B&B+CPLEX approach failed to give a feasible solution. In contrast, the LR+B&B+Approx. solution approach can obtain the exact optimal solutions in less than 2 minutes for the first 3 cases. For $n \in \{7, 8, 10, 15\}$, the optimality gaps after 1 hour of computation are 0.408%, 6.258%, 16.699%, and 26.570%, respectively. As such, the proposed LR+B&B+Approx. approach clearly outperforms the other two methods in terms of both solution quality and computation time.

4.4.2 Railroad Emergency Response

Many states in the U.S. Midwest have expressed strong concerns over the close proximity of hazardous material trains to densely-populated urban areas[c], and the long blockage of rail crossing by train traffic which may disrupt emergency response efforts[d]. The U.S. federal and local regulators have issued a number of orders on railroad incidents prevention and emergency response resource deployment so as to enhance rail crossing safety and reliability Gold & Stevens (2014). This calls for careful designs of emergency response facility locations (e.g., fire stations, hospitals, etc.) such that critical resources can be delivered efficiently even under emergency situations.

We now consider the Chicago area, a region with strong railroad network presence as shown in Figure 4.2(a). Target areas (e.g., towns and districts) are partitioned and sur-

[c]See http://www.dot.state.mn.us/newsrels/15/03/19oiltrains.html.
[d]See http://www.startribune.com/politics/statelocal/286633141.html.

rounded by railroad segments. We assume there is one major access point (at-grade crossing)[e] on each railroad segment that allow first-responders to reach the regions. A limited number of emergency resource facilities are to be deployed among these regions in anticipation of random emergencies (e.g., fire, incidents). However, the rail crossings are subject to blockages, and hence the emergency resources of a facility might not be accessible if all of its surrounding rail crossings are blocked. The railroad network in Chicago contains $|J| = 23$ candidate facility locations, $|I| = 23$ customers (e.g., cities and towns), and $|K| = 38$ railway-highway crossings. In Figure 4.2(b), each line represents a railway segment, each dot represents a railway crossing (access point), and each square (surrounded by multiple railway segments) represents a target demand area as well as a candidate facility location. The demand and fixed cost of each area are set to be proportional to its population and housing price, respectively. The railway crossings serve as supporting stations to built facilities, and they are categorized into three groups, each having a high, median, or low risk of being blocked based on their annual train traffic volumes (denoted by $\mathcal{K}_h, \mathcal{K}_m, \mathcal{K}_l$, respectively). We further assume that blockage probability of each group can be specified as follows:

$$q_k = \begin{cases} \bar{q} + \hat{q} & \text{if } k \in \mathcal{K}_h \\ \bar{q} & \text{if } k \in \mathcal{K}_m \\ \bar{q} - \hat{q} & \text{if } k \in \mathcal{K}_l \end{cases}$$

where $\bar{q}$ is the average probability and $\hat{q}$ marks the level of spatial variation. A simplified graph of the network is shown in Figure 4.2(c), where each node is a candidate facility location and each link is a railway crossing. The distance d_{ikj} is calculated as the shortest path distance between node i and j through link k based on Figure 4.2(c). We assume that a customer receiving service from a facility elsewhere must pass through one of the railway crossings surrounding the facility.

We test our model with a range of $\bar{q}, \hat{q}$, and R, so as to examine their impacts on the optimal facility location design and algorithm performances. Case 10 (i.e., $\bar{q} = \hat{q} = 0$) represents the degenerated situation where crossings never get blocked, and hence backup assignments are not necessary (i.e. $R = 1$). For other cases, we assume that $\bar{q} = 0.20$, and $\hat{q} \in \{0, 0.10, 0.20\}$ for identical probability, slight site-dependent probabilities, and high site-dependent probabilities, respectively. The value of R varies from 2 to 4.

Solutions from our approximate algorithm (LR+B&B+Approx.) are presented in Table 4.2. The relatively large values of station failure probabilities have led to longer computation times, i.e., not all cases can be solved to optimality within 2 hours. As R increases, the total cost decreases, possibly due to a slightly lower likelihood for the customers to receive the penalty of losing service. In addition, the value of R does have observable impacts on the computation time and the optimal facility location design. These observations are consistent with those in earlier studies by Cui et al. (2010); Li & Ouyang (2012). Existence of

[e]Each segment may actually include multiple access points. Since a segment cannot be passed through if and only if all access points on it are disrupted, we can approximately consolidate these access points into one "representative" with the "composite" disruption probability $q = \prod_{k \in L} q_k$, where L is the set of all actual access points on this segment. Note that when a segment is long, the distances of passing through these different access points will likely be different. This issue is not addressed in this paper but deserves further study.

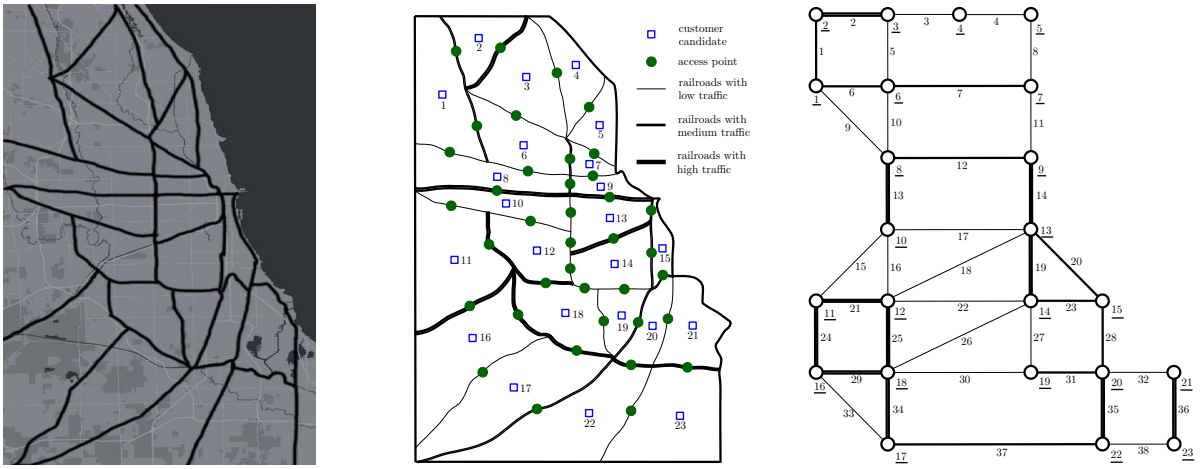

(a) The Chicago map (b) The railroad network (c) The abstract representation

Figure 4.2: The railroads network setup in Chicago area.

station failures generally has a noticeable impact on the optimal facility locations, total cost (including transportation cost), and the required computation time, if we use the no-failure counterpart (case 10) as the benchmark. Moreover, the spatial heterogeneity (as reflected by the value of $\hat{q}$) is possible to affect the optimal design, e.g., solutions to case 3 (with $\hat{q} = 0.20$), case 6 (with $\hat{q} = 0.10$), and case 9 (with $\hat{q} = 0$) are all quite different. It is worth noting that failing to consider site-dependent probabilities may lead to a cost increase, especially for transportation. For example, if we hold the failure probabilities of case 3 as the ground truth (where $\hat{q} = 0.20$), but solve the problem as if $\hat{q} = 0$. The corresponding solution (the one for case 9) will yield an actual total cost of 68596.4 and a transportation cost of 45636.4 under the assumed ground truth, which are 8.91% and 33.03% larger than the corresponding total cost of 62896.0 and transportation cost of 34566.0 obtained for case 3 (with $\hat{q} = 0.20$), respectively. It shall be also noted, however, that for many other cases, the cost "error" from ignoring station failure heterogeneity is not as high as those observed in other studies (which directly consider facility failure heterogeneity). This result is somewhat intuitive because the presence of shared access points among the facilities tends to serve as another layer of "buffer" that averages out the spatial heterogeneity.

Figure 4.3 presents the location decisions and assignment path of each customer to access the facilities at each backup level (i.e., 1^{st} and 2^{nd}) for cases 3 and 9 (with $R = 2$). Generally, five facilities $\{5, 6, 12, 14, 20\}$ are built in case 3, as marked by the solid red squares, while another 4 facilities $\{5, 8, 14, 22\}$ are built in case 9. For both cases, the built facilities are located at regions with a higher concentration of demands. Specifically, in the southern half of the metropolitan area, due to low demand, only one candidate location (e.g., 20 in case 3 and 22 in case 9) is selected. In contrast, the densely populated northern half always has two or even more built facilities. Moreover, regions/nodes with more access points (e.g., location 14) are more likely to be chosen since they can provide more backup access points/opportunities. As for the customer assignments, the 1^{st}-level assignments can be segregated into multiple groups, with each group clustered around one facility, while the 2^{nd}-level assignments are more intertwined with each other. In addition, a customer may

Table 4.2: Algorithm performance comparison for the Chicago cases.

Index	Failure Prob.		R	Opt. facility locations	Root UB	Root LB	Root gap (%)	Final Objective	Final gap (%)	Time (s)
	$\bar{q}$	$\hat{q}$								
1	0.20	0.20	4	5, 6, 10, 14, 22	61376.0	33161.9	46.0	60282.3	0	7054
2	0.20	0.20	3	5, 6, 10, 14, 22	61594.4	33151.8	46.2	60881.2	2.91	7200
3	0.20	0.20	2	5, 6, 12, 14, 20	64719.2	33625.9	48.0	62986.0	6.56	6936
4	0.20	0.10	4	5, 6, 10, 14, 22	61906.3	33498.8	45.9	61377.6	0	7200
5	0.20	0.10	3	5, 6, 10, 14, 22	64663.3	33525.5	48.2	62629.9	2.50	7200
6	0.20	0.10	2	5, 6, 12, 19, 20	70293.7	33889.6	51.8	70115.3	13.07	7200
7	0.20	0	4	3, 7, 10, 14, 22	62690.3	33570.7	46.5	62355.2	4.84	7200
8	0.20	0	3	3, 7, 10, 14, 22	65100.8	33557.2	48.5	64454.7	8.40	7200
9	0.20	0	2	5, 8, 14, 22	76727.2	33908.5	55.8	75635.2	22.35	7200
10	0	0	1	6, 14, 21	57120.0	36442.5	36.2	57120.0	0	89

visit the same facility or two different facilities through two different crossings at the two backup levels. For example, in the solution for case 3, customer 4 is first assigned to facility 5 through crossing 4 at level 1, then to facility 6 through crossing 5 at level 2; while customer 1 is first assigned to facility 6 through crossing 6 at level 1, then to facility 6 again through crossing 5 at level 2.

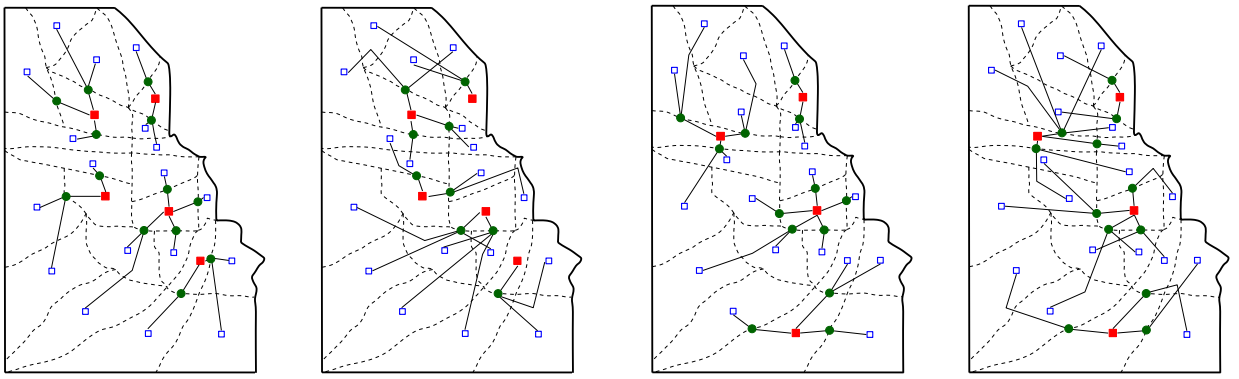

(a) 1st level assignment for case 3 (b) 2nd level assignment for case 3 (c) 1st level assignment for case 9 (d) 2nd level assignment for case 9

Figure 4.3: Facility locations and customer assignments at different backup levels of cases 3 and 9.

4.4.3 Earthquake

Figure 4.4(a) depicts an example from S. Xie et al. (2015), where a square urban area is subject to earthquake risks. The area is evenly divided into 16 indexed square cells, and the centroid of each represents a candidate facility location as well as a population center, i.e. $|J| = |I| = 16$. Each point generates an equal demand of $\mu_i = 1.25, \forall i$, and this adds up to a city-wide total demand of 20. The epicenter of a potential earthquake is assumed to be at location 1[f]. Since earthquake intensity drops with distance, facilities closer to the epicenter are more likely to be disrupted. We thus divide the city region into 10 rings centered at location 1. The facilities in each ring will fail together, and if that happens, all other facilities closer to the epicenter are already disrupted. The recipe in S. Xie et al. (2015) transforms a scenario-based correlated disruption profile (see Table 4 in S. Xie et al. (2015)) into an additional layer of 10 virtual stations as in Figure 4.4(b), each with a different failure propensity (as marked near the station). The construction cost of each facility is $f_j = 30, \forall j$. Euclidean distance between customer i and facility j (regardless of virtual supporting station k) is used to measure d_{ikj}. Penalty for loss of unit demand is $\pi_i = 60, \forall i$. The maximum assignment level is $R = 10$, which is equal to the number of added virtual stations. For comparison, we also study other cases when there is no correlation, and when customer demand displays heterogeneity. When there is no correlation, we assume that facility disruptions are independent but maintain the same marginal probabilities; the

[f]In real-world applications, we can extract the probability profile directly from historic data (Xie et al., 2015) and do not necessarily need information on the earthquake epicenter.

optimization model degrades to the one in Cui et al. (2010). For the heterogeneous cases, we assume that $\mu_i = 3.0 - 0.5d_i$ (such that $\sum_i \mu_i = 20$), where d_i is the Euclidean distance from location i to the city center. The computational time for every case is within 1.5 minutes. Figures 4.5(a)-4.5(d) depict the optimal facility location design for each of the four cases (correlated vs. uncorrelated disruption, homogeneous vs. heterogeneous demand).

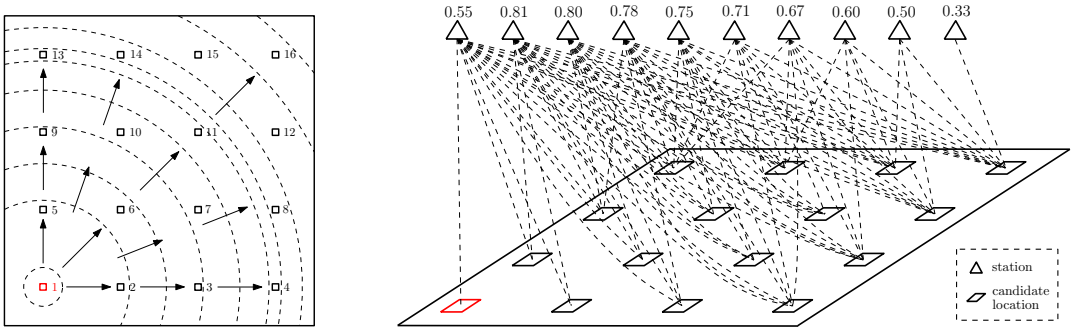

(a) Network input. (b) Facility-station system input.

Figure 4.4: Model input for the earthquake case.

It can be seen that disruption correlations and demand heterogeneity both have significant impacts on the optimal facility locations. In the first case (with correlated disruption and homogeneous demand), the four built facilities are quite spatially dispersed so as to minimize the positive correlations among these facilities. For example, at most one facility is selected in each ring, because those in the same ring will suffer simultaneous disruptions and will not be able to back up each other. In Figure 4.5(b), facilities are more clustered toward the city center when there is no disruption correlation. Facilities at locations 7 and 12 (which are closest to the city center) in this case are obviously geographically more advantageous over those at corner locations 4 and 16 in Figure 4.5(a). Meanwhile, we also observe that the existence of disruption correlation pushes the facilities away from the epicenter: the facility at location 4 is two rings farther than that at location 7, and the one at 16 is one ring farther than the one at 12. The same impact of disruption correlation can be found under heterogeneous demands. To study the impact of demand heterogeneity, we now compare Figure 4.5(a) with 4.5(c), and also Figure 4.5(b) with 4.5(d). Intuitively, candidate locations with high customer demand are more favorable, and hence the facilities in Figure 4.5(b) and 4.5(d) are somewhat more clustered toward the city center than their respective counterparts. The facility number is also reduced by 1 due to the economic benefits of demand concentration.

Table 4.3 summarizes the computational results. For each case, we list the optimal objective value from the respective model (e.g., ignoring correlation), as well as the evaluated system-wide cost assuming the ground-truth that disruption correlation does exist. It can be seen that the model without considering correlation results in a sub-optimal facility design (i.e., with higher system costs) for both homogeneous and heterogeneous demand. Heterogeneity in demand further exacerbates the cost difference to up to 28.6%.

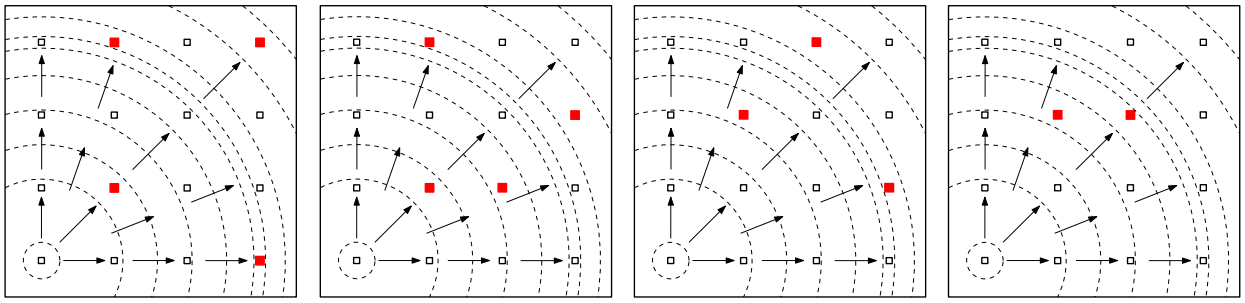

(a) correlation & homogeneous demand (b) no correlation & homogeneous demand (c) correlation & heterogeneous demand (d) no correlation & heterogeneous demand

Figure 4.5: Optimal facility locations for the four earthquake cases.

Table 4.3: Solution statistics for the earthquake cases.

Case		Facility	Objective	Evaluated cost	Cost	Comp.
Corr	Homo	location		under correlation	difference (%)	time (s)
Yes	Yes	4,6,14,16	339	339	–	83
No	Yes	6,7,12,14	315	349	2.9	70
Yes	No	8,10,15	325	325	–	69
No	No	10,11	302	418	28.6	2

4.4.4 Flooding

S. Xie et al. (2015) also considered a flooding case, as shown in Figure 4.6(a), in which the same city area is threatened by flooding from a river passing diagonally. Flooding may start randomly at any point along the river, i.e. locations 1, 6, 11, 16, and once it happens, water will spread in all directions and may disrupt nearby facilities. On the other hand, releasing flood water at one point could release the pressure and reduce the risk of flooding at other points. Hence, the facility disruptions exhibit both positive (e.g., along the lateral direction) and negative correlations (e.g., along the longitudinal direction). A general correlation profile involving a mixture of positive and negative correlations, described by the scenarios in Table 8 of S. Xie et al. (2015), can be represented equivalently by 16 additional virtual stations as in Figure 4.6(b). Note that some of the failure propensity values are now larger than 1. Other system parameters are similar to those in the earthquake case, except that the maximum customer assignment level is now $R = 16$, and we also examine four cases (correlated vs. uncorrelated disruption, homogeneous vs. heterogeneous demand). The optimal facility location designs are shown in Figure 4.7.

Again, disruption correlation and demand heterogeneity are observed to influence the optimal facility locations to some extent. Under homogeneous demand, our model determines that at optimality four facilities should be built somewhat evenly along the river, each at a different distance to the river. It shall be noted that the facility layouts in Figures 4.7(a) and 4.7(b) are actually identical since the failure disruption scenarios are set to be symmetric along the river. It indicates that correlation does not affect the facility locations

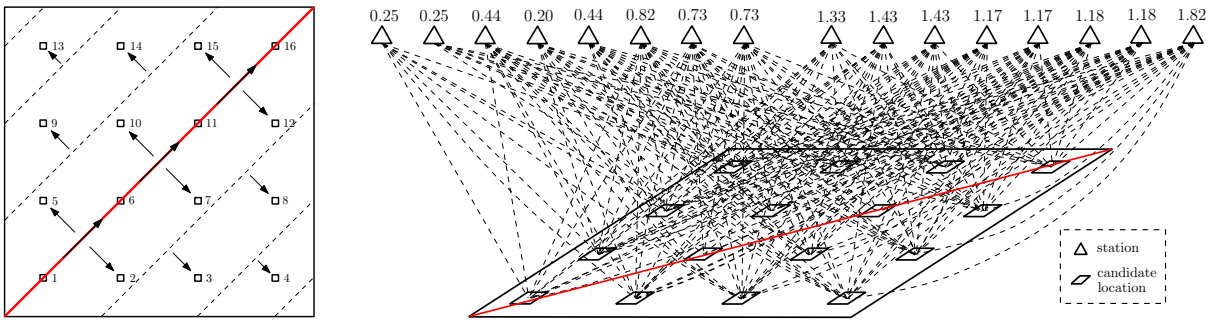

(a) Network input.

(b) Facility-station system.

Figure 4.6: Model input for the flooding case.

under homogeneous demand, probably because (i) facilities at locations 3, 5, 12, 14 or 2, 8, 9, 15 have relative low individual failure probabilities, and (ii) there are only very weak correlation among them (due to co-existence of positive and negative correlations). Under heterogeneous demand, three facilities are clustered toward the concentrated demand near the city center. Particularly, facilities in Figure 4.7(d) (with no correlation) are more clustered than those in Figure 4.7(c). The expected system cost and the cost difference for the four cases are summarized in Table 4.4. Similar to those for the earthquake cases, heterogeneous demand could reduce the system cost, and ignoring negative correlation leads to sub-optimal solutions. The computation time is a little larger as a result of having more virtual stations, but our proposed algorithm still solves the problem quite effectively.

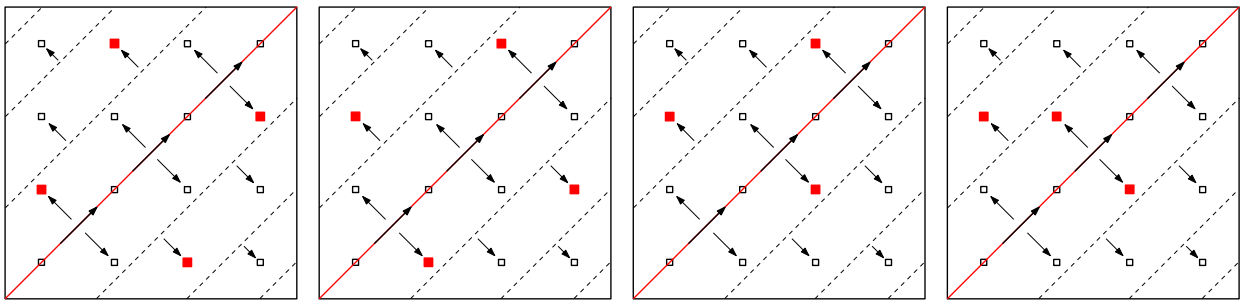

(a) correlation & homogeneous demand

(b) no correlation & homogeneous demand

(c) correlation & heterogeneous demand

(d) no correlation & heterogeneous demand

Figure 4.7: Optimal facility locations for the four flooding cases.

4.4.5 Terrorist Attack

We finally study the terrorist attack case in S. Xie et al. (2015) as shown in Figure 4.8(a), in which the same city area is under the risk of terrorist attacks. The terrorists are assumed to have limited resources and are only able to threat regions I and IV, and their threats to these two regions are independent. The detailed attack patterns are as follows: (i) in region I, location 1 is always attacked first, and only after facility 1 is attacked (i.e., disrupted)

Table 4.4: Solution statistics for the flooding cases.

Case		Facility	Objective	Evaluated cost	Cost	Comp.
Corr	Homo	location		under correlation	difference (%)	time (s)
Yes	Yes	2,8,9,15	294	294	–	189
No	Yes	3,5,12,14	284	294	0.0	4
Yes	No	7,9,15	291	291	–	155
No	No	7,9,10	278	320	10.0	12

can facilities 2 and 5 be possibly attacked; further, only after facilities 1, 2 and 5 are all disrupted can facility 6 be possibly attacked; and (ii) in region IV, facilities 11 and 16 are the two priority targets, and they two must both have been disrupted before possible attacks may occur to facilities 12 and 15. The correlations are described by the conditional probabilities in Table 10 of S. Xie et al. (2015). Calculations using (3.10) show that the number of scenarios for this case is 42, while the equivalent virtual station structure only involves 11 stations, as shown in Figure 4.8(b). This demonstrates the compactness of our station structure when the facility disruptions are locally correlated, per Proposition 5. The optimal facility location designs for four cases (correlated vs. uncorrelated disruptions, homogeneous vs. heterogeneous demand) are depicted in Figure 4.9. The expected system costs and the cost differences for the four cases are summarized in Table 4.5.

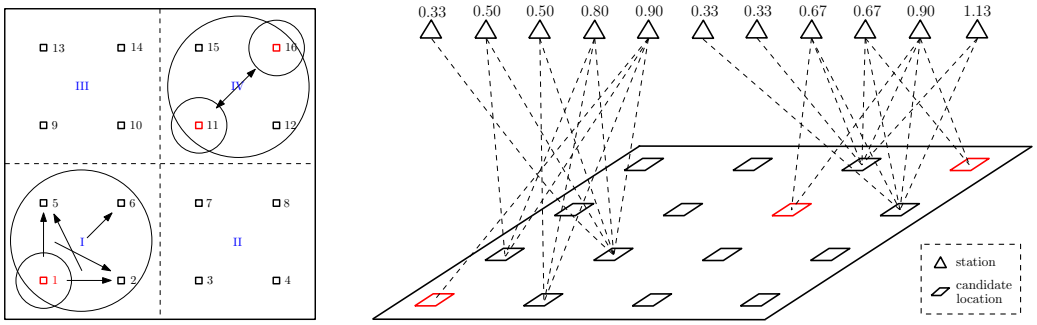

(a) Network input.

(b) Facility-station system.

Figure 4.8: Model input for the terrorist attack case.

Table 4.5: Solution statistics for the terrorist attack cases.

Case		Facility	Objective	Evaluated cost	Cost	Comp.
Corr	Homo	location		under correlation	difference (%)	time (s)
Yes	Yes	6,12,15	316	316	–	20
No	Yes	7,9,15	287	613	94.0	3
Yes	No	6,12,15	288	288	–	18
No	No	6,7,10	248	417	44.8	5

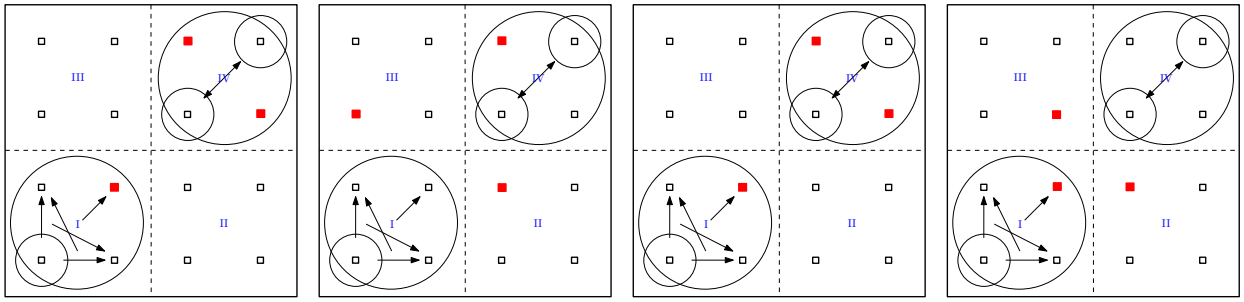

(a) correlation & homogeneous demand (b) no correlation & homogeneous demand (c) correlation & heterogeneous demand (d) no correlation & heterogeneous demand

Figure 4.9: Optimal facility locations for the four terrorist attack cases.

Chapter 5

RFL with Facility Combinations: Reliable Sensor Deployment for Positioning/Surveillance via Trilateration

5.1 Introduction

High-accuracy object positioning has been playing a critical role in various application contexts such as: (i) civilian uses, including vehicle navigation, driver guidance, activity tracking; (ii) industrial uses, such as aircraft tracking, regional surveillance, extrasolar planets detection; and (iii) military uses, such as search/rescue missions, missile and projectile guidance. In recent years, massive availability of mobile devices has stimulated demand for many location-aware applications. In a typical such system, multiple sensors are required to provide coverage jointly, and the effectiveness of the system highly depends on the quality (working range and precision level) and quantity of sensor coverage in the local area.

Trilateration is one of the most popular mathematical techniques used by many systems to geographically positioning or surveil an object. An object is positioned based on distance measurements received from a combination of sensors. Since various sensor combinations could share some common unreliable sensors, failure of a combination could be directly related to that of another combination. This leads to internal correlation among the functionality of sensor combinations. In this case, where to deploy sensors, which combinations of sensors to use, and in what sequence and probability to use backup combinations in case of disruptions, are nontrivial questions. It remains an open challenge to optimize sensor deployment locations that maximize the overall system-wide surveillance or positioning benefits under the risk of site-dependent sensor failures.

In this chapter, we incorporate the impacts of sensor disruptions into a reliable sensor deployment framework by extending the ideas of assigning backup sensors as well as correlation decomposition via supporting stations. Specifically, we formulate the reliable sensor deployment problem as a compact mixed-integer linear program and develop solution approaches based on a customized Lagrangian relaxation algorithm with several embedded

approximation subroutines. A series of hypothetical examples and a real-world Wi-Fi access points design problem for Chicago O'Hare Airport Terminal 5 are conducted to illustrate the applicability and performance of the model and solution algorithms. Managerial insights are also presented.

5.2 Model Formulation

We consider an area (e.g., airport, shopping mall) which contains a set of spatial neighborhoods $I := \{i\}$ that need surveillance coverage. In airports, such neighborhoods can be security check gates, boarding gates and restaurants where accidents are more likely to occur due to crowds' gathering. Each point $i \in I$ attracts v_i customers per day. Let J be the set of candidate locations for potential sensor installations. At most one sensor can be installed at each location $j \in J$ at a construction cost f_j. Let d_{ij} denote the distance from surveillance neighborhood i to sensor location j. A sensor located at j could be disrupted with a probability of p_j. For a neighborhood $i \in I$, the sensors are assigned with different backup levels. We assume the receiver (can be the mobile device/object itself) always uses N, where $N \geq 3$, sensors with the lowest backup levels to calculate the position of the object. Without loss of generality, for modeling convenience, N dummy sensors (located at $|J|+1, \cdots, |J|+N$) are added to the system to ensure there are always at least N sensors available even under the worst case scenario in which all sensors are disrupted. Let $\tilde{J}$ be the set of dummy sensors and $\mathcal{J} = J \cup \tilde{J}$ be the set of all sensors. The dummy sensors incur 0 installation cost and are not subject to failure, but make no contribution to object positioning. Let K be the set of candidate sensor combinations to locate customers. Each combination $k \in K$ contains exactly N sensors (including the dummy ones) and could monitor i with accuracy e_{ik}. Let α be the ratio of sensor cost to sensing accuracy. We introduce incidence matrix $\{a_{kj}\}$ to represent the mapping relationships between combinations and sensors, where $a_{kj} = 1$ if combination k contains sensor j, or 0 otherwise. The maximum number of combinations is $\sum_{t=0}^{N} \binom{|J|}{t}$, where t indicates that t regular sensors and $N-t$ dummy sensors are used in the combination.

As such, the receiver/object will search from the sensor with the lowest backup level until N sensors have been found. The key decision variables $\mathbf{X} := \{X_j\}$ determine sensor locations, where $X_j = 1$ if a sensor is installed at location j or $X_j = 0$ otherwise. For each surveillance neighborhood, the installed sensors are assigned to it at different levels. Variables $\mathbf{Z} := \{Z_{ijr}\}$ determine the relative sensor levels, where binary variable $Z_{ijr} = 1$ if sensor j is installed and is assigned with level r to neighborhood i, or 0 otherwise; $\mathbf{Y} := \{Y_{ikr}\}$ denote the sensor combination assignment to the customers, where $Y_{ikr} = 1$ if neighborhood i uses combination k whose highest level element sensor has level r, or 0 otherwise. Note that a combination k corresponds to only one level r, while there may exist multiple combinations corresponding to the same level r. The backup levels are initially assigned to the sensors. A level r, if associated with a sensor combination k, indicates the highest level of any sensor contained in k; it can be uniquely determined from the backup levels of sensors that are assigned to an object, i.e., $\{Z_{ijr}\}$. $\mathbf{P} := \{P_{ikr}\}$ are quasi-probability variables where P_{ikr} defines the probability to use combination k to monitor neighborhood i if $Y_{ikr} = 1$, and is a state variable if $Y_{ikr} = 0$.

This sensor location problem (SLP) can now be formulated as the following mixed-integer non-linear program:

$$\text{(SLP)} \quad \min_{\mathbf{X},\mathbf{Y},\mathbf{Z},\mathbf{P}} \quad \sum_{j\in J} f_j X_j - \alpha \sum_{i\in I}\sum_{k\in K}\sum_{r=1}^{|\mathcal{J}|} v_i e_{ik} P_{ikr} Y_{ikr} \tag{5.1a}$$

$$\text{s.t.} \quad \sum_{r=1}^{|\mathcal{J}|} Z_{ijr} \le X_j,\ \forall j \in J, i \in I, \tag{5.1b}$$

$$\sum_{r=1}^{|\mathcal{J}|} Z_{ijr} \le 1,\ \forall j \in J, i \in I, \tag{5.1c}$$

$$\sum_{r=1}^{|\mathcal{J}|} Z_{ijr} = 1,\ \forall j \in \tilde{J}, i \in I, \tag{5.1d}$$

$$Z_{ijr} = Z_{i,j+1,r+1},\ \forall r = 1, 2, \cdots, |\mathcal{J}| - 1, j \in \tilde{J}\backslash(|J| + N), i \in I, \tag{5.1e}$$

$$\sum_{j\in J} Z_{ijr} + \sum_{s=1}^{r} Z_{i,|J+1|,s} = 1,\ \forall r = 1, \cdots, |\mathcal{J}|, i \in I, \tag{5.1f}$$

$$Y_{ikr} \le \frac{1}{N} \sum_{j\in\mathcal{J}} \sum_{s=1}^{r} a_{kj} Z_{ijs},\ \forall k \in K, r = 1, \cdots, |\mathcal{J}|, i \in I, \tag{5.1g}$$

$$Y_{ikr} \le \sum_{j\in\mathcal{J}} a_{kj} Z_{ijr},\ \forall k \in K, r = 1, \cdots, |\mathcal{J}|, i \in I, \tag{5.1h}$$

$$P_{ikr} = \sum_{j\in\mathcal{J}} (p_j)^{1_{[j\in J]}} Z_{ijr} P_{ik,r-1},\ \forall k \in K, r = 1, \cdots, |\mathcal{J}|, i \in I, \tag{5.1i}$$

$$P_{ik0} = \prod_{j\in J} (1 - p_j)^{a_{kj}} (p_j)^{-a_{kj}},\ \forall k \in K, i \in I, \tag{5.1j}$$

$$X_j, Z_{ijr}, Y_{ikr} \in \{0, 1\},\ \forall k \in K, j \in \mathcal{J}, r = 1, \cdots, |\mathcal{J}|, i \in I. \tag{5.1k}$$

The objective function (5.1a) presents the expected system cost including the sensor installation cost and the expected total inaccuracy penalty, where $P_{ikr}Y_{ikr}$ is the probability that combination k is used by neighborhood i at the r-th level. Constraints (5.1b) enforce that customers can only use installed sensors. Constraints (5.1c) indicate that for a certain surveillance neighborhood, each regular sensor can only be assigned to at most one level. Constraints (5.1d) ensure for a certain surveillance neighborhood, each dummy sensor must be assigned to it at a certain backup level. The same dummy sensor could be assigned to other surveillance neighborhoods at different levels. Constraints (5.1e) postulate that if a dummy sensor $j \in \tilde{J}$ is assigned to surveillance neighborhood i at level r, then dummy sensor $j + 1$ must be assigned to i at level $r + 1$. Constraints (5.1f) require that at each level r, a surveillance neighborhood i either uses a regular sensor, or it has used the first dummy sensor at level $s \le r$. Constraints (5.1g) enforce that combination k is available to surveillance neighborhood i only if the N sensors in k are all installed. Constraints (5.1h) require that combination k is available to surveillance neighborhood i when its highest level element serves at level r. Constraints (5.1i) and (5.1j) recursively define the assignment

probability P_{ikr} for $Y_{ikr} = 1$ to happen, where the indicator function $1_{[\cdot]} = 1$ when condition $[\cdot]$ holds, or 0 otherwise. Please note that P_{ikr} does not have physical meaning when $Y_{ikr} = 0$ and its value will not affect the value of the objective function. Given that the lower level sensors are used earlier, a combination k is used if and only if its element sensors are all functioning, and the other constructed sensors which has level lower than the highest level in k are all disrupted. The derivation of P_{ikr} is shown as follows.

Proposition 6. *The assignment probability P_{ikr} (for $Y_{ikr} = 1$ to happen) can be calculated recursively by* (5.1i)*, given its initial state value defined by* (5.1j)*.*

In (SLP), the surveillance neighbourhood i can choose any installed sensors and assign them to various levels flexibly to minimize the inaccuracy penalty. However, at optimality, each neighbourhood i will use all installed sensors, and the backup level of each sensor solely depends on its relative distance to the neighbourhood (i.e., irrelevant to its failure probability), as proved in the following proposition.

Proposition 7. *In any optimal solution $\{\mathbf{X}, \mathbf{Z}, \mathbf{Y}\}$, for each surveillance neighborhood i, an installed sensor must be assigned to a backup level, and a nearer sensor must be assigned to an earlier level; i.e. the following two properties must hold (i) if $X_j = 1$, then $\sum_{r=1}^{|\mathcal{J}|} Z_{ijr} = 1$; (ii) if $Z_{ij_1r} = Z_{ij_2r+1} = 1$ for some i, r, then $d_{ij_1} \leq d_{ij_2}$.*

The current model is nonlinear due to the existence of nonlinear terms $P_{ikr}Y_{ikr}$ in (5.1a) and $Z_{ijr}P_{ikr-1}$ in (5.1i). Linearization techniques introduced by Sherali and Alameddine (1992) (similar to those in Li and Ouyang (2012)) can be applied: i.e., we replace each $P_{ikr}Y_{ikr}$ and $Z_{ijr}P_{ikr-1}$ by new continuous variables W_{ikr} and V_{ikjr}, respectively, and enforce their equivalence by adding the following sets of constraints where M_k is the maximum value of P_{ijr} with $M_k = \prod_{j\in J}(1-p_j)^{a_{kj}} p_j^{-a_{kj}}$.

$$W_{ikr} \leq P_{ikr} + M_k\,(1 - Y_{ikr})\,,\ \forall k \in K, r = 1, \cdots, |\mathcal{J}|, i \in I, \tag{5.2a}$$
$$W_{ikr} \geq P_{ikr} + M_k\,(Y_{ikr} - 1)\,,\ \forall k \in K, r = 1, \cdots, |\mathcal{J}|, i \in I, \tag{5.2b}$$
$$W_{ikr} \leq M_k Y_{ikr},\ \forall k \in K, r = 1, \cdots, |\mathcal{J}|, i \in I, \tag{5.2c}$$
$$W_{ikr} \geq -M_k Y_{ikr},\ \forall k \in K, r = 1, \cdots, |\mathcal{J}|, i \in I, \tag{5.2d}$$
$$V_{ikjr} \leq P_{ikr-1} + M_k\,(1 - Z_{ijr})\,,\ \forall k \in K, j \in \mathcal{J}, r = 1, \cdots, |\mathcal{J}|, i \in I, \tag{5.2e}$$
$$V_{ikjr} \geq P_{ikr-1} + M_k\,(Z_{ijr} - 1)\,,\ \forall k \in K, j \in \mathcal{J}, r = 1, \cdots, |\mathcal{J}|, i \in I, \tag{5.2f}$$
$$V_{ikjr} \leq M_k Z_{ijr},\ \forall k \in K, j \in \mathcal{J}, r = 1, \cdots, |\mathcal{J}|, i \in I, \tag{5.2g}$$
$$V_{ikjr} \geq -M_k Z_{ijr},\ \forall k \in K, j \in \mathcal{J}, r = 1, \cdots, |\mathcal{J}|, i \in I. \tag{5.2h}$$

The original (SLP) is then transformed into the following mixed integer linear program, which we call the linearized sensor location problem (LSLP). It remains an NP hard problem,

but small instances can be readily solved by existing solvers (such as CPLEX).

$$\text{(LSLP)} \quad \min_{\mathbf{X},\mathbf{Y},\mathbf{Z},\mathbf{P},\mathbf{W},\mathbf{V}} \quad \sum_{j\in J} f_j X_j - \alpha \sum_{i\in I}\sum_{k\in K}\sum_{r=N}^{|\mathcal{J}|} v_i e_{ik} W_{ikr} \tag{5.3a}$$

$$\text{s.t.} \quad (5.1b)-(5.1h), (5.1j)-(5.1k), (5.2a)-(5.2h),$$

$$P_{ikr} = \sum_{j\in\mathcal{J}} p_j^{1_{[j\in J]}} V_{ikjr},\ \forall k\in K, r=1,\cdots,|\mathcal{J}|, i\in I, \tag{5.3b}$$

$$W_{ikr}\geq 0, V_{ikjr}\geq 0,\ \forall k\in K, j\in\mathcal{J}, r=1,\cdots,|\mathcal{J}|, i\in I. \tag{5.3c}$$

Owning to the formidable size of variables in the model, solving (LSLP) by commercial solvers is still not an easy job. CPLEX fails to obtain a feasible solution for a small size network even after several hours of computation. In the following section, more sophisticated solution approaches are developed to overcome such computational difficulties.

5.3 Solution Approach

5.3.1 Lagrangian relaxation

In (LSLP), the sensor location variables $\mathbf{X}$ are correlated with the sensor level assignment variables $\mathbf{Z}$ by constraints (5.1b), which is further correlated with the sensor combination assignment variables $\mathbf{Y}$ through constraints (5.1g) and (5.1h). Such correlation complicates the model and makes the computation challenging. Moreover, a great amount of continuous variables are introduced for linearization, which adds to the computation burden significantly. In the following, we will work with the original (SLP) directly to tackle the problems through various relaxation and approximation techniques. To decouple the correlation between $\mathbf{X}$ and $\mathbf{Z}$, we relax constraints (5.1b) in (SLP) and add them to objective function (5.1a) with nonnegative Lagrangian multipliers $\boldsymbol{\mu} = \{\mu_{ij}, \forall i\in I, j\in J\}$. The relaxed problem becomes:

$$\text{(RSLP)} \quad \min_{\mathbf{X},\mathbf{Y},\mathbf{Z},\mathbf{P}} \quad \sum_{j\in J}(f_j - \sum_{i\in I}\mu_{ij})X_j - \alpha\sum_{i\in I}\sum_{k\in K}\sum_{r=N}^{|\mathcal{J}|} v_i e_{ik} P_{ikr} Y_{ikr} + \sum_{i\in I}\sum_{j\in J}\mu_{ij}\sum_{r=1}^{|\mathcal{J}|} Z_{ijr} \tag{5.4a}$$

$$\text{s.t.} \quad (5.1c)-(5.1k).$$

Given $\boldsymbol{\mu}$, the optimal solution of (RSLP) provides a lower bound to the original (SLP) problem. After the above relaxation, the (RSLP) reduces to two parts, which can be solved separately. The part involving $\mathbf{X}$,

$$\min_{X_j\in\{0,1\}} \sum_{j\in J}\left(f_j - \sum_{i\in I}\mu_{ij}\right)X_j,$$

can be solved by simple inspection; i.e., given any $\{\mu_{ij}\}$, we can easily find the optimal $\mathbf{X}$ as follows:

$$X_j = \begin{cases} 1 & \text{if } f_j - \sum_{i\in I} \mu_{ij} < 0, \\ 0 & \text{otherwise.} \end{cases}$$

The part involving $\mathbf{Z}$ and $\mathbf{Y}$ can be further separated into individual sub-problems, one for each neighborhood i. For ease of notation, we omit the subscripts i in Z_{ijr}, Y_{ikr} and P_{ikr}. The sub-problem (RSLP$_i$) with respect to neighborhood i is:

$$(\text{RSLP}_i) \quad \min -\alpha \sum_{k\in K} \sum_{r=N}^{|\mathcal{J}|} v_i e_{ik} P_{kr} Y_{kr} + \sum_{j\in J} \mu_{ij} \sum_{r=1}^{|J|} Z_{jr} \tag{5.5a}$$

$$\text{s.t.} \quad \sum_{r=1}^{|\mathcal{J}|} Z_{jr} \le 1, \ \forall j \in J, \tag{5.5b}$$

$$\sum_{r=1}^{|\mathcal{J}|} Z_{jr} = 1, \ \forall j \in \tilde{J}, \tag{5.5c}$$

$$Z_{jr} = Z_{j+1,r+1}, \ \forall r = 1, \cdots, |\mathcal{J}| - 1, j \in \tilde{J} \backslash |J| + N, \tag{5.5d}$$

$$\sum_{j\in J} Z_{jr} + \sum_{s=1}^{r} Z_{|J|+1,s} = 1, \ \forall r = 1, \cdots, |\mathcal{J}|, \tag{5.5e}$$

$$Y_{kr} \le \frac{1}{N} \sum_{j\in\mathcal{J}} \sum_{s=1}^{r} a_{kj} Z_{js}, \ \forall k \in K, r = 1, \cdots, |\mathcal{J}|, \tag{5.5f}$$

$$Y_{kr} \le \sum_{j\in\mathcal{J}} a_{kj} Z_{jr}, \ \forall k \in K, r = 1, \cdots, |\mathcal{J}|, \tag{5.5g}$$

$$P_{kr} \le \sum_{j\in\mathcal{J}} p_j Z_{jr} P_{kr-1}, \ \forall k \in K, r = 1, \cdots, |\mathcal{J}|, \tag{5.5h}$$

$$P_{k0} = \prod_{j\in J} (1 - p_j)^{a_{kj}} (p_j)^{-a_{kj}}, \ \forall k \in K, \tag{5.5i}$$

$$Z_{jr}, Y_{kr} \in \{0, 1\}, \ \forall k \in K, j \in \mathcal{J}, r = 1, \cdots, |\mathcal{J}|. \tag{5.5j}$$

(RSLP$_i$) can be linearized the same way as (SLP) by adding (5.2a)-(5.2h). It is well-known that the optimal objective value of the above (RSLP) for any given $\boldsymbol{\mu}$ provides a lower bound to the original (SLP) problem. According to Proposition 7, a nearer sensor must be assigned to an earlier level at optimum. Based on this property, we can find an upper bound to the original (SLP) quickly through fixing the optimal sensor location decisions $\mathbf{X}$ obtained from the relaxed problem (RSLP) and assigning neighbourhoods accordingly. For each neighbourhood i, we sort all constructed sensors (i.e., $X_j = 1$) in ascending order of d_{ij} and assign each sensor with a level r equal to its rank in distance (i.e., $Z_{ijr} = 1$ if sensor j is installed to be the r^{th} nearest sensor to neighborhood i). Based on the level assignment of the installed sensors (the value of $\mathbf{Z}$), we enumerate all possible combinations $\mathbf{Y}$ to get their total accuracy contribution.

In the remainder of the Lagrangian relaxation solution framework, we use standard subgradient technique (Fisher, 1981) to update the multipliers μ; i.e.,

$$\mu_{ij}^{n+1} = \mu_{ij}^{n} + s_j^n \left(\sum_{r=1}^{|\mathcal{J}|} Z_{ijr}^n \leq X_j^n \right), \tag{5.6}$$

$$s_j^n = \frac{\xi^n \left(g^* - g_D(\mu^n) \right)}{\left\| \sum_{r=1}^{|\mathcal{J}|} Z_{ijr}^n - X_j^n \right\|^2}, \tag{5.7}$$

where μ_{ij}^n represents a multiplier in the n^{th} iteration, s_j^n is the step size, ξ^n is a scalar and g^* and $g_D(\mu^n)$ are the best upper bound and the current lower bound, respectively. If the Lagrangian relaxation algorithm fails to find a solution with small enough gap in a certain number of iterations, we embed it into a branch-and-bound (B&B) framework to further close the gap.

However, solving the mixed integer program (RSLP$_i$) repeatedly for each neighborhood and across Lagrangian relaxation iterations could still be time-consuming. As such, an approximation approach is developed to quickly identify lower bounds to the relaxed subproblems (RSLP$_i$).

5.3.2 Approximation of P_{kr}

Equations (5.5h) show that P_{kr} depends on P_{kr-1} and Z_{jr}, which builds connections across the decision variables and brings difficulties in solving the sub-problem. Similar to Cui et al. (2010), we approximate the variable probability P_{kr} with fixed numbers. For each combination k with its highest level element sensor assigned at level r, we select the regular sensors which are not in k and are closer to the monitored neighborhood than its most remote sensor in k. Let the number of qualified regular sensors be κ, where $\kappa < |J|$. We rank those κ regular sensors based on their failure probabilities and let $j_1, j_2, \cdots, j_\kappa$ be an ordering of the sensors such that $p_{j_1} \geq p_{j_2} \geq \cdots \geq p_{j_\kappa}$. For $N \leq r \leq N + \kappa$, we define one set of variables $\beta_{kr} = \prod_{j' \in J} (1 - p_{j'})^{a_{kj'}} \prod_{l=1}^{r-N} p_{j_l}$. While for $r < N$ or $r > N + \kappa$, we set $\beta_{kr} = 0$. Replacing P_{kr} with β_{kr}, we can modify the (RSLP$_i$) as:

$$\text{(DRSLP}_i\text{)} \quad \min -\alpha \sum_{k \in K} \sum_{r=N}^{|\mathcal{J}|} v_i e_{ik} \beta_{kr} Y_{kr} + \sum_{j \in J} \mu_{ij} \sum_{r=1}^{|J|} Z_{jr} \tag{5.8a}$$

$$\text{s.t.} \quad \text{(5.5b)} - \text{(5.5g)}, \text{(5.5j)}.$$

Proposition 8. *The solution to (DRSLP$_i$) provides a lower bound to the relaxed subproblem (RSLP$_i$).*

Proof. (DRSLP$_i$) is constructed through replacing P_{kr} with β_{kr} and removing constraints (5.5h)-(5.5i). As removing constraints enlarges the feasible region of (RSLP$_i$), it will never increase the objective value of this minimization problem. The effect of replacing P_{kr} with β_{kr} in the objective function is studied under two scenarios where $Y_{kr} = 1$ or $Y_{kr} = 0$. If $Y_{kr} = 0$, the value of β_{kr} won't affect the optimal objective value as $\beta_{kr} Y_{kr} = P_{kr} Y_{kr} = 0$.

When $r < N$, $Y_{kr} = 0$ must hold since the most remote sensor in k must be assigned at a higher level than N. When $r > N + \kappa$, we also have $Y_{kr} = 0$ since a sensor can't be assigned to a level higher than the total number of sensors who are closer than it. When $Y_{kr} = 1$, the probability of using combination k is $P_{kr} = \prod_{j\in J}(1-p_j)^{a_{kj}} \prod_{s\le r}\left[\sum_{j\in\mathcal{J}} Z_{ijs}(p_j)^{1-a_{kj}}\right]$ according to the proof to Proposition 1. P_{kr} calculates the probability to have the N sensors in k working and $r - N$ regular sensors disrupted. Based on the construction of β_{kr} where $N \le r \le N + \kappa$, β_{kr} provides an upper bound to P_{kr} if $Y_{kr} = 1$. Therefore, $\beta_{kr}Y_{kr}$ must be an upper bound to $P_{kr}Y_{kr}$ for any $k \in K, r = N, \cdots, |\mathcal{J}|$ and the optimal objective value of (DRSLP$_i$) is a lower bound to the optimal objective value of (RSLP$_i$). □

5.3.3 Approximation of Y_{kr}

In this section, constraints (5.5f) and (5.5g) are replaced by a simple equality formula to decouple the connection between Z_{jr} and Y_{kr}. For a neighborhood i, the Lagrangian multiplier μ_{ij} in (5.8a) can be interpreted as an extra installation cost of sensor j and the first term $\sum_{k\in K}\sum_{r=N}^{|\mathcal{J}|} v_i e_{ik}\beta_{kr}Y_{kr}$ represents the total accuracy contribution of the installed sensors to the system. Given that the N dummy sensors are always installed and assigned to the highest levels, we let the regular sensors be installed sequentially from level 1 to level $|J|$. Let binary variables $\{y_{krt} : \forall k, r\}$ be the combination assignments when t regular sensors are installed. $y_{krt} = 1$ if combination k is used ($Y_{kr} = 1$) given t regular sensors are installed. As such, the total accuracy can be decomposed into $|J|$ portions, one for each level t. The tth portion calculates the additional benefits contributed by installing a sensor j at level t.

The accuracy contribution of all sensors, i.e. the first term in (5.8a) omitting the constant v_i, can be reformulated as:

$$AC = \sum_{k\in K}\sum_{r=N}^{|\mathcal{J}|} e_{ik}\beta_{kr}Y_{kr} = \sum_{r=N}^{N}\sum_{k\in K} e_{ik}\beta_{kr}y_{kr0} + \sum_{t=1}^{|J|}\left[\sum_{r=N}^{N+t}\sum_{k\in K} e_{ik}\beta_{kr}y_{krt} - \sum_{r=N}^{N+t-1}\sum_{k\in K} e_{ik}\beta_{kr}y_{kr,t-1}\right], \tag{5.9}$$

where $\sum_{r=N}^{N}\sum_{k\in K} e_{ik}\beta_{kr}y_{kr0}$ represents the accuracy contribution of the N dummy sensors, which is 0 by definition; $\sum_{r=N}^{N+t}\sum_{k\in K} e_{ik}\beta_{kr}y_{krt}$ states the accuracy level of the system with N dummy sensors and t regular sensors; difference of the two terms in the parentheses represents the accuracy improvement by adding one regular sensor at level t given that $t-1$ regular sensors are already installed. If we expand the summation terms in (5.9), the intermediate accuracy level $\sum_{r=N}^{N+t}\sum_{k\in K} e_{ik}\beta_{kr}y_{krt}$ for any t where $t < |J|$ will be cancelled out. As such, AC will be simplified as $AC = \sum_{r=N}^{N+|J|}\sum_{k\in K} e_{ik}\beta_{kr}y_{krt} = \sum_{k\in K}\sum_{r=N}^{|\mathcal{J}|} e_{ik}\beta_{kr}Y_{kr}$, which mathematically proves the second equivalence in (5.9).

Adding one regular sensor j at level t is equivalent to replacing the dummy sensor $|J|+1$ with j and moving all the dummy sensors upward by one level. The resultant accuracy difference for the two systems with t or $t-1$ regular sensors can be calculated by updating the accuracy level of every combination relating to sensor j. The total system accuracy is

reformulated as:

$$AC = \sum_{t=1}^{|J|} \sum_{r=\max\{t,N\}}^{N+t} \sum_{k\in K} \left(e_{ik}\beta_{kr} - (1-p_j)e_{ik'}\beta_{k'r}\right) 1_{[J_k \backslash J_{k'}=j \&\& b_{kj}=1]} y_{krt}, \tag{5.10}$$

where J_k represents the set of regular sensors in combination k and parameter $b_{kj} = 1$ if j is the most remote regular sensor in k and is 0 otherwise. In the indicator function $1_{[\cdot]}$, $J_k \backslash J_{k'} = j$ identifies the updated combination k who has one additional regular sensor j comparing with an existing combination k'; $b_{kj} = 1$ forces this sensor j to be the most remote regular sensor in k. Inserting j at level t brings new combinations – the term $e_{ik}\beta_{kr}1_{[J_k \backslash J_{k'}=j \&\& b_{kj}=1]}$ calculates the accuracy contribution of a new combination k which uses j as its most remote regular sensor. Moreover, inserting j at level t changes the assignment level of all dummy sensors. An existing combination k' who contains dummy sensors in the old system (with $t-1$ regular sensors) will be used in the new system (with t regular sensors) only when sensor j is disrupted – the term $(1-p_j)e_{ik'}\beta_{k'r}1_{[J_k \backslash J_{k'}=j \&\& b_{kj}=1]}$ in (5.10) calculates the contribution deduction due to the probability decrease of using combination k'.

Fig. 5.1 illustrates the decomposition process in order to calculate the total accuracy level of the system with 3 dummy sensors and $|J|$ regular sensors. Sensors $a, b, c, \cdots, j$ are sequentially added to the system to calculate their contribution. For example, contribution of sensor c is equal to the difference in system accuracy when $t = 3$ or $t = 2$. Let the element sensors-combination index be defined as: abc-1, abD_1-2, acD_1-3, bcD_1-4, aD_1D_2-5, bD_1D_2-6, cD_1D_2-7, $D_1D_2D_3$-8. The system accuracy when $t = 3$ and $t = 2$ respectively are

$$AC|_{t=3} = \sum_{r=N}^{N+3} \sum_{k\in K} e_{ik}\beta_{kr}y_{kr3} = e_1\beta_{13} + e_2\beta_{24} + e_3\beta_{34} + e_4\beta_{44} + e_5\beta_{55} + e_6\beta_{65} + e_7\beta_{75} + e_8\beta_{86},$$

$$AC|_{t=2} = \sum_{r=N}^{N+2} \sum_{k\in K} e_{ik}\beta_{kr}y_{kr2} = e_2\beta_{23} + e_5\beta_{54} + e_6\beta_{64} + e_8\beta_{85}.$$

The contribution of inserting sensor c at level $t = 3$ is

$$\begin{aligned} AC|_{t=3} - AC|_{t=2} = {} & [e_1\beta_{13} - e_2(\beta_{23} - \beta_{24})] + [e_3\beta_{34} - e_5(\beta_{54} - \beta_{55})] \\ & + [e_4\beta_{44} - e_6(\beta_{64} - \beta_{65})] + [e_7\beta_{75} - e_8(\beta_{85} - \beta_{86})], \end{aligned} \tag{5.11}$$

where each combination k, $k = 1, 3, 4$ or 7, has element sensor c as its most remote regular sensor, namely $b_{kc} = 1$; the combinations paired up in brackets (1 and 2; 3 and 5; 4 and 6; 7 and 8) have the same regular sensors except for sensor c, namely $J_k \backslash J_{k'} = c$. According to the construction of β_{kr}, the paired probabilities in the parentheses satisfy $\beta_{24} = p_c\beta_{23}, \beta_{55} = p_c\beta_{54}, \beta_{65} = p_c\beta_{64}$ and $\beta_{86} = p_c\beta_{85}$. Substituting $\beta_{k'r+1}$ by $p_c\beta_{k'r}$ in the parentheses, we can simplify (5.11) as follows:

$$\begin{aligned} AC|_{t=3} - AC|_{t=2} = {} & [e_1\beta_{13} - e_2\beta_{23}(1-p_c)] + [e_3\beta_{34} - e_5\beta_{54}(1-p_c)] \\ & + [e_4\beta_{44} - e_6\beta_{64}(1-p_c)] + [e_7\beta_{75} - e_8\beta_{85}(1-p_c)]. \end{aligned} \tag{5.12}$$

For any t and r satisfying $1 \le t \le |J|$, $\max\{t, N\} \le r \le N + t$, a combination k fulfilling $1_{[J_k \backslash J_{k'}=j \&\& b_{kj}=1]} y_{krt} = 1$ must have j as its most remote regular sensor, have its most remote

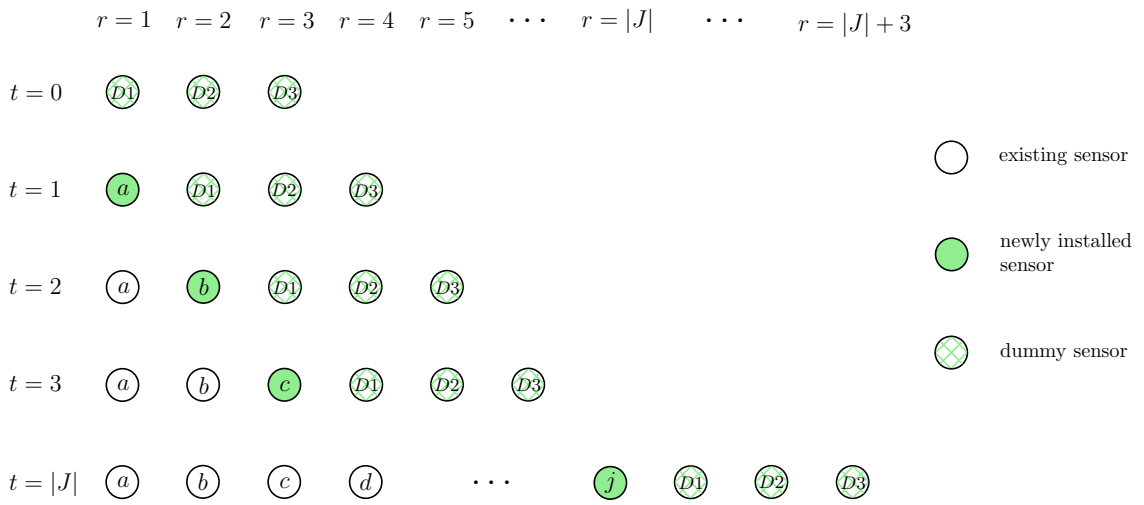

Figure 5.1: Decomposition scheme of sensor contributions.

sensor assigned at level r and thus have $r-t$ dummy sensors. Hence we only need to choose $N-1-(r-t)$ regular sensors from the $t-1$ alternatives to get a qualified k. We denote the maximum number of such updated combinations by $n_{tr} = \binom{t-1}{N-1-r+t}$. We also let $C_{ijrk} = (e_{ik}\beta_{kr} - (1-p_j)e_{ik'}\beta_{k'r})\,1_{[J_k \setminus J_{k'}=j \&\& b_{kj}=1]}$. For each $1 \le t \le |J|$, $\max\{t, N\} \le r \le N+t, 1 \le j \le |J|$, let $k_1, k_2, \cdots, k_{|K|}$ be an ordering of the coefficients C_{ijrk} such that $C_{ijrk_1} \ge C_{ijrk_2} \ge \cdots \ge C_{ijrk_{|K|}}$. We define $\gamma_{ijt} = \sum_{r=\max\{t,N\}}^{N+t} \sum_{l=1}^{n_{tr}} C_{ijrk_1}$. Based on the construction of γ_{ijt}, $\gamma_{ijt}Z_{jt}$ provides an upper bound to the accuracy improvement from inserting sensor j at level t. Replacing AC by its upper bound $\sum_{t=1}^{|J|}\sum_{j\in J}\gamma_{ijt}Z_{jt}$, (DRSLP$_i$) further reduces to the following simple assignment problem (TRSLP$_i$), which can be solved by the Hungarian algorithm.

$$\text{(TRSLP}_i\text{)} \quad \min -\sum_{t=1}^{|J|}\sum_{j\in\mathcal{J}} v_i\gamma_{ijt}Z_{jt} + \sum_{r=1}^{|J|}\sum_{j\in\mathcal{J}}\mu_{ij}Z_{jr} \tag{5.13a}$$

$$\text{s.t.} \quad \text{(5.5b)} - \text{(5.5e)},$$

$$Z_{jr} \in \{0,1\},\ \forall j \in \mathcal{J}, r = 1, \cdots, |\mathcal{J}|. \tag{5.13b}$$

Proposition 9. *The solution to (TRSLP$_i$) provides a lower bound to the relaxed sub-problem (RSLP$_i$).*

Proof. (TRSLP$_i$) is constructed from (DRSLP$_i$) through replacing $\sum_{k\in K}\sum_{r=N}^{|\mathcal{J}|} v_i e_{ik}\beta_{kr}Y_{kr}$ with $\sum_{r=1}^{|J|}\sum_{j\in\mathcal{J}} v_i\gamma_{ijr}Z_{jr}$ and removing constraints (5.5f)-(5.5g). As removing constraints enlarges the feasible region of (DRSLP$_i$), it will never increase the objective value of this minimization problem. Based on the construction of γ_{ijr}, $\sum_{r=1}^{|J|}\sum_{j\in\mathcal{J}} v_i\gamma_{ijr}Z_{jr}$ provides an upper bound to $\sum_{k\in K}\sum_{r=N}^{|\mathcal{J}|} v_i e_{ik}\beta_{kr}Y_{kr}$. Therefore, the optimal objective value of (TRSLP$_i$) is a lower bound to the optimal objective value of (DRSLP$_i$). Together with the result in Proposition 8, the solution of (TRSLP$_i$) is a lower bound to the relaxed sub-problem (RSLP$_i$). □

5.4 Numerical Case Studies

To demonstrate the applicability of the proposed models and algorithms, we apply them to a series of hypothetical grid networks as well as a more realistic Wi-Fi Access Point (AP) network in Terminal 5 of the Chicago O'Hare Airport. The proposed solution algorithms are programmed in C++ and run on a 64-bit Intel i7-3770 computer with 3.40 GHz CPU and 8G RAM. The linearized LSLP are tackled by commercial solver CPLEX 12.4 using up to 4 threads. We set the overall solution time limit to be 3600 seconds.

5.4.1 Hypothetical grid networks

A 2×3 rectangle grid network and six $n \times n$ square grid networks for $n \in \{3, 4, 5, 6, 7, 8\}$ are generated to represent various hypothetical study regions. In the square grid networks, each network contains $(n-1)^2$ cells. The four corners of each cell represent the candidate sensor locations, adding to a total number of n^2 candidate sensor locations. The centroid of each cell is constructed to be a surveillance neighborhood, adding to $(n-1)^2$ neighborhoods. The network layouts are shown in Fig. 5.2. We omit the surveillance neighborhoods in some of the larger networks (i.e., from 5×5 to 8×8) for cleaner figure presentation. The edge length of each cell is set to 1. The customer demand of each neighborhood i is $v_i = 10$, the value of α is 1, and the fixed sensor installment cost is 10. The value of coverage is 1. The site-dependent failure probability of sensor location j is assumed to vary from 0.1 to 0.2 based on its Euclidean distance to the center of the study region. The sensor(s) located nearest to the center have the highest failure probability of 0.2, the sensor(s) located farthest away have the lowest probability of 0.1. The failure probability of a sensor in the middle linearly decreases with the distance to the center. Each combination uses $N = 3$ sensors. Combination accuracy is computed based on $e_{ik} = \sum_{j \in J} \frac{a_{kj}}{(d_{ij})^2+\epsilon}, \forall i \in I, k \in K$, where d_{ij} is the Euclidean distance and ϵ is a small positive number. The reliable sensor location problems are solved by two approaches: (i) CPLEX directly applied to the mixed-integer linear program LSLP and (ii) Lagrangian relaxation based branch-and-bound method with approximation algorithm (LR+B&B+Approx.). Table 5.1 summarizes and compares the results from the two approaches.

As one can observe from the table, the solution time and solution quality rapidly deteriorate with the network size, due to the significant increase in the number of integer variables $\mathbf{Y}$ and $\mathbf{Z}$. CPLEX could only find the optimal solution to the specifically constructed small rectangle network. In the second case, CPLEX identified a feasible solution but failed to find a lower bound, despite its rather small network size. For the other larger networks, CPLEX ran out of memory and could not provide a feasible solution or a lower bound. In contrast, optimal solutions to the first 6 cases were obtained by the LR+B&B+Approx. approach within 3 minutes. For the 8×8 network, there is a residue gap of 2.32% after 1 hour of computation.

In Fig. 5.2, the installed sensors in the best solutions from the LR+B&B+Approx. approach are marked green. We can observe that more sensors are installed in order to monitor a larger region. In the first three cases, the installed sensors are clustered in the center of the study region mainly owning to their short distances to all the surveillance neighborhoods, which provides better accuracy with a limited number of sensors. In the

Table 5.1: Algorithm performance comparison for the 7 hypothetical cases.

	Sensor network	Neighborhood network	No. of sensors	Final UB	Final LB	Final gap (%)	CPU time (s)
CPLEX	2×3	1×2	2	-1.31	-1.30	0	1.6
	3×3	2×2	4	-14.01	fail	100	3600
	4×4	3×3	-	-	-	fail	3600
	$\cdots$	$\cdots$	-	-	-	fail	3600
	8×8	7×7	-	-	-	fail	3600
LR+B&B	2×3	1×2	2	-1.31	-1.31	0	0.1
	3×3	2×2	4	-24.28	-24.28	0	0.1
	4×4	3×3	5	-77.38	-77.38	0	0.4
	5×5	4×4	8	-150.78	-150.78	0	0.8
	6×6	5×5	14	-243.48	-243.48	0	38
	7×7	6×6	21	-360.99	-360.99	0	181
	8×8	7×7	29	-489.07	-500.41	2.32	3600

four larger cases, it is interesting to observe that the sensors are installed symmetrically along the diagonal lines. Moreover, no sensor is installed immediately next to the boundary, while all nearby candidate locations (e.g., slightly closer to the region center) are selected. Those properties indicate the possibility to decompose a larger yet symmetrical network into several smaller ones to obtain the sensor deployment effectively. Take the 8×8 network for example, if the sensor at coordinate (1, 1) is installed (assuming the bottom left sensor is located at the origin (0, 0)), then we can automatically install the sensor at (6, 6), which could significantly speed up solution process. As such, the proposed algorithm could possibly handle an even larger symmetrical network efficiently.

Fig. 5.3 illustrates how the sensor combinations are used by the customers in neighborhood $i = 1$ (i.e., indicated by the dark star in Fig. 5.2) in the 3-by-3 case. The installed sensors 4, 5, 6, 8 are assigned to levels 1 - 4 based on distance, while the dummy sensors are assigned at levels 5 - 7. Some representative combinations are illustrated in this figure. For example, the shaded combination ($k = u$) will be used to monitor this neighborhood if and only if sensors 5, 6 and 8 are functioning and sensor 4 has been disrupted. The most remote sensor in this combination is 8, which is ranked at level $r = 4$. Hence combination u corresponds to backup level $r = 4$ and it will be used with a probability of $P_{1u4} = p_4(1 - p_5)(1 - p_6)(1 - p_8) = 0.15 \times 0.8 \times 0.75 \times 0.75 = 0.0675$ based on the sensor failure probability settings.

5.4.2 Wi-Fi Access Point Network for Chicago O'Hare Airport Terminal 5

The Chicago O'Hare International Airport is one of the busiest airports in the world. In June 2016 alone, a total of 7,329,084 travelers passed through the airport (CDA, 2016). Boingo, the O'Hare Airport's Wi-Fi provider, has pioneered a new "S.M.A.R.T" network design

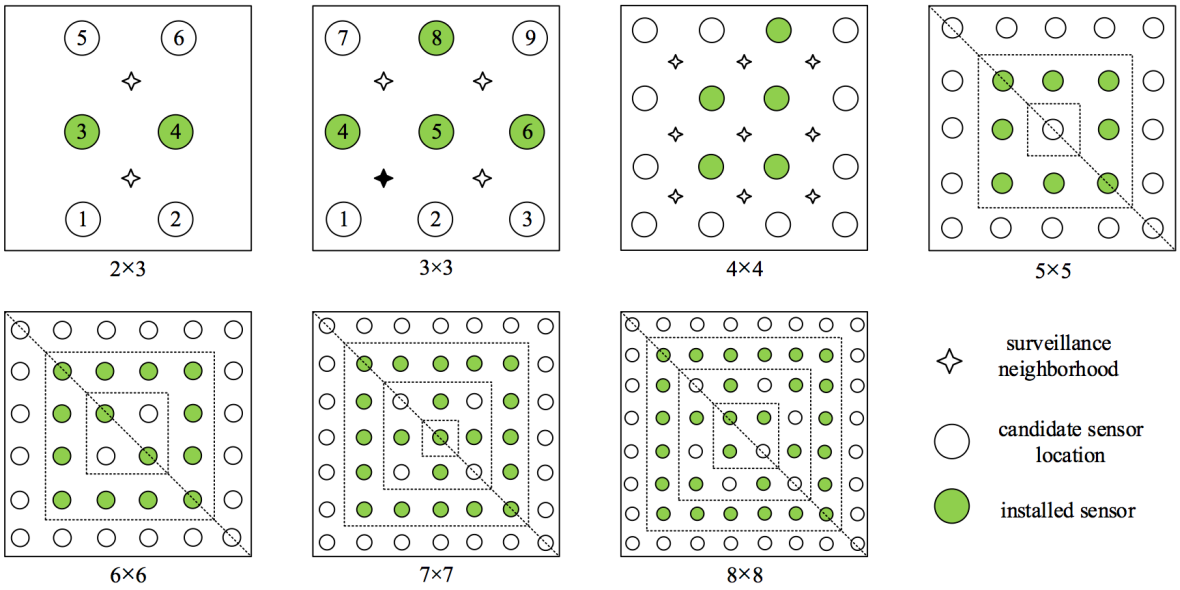

Figure 5.2: Optimal sensor deployment for the 7 hypothetical cases.

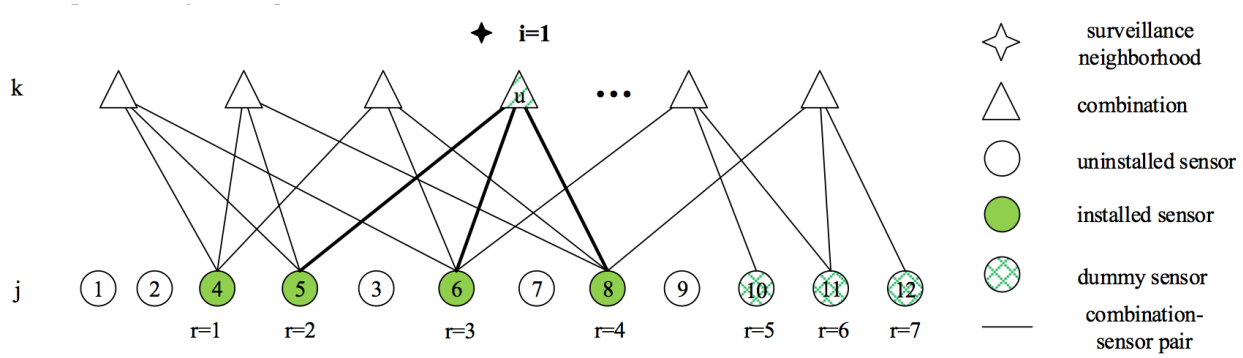

Figure 5.3: Detailed assignment plan of sensor combinations to neighborhood $i = 1$.

(Secure, Multi-platform, Analytics-Driver, Responsive and Tiered) which allows increased access point density for location-based services like queue management, advertising, and passenger guidance. Such a system is expected to deliver valuable business intelligence and actionable insights to enable high-quality passenger service.

In this case study, we select the departure level of Terminal 5 to investigate Wi-Fi Access Point deployment for better location-based services. Terminal 5 contains Concourse M, which is used for all international arrivals and part of the international departures (those of most non-US carriers). We select 52 heavy-traffic venues inside the terminal, including 21 gates, 10 restaurants, 13 shops, 6 airline lounges and 1 security check point, as key surveillance neighborhoods; see Fig. 5.4. Average hourly surveillance demand at each neighborhood is assumed to be proportional to the local passenger flow per the monthly statistics report of the Chicago Department of Aviation (CDA, 2016). The terminal is further divided into square

cells with an edge length of 10 meters[a]. The corners of every square cell are considered candidate sensor/AP locations. There are 222 candidate locations in total. Boingo uses Cisco's AP systems with chipsets featuring 802.11ac standard, with an installation cost of about US$200 each (maintenance cost or other capital cost is not considered). The received signal strength (RSS) follows a logarithm function of distance (Shchekotov, 2014), and hence we assume a combination of sensors will yield an accuracy measure of $e_{ik} = \sum_{j \in J} 22 a_{kj} \log_{10} \left(\frac{40}{d_{ij}+\epsilon} \right), \forall i \in I, k \in K$, where d_{ij} is the Euclidean distance in meters, and 40 (meters) is the effective range of a Cisco AP. Each combination uses $N = 3$ sensors.

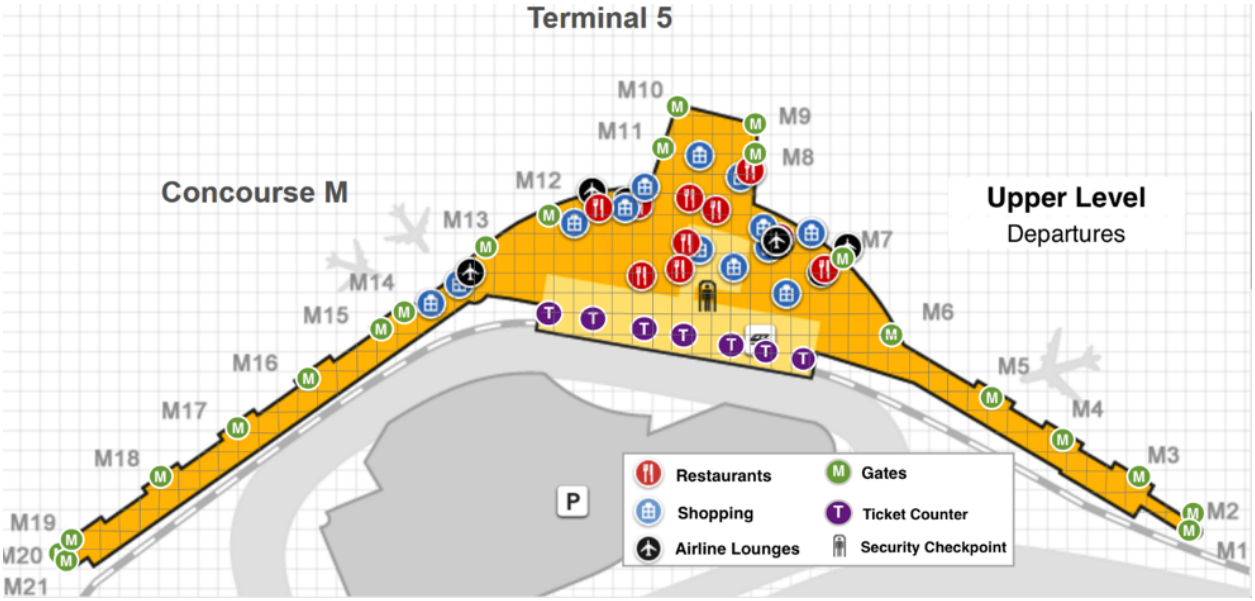

Figure 5.4: O'Hare terminal 5 map (Source: `http://www.flychicago.com/OHare/EN/AtAirport/map`).

We consider site-independent, yet low, median and high levels of sensor disruption probabilities; i.e., $p_j = p \in \{0.01, 0.2, 0.5\}, \forall j$. The system performance measures under these scenarios are presented in Table 5.2. All results are obtained from the proposed LR+B&B+Approx algorithm within 3600 seconds. Overall, a higher sensor failure probability leads to a fewer number of installed sensors as well as a significant deterioration in the best objective value (i.e., the final UB). The residue gap also increases slightly with the failure probability. The value of α reflects the tradeoff between the positioning accuracy e_{ik} and the unit sensor installation cost f_j. Very often the value of α may be subject to speculation and interpretation. We thus conduct sensitivity analysis over α while keeping the same formula for e_{ik}, and when $f_j = 200, p_j = 0.01$. When α increases from 0.025 to 0.4, the number of installed sensors increases drastically from 17 to 111, and the objective function drops by about two orders of magnitude. These results indicate that the benefits of deploying more sensors far outweigh the installation costs in the O'hare case study.

[a]Generally, access points should be separated by at least 10 feet in order to reduce adjacent channel interference, and it is recommended that APs are mounted at 30-40 feet (or approximately 10 meters) from one another (`https://supportforums.adtran.com/docs/DOC-7257`).

(a) $p = 0.01$

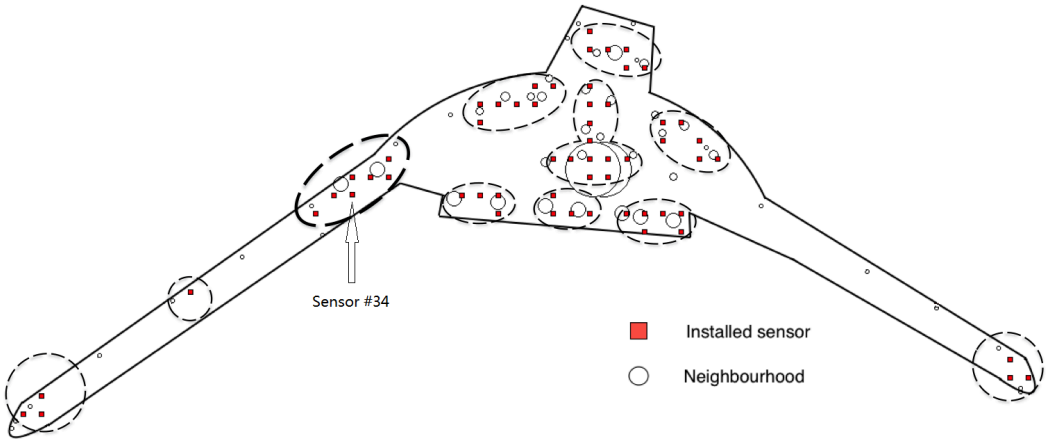

(b) $p = 0.2$

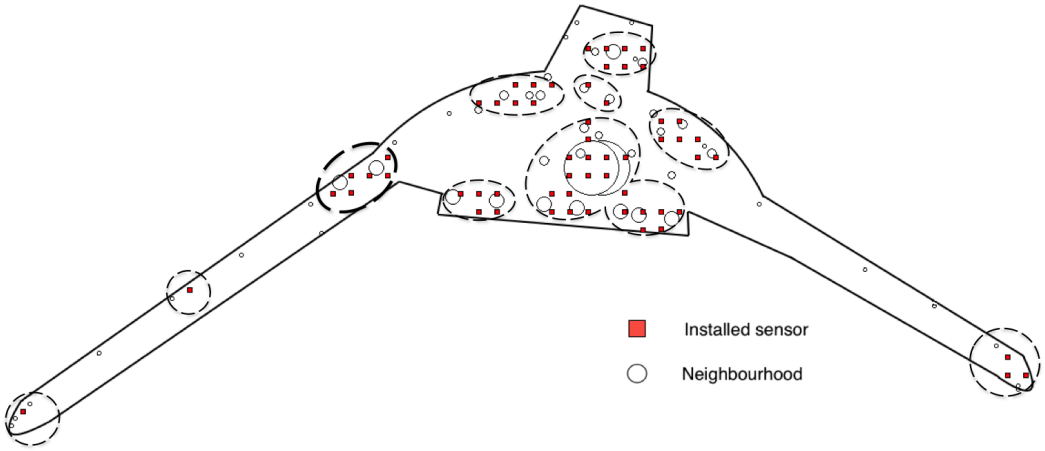

(c) $p = 0.5$

Figure 5.5: Optimal sensor locations under (a) low, (b) median, and (c) high sensor disruption probabilities.

Table 5.2: Performance measures for the O'Hare Airport case.

Failure prob	α	No. of candidate sensors	No. of neighbor -hoods	No. of installed sensors	Final UB	Final LB	Final gap(%)	CPU time(s)
0.01	0.1	222	52	61	-32306.5	-33795.4	4.6	3600
0.2	0.1	222	52	58	-27720.0	-29147.4	5.1	3600
0.5	0.1	222	52	56	-18761.6	-19786.5	5.5	3600
0.01	0.025	222	52	17	-3417.3	-3739.3	8.5	3600
0.01	0.050	222	52	34	-11732.2	-12355.9	5.0	3600
0.01	0.2	222	52	92	-79741.0	-82682.9	3.6	3600
0.01	0.4	222	52	111	-180132.0	-186298.0	3.3	3600

The optimal sensor locations for the three cases are shown in Fig. 5.5. The solid-line circles represent the surveillance neighborhoods, and their size indicates the volume of surveillance demand. The installed sensors are marked by shaded squares. They can be roughly clustered into groups, as shown by the dotted ellipses, in which the distances between any adjacent sensors do not exceed 15 meters – i.e., these sensors are likely to provide effective backups to each other. Under a low failure probability, the installed sensors can be clustered into 16 groups, and the sensor nearest to every surveillance neighborhood is always installed. This forms a rather dispersed sensor network overall. In the two wings of the airport, 5 isolated sensors are installed in order to monitor their most adjacent neighborhoods, although these sensors only make marginal contributions to other neighborhoods.

When the sensor disruption probability increases to 0.2 and 0.5, the number of sensor groups drops to 12 and 10, respectively, and fewer isolated sensors are installed. Sensors within a group tend to become more clustered so as to better back each other up. This is clearly illustrated, for example, by the highlighted group (see the bold ellipse). Meanwhile, sensors also tend to cluster around the center of the concourse where demand is the heaviest. For example, 10 sensors are clustered within 20 meters from at the security checkpoint when $p = 0.5$, while there are only 7 when $p = 0.2$ and 5 when $p = 0.01$. In summary, under higher failure probability, the model tends to yield a higher degree of sensor clustering especially around the heavy-demand neighborhoods, while at the same time a smaller total number of sensors would be installed especially around the less crowded neighborhoods.

A closer look at the sensor deployment in the highlighted group (bold ellipse) reveals some interesting points. When p increases from 0.01 to 0.2, sensor #29 is removed from the low demand neighborhood while sensor #34 is added to the high demand neighborhood. Such changes can be explained by the marginal costs and marginal benefits of these sensors. In the case of $p = 0.2$, if we add sensor #29 back, the marginal coverage benefit is \$185.7, which is lower than its installation cost \$200. On the other hand, if we remove sensor #34, the coverage accuracy loss is \$252.1 when $p = 0.2$, which is higher than \$200. This result can be generalized. When the disruption probability increases, the sensors become less reliable, and more sensors will be needed to maintain the same coverage accuracy. In high-demand neighborhoods, the net marginal benefit of installing an extra "back-up" sensor (e.g., to

maintain the accuracy) may be high enough to outweigh the installation cost. We hence may observe an increase in the sensor number near those neighborhoods. In low-demand neighborhoods, however, the net marginal benefit of adding a sensor may not justify its cost, and we will therefore expect reduction of sensors. In other words, the spatial distribution of sensors tends to be more clustered near high-demand neighborhoods under high disruption probabilities, but at the same time more sparse near low-demand neighborhoods. The total number of sensors across all neighborhoods may not exhibit a monotonic relationship with the value of p.

Chapter 6

Conclusion

Railroad has witnessed significant increases in shipment of hazmat such as oil, gas, and ethanol in recent years. Accordingly, railroad related incidents, particularly those involving hazardous material (hazmat), has caused severe consequences and posed significant threats to safety, public health and the environment. As many hazmat trains these days are passing through Chicago, the Twin Cities, and many other towns, rail safety is becoming a huge issue in Midwestern states such as Illinois, Wisconsin, and Minnesota.

Considering the huge potential impacts of rail safety issues, the planning of emergency responses to railroad incidents, i.e., developing coordinated and efficient response to emergence and determining optimal operations for a random combination of large-scale incidents, is now a very important topic. This planning problem essentially involves facilty location and resource assignment decisions to balance between fixed investment of facility construction and transportation cost of serving demands. This project aimed at strategically positioning and allocating emergency responders and resources in anticipation of potential accidents in a region that may be impacted by rail incidents.

In particular, we develop a series of mathematical models and efficient solution techniques to enable systematic analysis of the emergency response system associated with railroad incidents. We develop advanced reliability models to characterize and guide positioning and utilization of first-responder resources taking into account its own vulnerability and complex interactions among multiple agencies and jurisdictions, e.g., positioning and allocation of emergency responders and resources in anticipation of potential accidents along spatially distributed railroad networks. Based on the results of these models, we provide fundamental understanding, operational guidelines, and practical tools to policy makers (e.g., federal and state agencies) to induce socio-economically favorable systems that support safe and efficient railroad industry operations.

References

Ahmed, A., Watling, D., & Ngoduy, D. (2014). Significance of sensor location in real-time traffic state estimation. *Procedia Engineering*, *77*, 114-122.

Atamtürk, A., Berenguer, G., & Shen, Z.-J. M. (2012). A conic integer programming approach to stochastic joint location-inventory problems. *Operations Research*, *60*(2), 366-381.

Berman, O., & Krass, D. (2011). On n-facility median problem with facilities subject to failure facing uniform demand. *Discrete Applied Mathematics*, *159*(6), 420-432.

Berman, O., Krass, D., & Menezes, M. B. C. (2007). Facility reliability issues in network p-median problems: Strategic centralization and co-location effects. *Operations Research*, *55*(2), 332-350.

Berman, O., Krass, D., & Menezes, M. B. C. (2009). Locating facilities in the presence of disruptions and incomplete information. *Decision Sciences*, *40*(4), 845-868.

Berman, O., Krass, D., & Menezes, M. B. C. (2013). Location and reliability problems on a line: Impact of objectives and correlated failures on optimal location patterns. *Omega*, *41*(4), 766-779.

Brualdi, R. A. (2004). *Introductory combinatorics, 4/e.* Pearson Education India.

CDA. (2016). *Chicago department of aviation.* `http://www.flychicago.com/ohare/en/home/Pages/default.aspx`. (Accessed: 2016-08-15)

Chen, Q., Li, X., & Ouyang, Y. (2011). Joint inventory-location problem under the risk of probabilistic facility disruptions. *Transportation Research Part B: Methodological*, *45*(7), 991-1003.

Church, R. L., Scaparra, M. P., & Middleton, R. S. (2004). Identifying critical infrastructure: The median and covering facility interdiction problems. *Annals of the Association of American Geographers*, *94*(3), 491-502.

Clouqueur, T., Phipatanasuphorn, V., Ramanathan, P., & Saluja, K. K. (2003). Sensor deployment strategy for detection of targets traversing a region. *Mobile Networks and Applications*, *8*(4), 453-461.

Crummy, B. (2013). *Mile-long train carrying crude oil derails, explodes in north dakota.* http://usnews.nbcnews.com/_news/2013/12/30/22113442-mile-long-train-carrying-crude-oil-derails-explodes-in-north-dakota?lite. (Accessed: 2014-03-17)

Cui, T., Ouyang, Y., & Shen, Z.-J. M. (2010). Reliable facility location design under the risk of disruptions. *Operations Research*, *58*(4), 998-1011.

Danczyk, A., Di, X., & Liu, H. X. (2016). A probabilistic optimization model for allocating freeway sensors. *Transportation Research Part C: Emerging Technologies*, *67*, 378-398.

Daskin, M. S. (2011). *Network and discrete location: Models, algorithms, and applications* (2nd ed.). New York: John Wiley & Sons.

De Stefano, M., Gherlone, M., Mattone, M., Di Sciuva, M., & Worden, K. (2015). Optimum sensor placement for impact location using trilateration. *Strain*, *51*(2), 89-100.

Drezner, Z. (1995). *Facility location: A survey of applications and methods.* New York: Springer Verlag.

Eisenman, S., Fei, X., Zhou, X., & Mahmassani, H. (2006). Number and location of sensors for real-time network traffic estimation and prediction: sensitivity analysis. *Transportation Research Record: Journal of the Transportation Research Board*, *1964*, 253-259.

Erdemir, E. T., Batta, R., Spielman, S., Rogerson, P. A., Blatt, A., & Flanigan, M. (2008). Location coverage models with demand originating from nodes and paths: Application to cellular network design. *European Journal of Operational Research*, *190*(3), 610-632.

Fei, X., & Mahmassani, H. S. (2011). Structural analysis of near-optimal sensor locations for a stochastic large-scale network. *Transportation Research Part C: Emerging Technologies*, *19*(3), 440-453.

Fisher, M. L. (1981). The lagrangian relaxation method for solving integer programming problems. *Management Science*, *27*(1), 1-18.

Geetla, T., Batta, R., Blatt, A., Flanigan, M., & Majka, K. (2014). Optimal placement of omnidirectional sensors in a transportation network for effective emergency response and crash characterization. *Transportation Research Part C: Emerging Technologies*, *45*, 64-82.

Gentili, M., & Mirchandani, P. (2012). Locating sensors on traffic networks: Models, challenges and research opportunities. *Transportation Research Part C: Emerging Technologies*, *24*, 227-255.

Gold, R., & Stevens, L. (2014). *U.S. issues emergency testing order to crude oil rail shippers: Move by transportation department response to crude-by-rail accidents.* http://on.wsj.com/1WQaKvt. (Accessed: 2014-03-17)

Gueye, S., & Menezes, M. B. C. (2015). General asymptotic and submodular results for the median problem with unreliable facilities. *Operations Research Letters*, *43*(5), 519-521.

He, S. (2013). A graphical approach to identify sensor locations for link flow inference. *Transportation Research Part B: Methodological*, *51*, 65-76.

Huang, R., Kim, S., & Menezes, M. B. C. (2010). Facility location for large-scale emergencies. *Annals of Operations Research*, *181*(1), 271-286.

Li, X., & Ouyang, Y. (2010). A continuum approximation approach to reliable facility location design under correlated probabilistic disruptions. *Transportation Research Part B: Methodological*, *44*(4), 535-548.

Li, X., & Ouyang, Y. (2011). Reliable sensor deployment for network traffic surveillance. *Transportation Research Part B: Methodological*, *45*(1), 218-231.

Li, X., & Ouyang, Y. (2012). Reliable traffic sensor deployment under probabilistic disruptions and generalized surveillance effectiveness measures. *Operations Research*, *60*(5), 1183-1198.

Li, X., Ouyang, Y., & Peng, F. (2013). A supporting station model for reliable infrastructure location design under interdependent disruptions. *Transportation Research Part E: Logistics and Transportation Review*, *60*, 80-93.

Liberatore, F., Scaparra, M. P., & Daskin, M. S. (2011). Analysis of facility protection strategies against an uncertain number of attacks: The stochastic r-interdiction median problem with fortification. *Computers & Operations Research*, *38*(1), 357-366.

Liberatore, F., Scaparra, M. P., & Daskin, M. S. (2012). Hedging against disruptions with ripple effects in location analysis. *Omega*, *40*(1), 21-30.

Liu, C., Fan, Y., & Ordóñez, F. (2009). A two-stage stochastic programming model for transportation network protection. *Computers & Operations Research*, *36*(5), 1582-1590.

Lu, M., Ran, L., & Shen, Z.-J. M. (2015). Reliable facility location design under uncertain correlated disruptions. *Manufacturing & Service Operations Management*, *17*(4), 445-455.

Mirchandani, P. B., Li, J.-Q., & Long, Y. (2010). Locating a surveillance infrastructure in and near ports or on other planar surfaces to monitor flows. *Computer-Aided Civil and Infrastructure Engineering*, *25*(2), 89-100.

NBC News. (2013). *Danger on the tracks: Unsafe rail cars carry oil through us towns.* `http://www.nbcnews.com/news/other/danger-tracks-unsafe-rail-cars-carry-oil-through-us-towns-f8C11082948`. (Accessed: 2014-03-17)

Ouyang, Y., Li, X., Barkan, C. P. L., Kawprasert, A., & Lai, Y.-C. (2009). Optimal locations of railroad wayside defect detection installations. *Computer-Aided Civil and Infrastructure Engineering*, *24*(5), 309-319.

Peng, F., Li, X., & Ouyang, Y. (2011). Installation of railroad wayside defect detectors. *Transportation Research Record: Journal of the Transportation Research Board*, *2261*, 148-154.

Roa, J. O., Jiménez, A. R., Seco, F., Prieto, J. C., & Ealo, J. (2007). Optimal placement of sensors for trilateration: Regular lattices vs meta-heuristic solutions. In R. Moreno Díaz, F. Pichler, & A. Quesada Arencibia (Eds.), *Computer aided systems theory – eurocast 2007: 11th international conference on computer aided systems theory, las palmas de gran canaria, spain, february 12-16, 2007, revised selected papers* (p. 780-787). Berlin, Heidelberg: Springer Berlin Heidelberg.

Russell, S., & Norvig, P. (2009). *Artificial intelligence: A modern approach* (3rd ed.). Upper Saddle River, NJ: Prentice Hall Press.

Scaparra, M. P., & Church, R. L. (2008a). A bilevel mixed-integer program for critical infrastructure protection planning. *Computers & Operations Research*, *35*(6), 1905-1923.

Scaparra, M. P., & Church, R. L. (2008b). An exact solution approach for the interdiction median problem with fortification. *European Journal of Operational Research*, *189*(1), 76-92.

Sherali, H., & Alameddine, A. (1992). A new reformulation-linearization technique for bilinear programming problems. *Journal of Global Optimization*, *2*(4), 379-410.

Snyder, L. V. (2006). Facility location under uncertainty: a review. *IIE Transactions*, *38*(7), 547-564.

Snyder, L. V., & Daskin, M. S. (2005). Reliability models for facility location: The expected failure cost case. *Transportation Science*, *39*(3), 400-416.

Wang, Y.-C., Hu, C.-C., & Tseng, Y.-C. (2005). Efficient deployment algorithms for ensuring coverage and connectivity of wireless sensor networks. In *First international conference on wireless internet (wicon'05)* (p. 114-121).

Xie, S., An, K., & Ouyang, Y. (2016). Planning of facility location under correlated facility disruptions. *Transportation Research Part B: Methodological*, Revision under review.

Xie, S., Li, X., & Ouyang, Y. (2015). Decomposition of general facility disruption correlations via augmentation of virtual supporting stations. *Transportation Research Part B: Methodological*, *80*, 64-81.

Xie, X., & Dai, J. B. (2014, Dec). Sensor placement in the ultrasonic positioning system. *International Journal of Management Science and Engineering Research*, *1*, 31-39.

Zou, Y., & Chakrabarty, K. (2004). Sensor deployment and target localization in distributed sensor networks. *ACM Transactions on Embedded Computing Systems*, *3*(1), 61-91.